Torbjørn Nguyen

Evaluation of environmental conditions on the sorption of PAHs onto synthetic and natural fibres

Master's thesis in Environmental Toxicology and Chemistry
Supervisor: Rudolf Schmid, Andy Booth, Lisbet Sørensen
May 2019

Master's thesis

NTNU
Norwegian University of Science and Technology
Faculty of Natural Sciences
Department of Chemistry

NTNU
Norwegian University of
Science and Technology

Acknowledgements

Abstract

Microplastics in the environment has been of increasing concern the last decade. Its abundance in the environment has greatly increased, posing as hazard to wildlife. Microplastic fibres are a common type of microplastics found in environmental sampling. These fibres are mainly derived from textiles, such as clothing, and are released to the environment through washing of clothes. Little to none research has been done on the impact of microplastic fibres in the environment and their interaction with organic pollutants.

In this study, the sorptive behaviour between the polycyclic aromatic hydrocarbons (PAHs) phenanthrene, 1-metylphenanthrene 1-, fluoranthene and 9-phenanthrol with the synthetic fibres polyester, polyamide and polyacrylonitrile and the natural fibre wool were studied. Sorption of phenanthrene on microplastics fibres and wool was investigated in seawater at three different temperatures (4 °C, 10 °C and 20 °C) and in freshwater at 20 °C, to determine the influence of temperature and salinity on degree of sorption. Additionally, the sorption of 1-methylphenanthrene, fluoranthene and 9-phenanthrol to microplastic fibres and wool was investigated in seawater at 20 °C to determine effect of different microplastics fibres physicochemical properties on organic contaminant sorption.

No significant sorption of any of the PAHs was observed for polyacrylonitrile microplastics fibres. It was found that phenanthrene,1-methylphenanthrene and fluoranthene have high degree of sorption onto polyamide microplastics fibres. When compared to polyamide, less degree of sorption of phenanthrene, 1-methylphenanthrene and fluoranthene onto both polyester and wool fibres was observed.

Sorption equilibrium between PAHs and microplastic fibres was achieved within 10 days in all cases and was influenced by several of the studied parameters. Importantly, wool achieved equilibrium with PAHs faster (within

few days) than any of the synthetic fibres. In general, it was observed that the degree of sorption increased with increasing temperature and decreasing salinity.

Adsorption isotherms fitted to the experimental data showed that the Redlich-Peterson model (RP) and the Sips model gave best fit in most cases. The Dubinin-Astakov model (DA) also gave good fit with much of the experimental data, especially with wool. The results indicate that adsorption on PES and PA mainly occurs as layer-by-layer sorption on heterogenous surface as indicated by the RP and Sips model. For wool, both layer-by-layer and pore filling sorption mechanisms was predicted due to good fit with both the Sips model and the DA model. Other isotherm models such as the Langmuir model, Freundlich model and Dubinin-Raduskevich model was also tested.

Sorption of toxic compounds, such as PAHs, to particles, such as microplastic fibres, present in aqueous environments, may affect the ultimate fate and bioavailability of such compounds. As evidenced by the current thesis, both MPF properties and environmental parameters will play a role and must be taken into consideration when researching and discussing implications of combined effects chemical and particulate pollutants. Importantly, naturally occurring particles may be as important as synthetic as a potential transport vector for pollutants.

Sammendrag

Mikroplast I miljøet har blitt en økende bekymring det siste tiåret. Tilstedeværelsen til mikroplast i miljøet har kraftig økt, og fremstår som en fare for dyreliv. En vanlig type mikroplast funnet i miljøet er mikroplastfibre. Disse fibrene kommer hovedsakelig fra tekstiler, som klær, og slippes ut i miljøet gjennom klesvask. Lite til ingen forskning har blitt gjort på innvirkningen av mikroplast fibre på miljøet og hvordan de samhandler med organiske giftstoffer.

I dette studiet ble sorpsjonen mellom de polysykliske aromatiske hydrokarbonene fenantren, 1-metylfenantren, fluoranten og 9-fenantrol med de syntetiske fibrene polyester, polyamid og polyakrylnitril og det naturlige fibret ull. Sorpsjon av fenantren på mikroplastfibre var undersøkt i sjøvann ved tre forskjellige temperaturer (4 °C, 10 °C & 20 °C) og i ferskvann ved 20 °C for å bestemme effekter av temperatur og salinitet. 1-metylfenantren, fluoranten og 9-fenantrol ble undersøkt i sjøvann ved 20 °C for å bestemme effekten av forskjellig fysisk-kjemiske egenskaper.

Ingen signifikant sorpsjon av noen av PAHs ble observert for polyakrylnitril mikroplastfibre. Det ble observert at fenantren, 1metylfenantren og fluoranten hadde høy grad av sorpsjon på polyamid mikroplastfibre. I tillegg ble mindre sorpsjon av fenantren, 1-metylfenantren og fluoranten observert på polyester og ull i forhold til polyamid.

Likevektstid mellom PAHs og mikroplast fibre ble oppnådd innen 10 dager i alle i tilfellene og ble påvirket av flere av studieparameterne. Mest merkbare er ull som hadde likevektstider med PAHs raskere (innen få dager) enn de syntetiske fibrene. Det ble generelt observert at grad av sorpsjon økte med økende temperatur og synkende salinitet.

Adsorpsjons isotermer ble tilpasset eksperimentell data. Redlich-Peterson (RP) modellen og Sips modellen viste seg å gi best tilpasning ved de fleste tilfeller. Dubinin-Astakov (DA) modellen ga også god tilpasning med mye av

de eksperimentelle dataene, spesielt med ull. Resultatene indikerer at sorpsjon på PES og PA hovedsakelig fremstår som lag-på-lag sorpsjon på en heterogen overflate, som indikert av RP og Sips modellen. For ull var både lag-på-lag og pore fylling mulige mekanismer grunnet gode tilpasninger med Sips og DA modellene. Andre isoterm modeller brukt var Langmuir modellen, Freundlich modellen og Dubinin-Raduskevich modellen.

Sorpsjon av PAHs som vist i denne oppgaven kan ha implikasjoner på mobiliteten til PAHs i det marine miljøet, og ha en innvirkning på skjebnen til disse stoffene. PAHs har potensiale til å overføres fra fibrene til dyreliv som svelger disse fibrene. En annen mulighet er at fibrene fremstår som en felle for PAHs ved å gjøre dem mindre tilgjengelig i vann.

Table of Contents

List of abbreviations

1-MP	1-methylphenanthrene
A	Area of peak in chromatogram
ACN	Acetonitrile
ARE	Average relative error
Cfree	Free concentration of PAHs in solution
DCM	Dichloromethane
EABS	Sum of absolute error
FLA	Fluoranthene
FW	Freshwater
GC	Gas chromatography
HCl	Hydrochloric acid
HPLC	High performance liquid chromatography
HYBRID	Hybrid fractional error
LLE	Liquid-liquid extraction
MeOH	Methanol
MS	Mass spectrometry
MPSD	Marquadt's percent standard deviation
MWSE	Mean weighed square error
OCs	Organochlorines
PA	Polyamide
PAC	Polyacrylonitrile
PAHs	Polycyclic aromatic compounds
PBDE	Polybrominated diethyl ethers
PCBs	Polychlorinated biphenyls
PES	Polyester
PES-B	Black polyester
PES-W	White polyester
PET	Polyethylene terephthalate
PHE	Phenanthrene
POPs	Persistent organic compounds
R^2	Coefficient of determination
SIM	Selected ion monitoring
SW	Seawater
US EPA	US Environmental Protection Agency
UV	Ultraviolet
WAF	Water accommodated fraction

1 Introduction

1.1 Plastic pollution

Due to the versatility, properties and multi-purpose applications, plastics have become an important cornerstone of modern society. Plastics are cheap, lightweight, strong, durable and corrosion resistant, and are therefore usable for a wide range of applications (Derraik, 2002). Though today life without plastics might seem unimaginable, industrial large-scale production of plastics only dates to the 1950s. Back then in 1950, plastic production was estimated to be around 2 million metric tonnes (Mt) a year. In 2015 the global production of plastics had risen to 381 million Mt, which is a near 200 times increase compared to production in 1950 (Geyer et al., 2017).

On a global basis, Asia is the largest producer of plastics, with 50,1 % of the global marked production, of which China has 29,4 % of the total global production. Europe on the other hand stands for 18,5 % of the global plastics production (PlasticsEurope, 2018). It is worth noting that this data does not include plastics produced as fibres. Today, the largest use of plastics is in packaging. An estimate of 146 million Mt of plastics was used for packaging purposes in 2015. In comparison, 65 million Mt of plastics was produced for building and construction and 59 million Mt was produced for the textile industry. In total, around 407 Mt of plastics was produced as part of primary production in 2015 (Geyer et al., 2017).

Since the beginning of large-scale plastic production, the amount of waste entering the environment has risen greatly and plastic pollution has gained an increased concern globally in recent years. Jambeck et al. estimated that 275 million Mt of plastic waste was generated from 192 coastal countries in 2010, whereas 4,8 to 12,7 million Mt entered the ocean (Jambeck et al., 2015). An increased use of disposable single-use packaging from reusable packaging has accelerated an increase if plastic waste in municipal solid waste (by mass) from less than 1 % in 1960 to more than 10 % by 2005

(Geyer et al., 2017). Plastic pollution in the environment can pose as a hazard to wildlife and ecosystems, and has been shown to affect organisms either by ingestion, entanglement or chemical effects (LI et al., 2016; Teuten et al., 2007).

1.2 Microplastics (MPs)

1.2.1 Definition and sources of microplastics

Microplastics are small plastic particles. Their size has been defined differently depending on the study, but can generally be defined as pieces of plastic smaller than 5 mm (Barnes et al., 2009; Cole et al., 2011; Lusher et al., 2017). Microplastics can be classified as either primary microplastics or secondary microplastics (Cole et al., 2011). Plastics that are produced to be of a microscopic size are defined as primary microplastics. These plastics can be used for several purposes, such as scrubbers in hand cleansers and facial scrubs, air blasting media or as vectors for drugs in medicine. Accidental discharge of such plastics can happen during shipping and transport. Secondary microplastics are plastics that have derived from larger pieces of plastic on sea or land. They are broken from larger pieces of plastic debris in the environment by means such as UV degradation, mechanical degradation and/or biodegradation.

1.2.2 Microplastics in the environment: distribution, abundance and fate

Plastic waste from terrestrial sources accommodates for approximately 80 % of the plastics found in the marine environment (Andrady, 2011). Such plastics include larger plastic debris that can breakdown to secondary microplastics and primary microplastics. It is estimated in 2014 that 15 to 51 trillion microplastic particles are present in the world's oceans, weighing between 93 and 236 thousand metric tonnes (Van Sebille et al., 2015).

Microplastics are widely distributed across terrestrial and marine systems (Zhang et al., 2019). Distribution of microplastics are affected by a wide

range of processes, such as runoff, infiltration, river discharge, wind, ocean currents and dispersal through animal and human activities. In the marine environment, microplastics can be the water column ranging from sediments to the water surface. The density of the microplastics determine how far down the microplastics are able to sink. Other processes such as biofouling can affect the density of the microplastics, resulting in sinking, neutral buoyancy or floating.

Little research has been conducted on microplastic in the terrestrial environment (Crawford and Quinn, 2016a). It has been found that soil applied with sewage sludge had much higher concentrations of plastic fibres, than soil without sewage sludge.

In the marine environment, it has been found that microplastic concentrations decrease with depth (Kooi et al., 2016). Due to their density most plastics are more likely to sink and be stored in the sediments. Despite this, observations of microplastics with higher densities than the seawater has occurred (Crawford and Quinn, 2016b). This could be because of vertical mixing at different depths, or that microplastics have incorporated air pockets, thus increasing their buoyancy.

Most microplastics that enter the ocean can't be accounted for. Estimations show much higher amounts of microplastics in the environment than what observations say (Cózar et al., 2014). Sinking and sedimentation can account for a large amount of microplastic that enter the ocean, as well as other processes such as degradation into smaller pieces.

1.2.3   Synthetic fibres in the environment

Synthetic fibres are one of the most abundant types of microplastics found in the environment. They are produced in large scale for garment and textile industry. Some of the most common polymer types are polyester (PES), polyamide (PA) and polyacrylonitrile (PAC) (Geyer et al., 2017). Fibres in the environment are most often secondary type source microplastics through

shedding of various textile products (Hartline et al., 2016). Washing of clothes have shown to be one of the most important sources of microplastic fibres in the environment. Microplastic fibres from washing are transported through waste water and enter the oceans directly as most waste water treatment plants don't have the ability to filter out these materials (Browne et al., 2011). Forensic study on microplastic in sediments have shown that the proportion of polyester and polyamide to those found in habitats that receive sewage discharges, which suggest that microplastic fibres origin from washing of clothes.

Fibres are found to be ubiquitous in the environment. They are commonly found in water and can be found on land. A study done by Dris et al. has shown that synthetic fibres can undergo atmospheric fallout (Dris et al., 2016). This indicates that microplastic fibres can take part in atmospheric transport, which can be a source of microplastic fibres in the environment.

1.2.4   Effects of microplastics on biota

Several cases of have been reported of microplastics entering the food chain. More than 180 species of animals have been documented to ingest some type of plastic debris (Teuten et al., 2009). This range from mammals, birds and reptilians to marine wildlife, indicating the spread of microplastics in the environment. Ingestion of microplastics can cause physical internal injuries, such as damage to digestive organs, reduced ingestion or compromise nutrition and energy uptake. Microplastics of really small sizes can invade various organs in creatures, such as liver, pancreas, ovaries and gill lamella which can cause physical damage. Additionally, observations have shown the microplastics in the nanoscale can cross membranes and tissues within organism. Research within this field has mostly been laboratory studies with relatively high microplastics concentrations.

1.3 Persistent organic pollutants (POPs) in the environment

The accumulation of natural and anthropogenic organic compounds has in recent decades been of concern, as their abundance in the environment has reached harmful levels to wildlife and humans (El-Shahawi et al., 2010). These compounds appear ubiquitous in the environment and are characterised by their persistency, as well as toxicity and bioavailability. Organic compounds that are persistent in the environment are often denoted as Persistent Organic Pollutants (POPs) and can be described as compounds with physical or chemical properties that makes them resistant to photolytic, biological and/or chemical degradation or transformation.

POPs can be divided between intentional and unintentional POPs (El-Shahawi et al., 2010). Intentional POPs are manmade compounds and are not naturally found in the environment. These compounds are halogenated through different reactions in order to be used for different purposes. Examples of such compounds are organochlorines (OCs) that are used as pesticides, polybrominated biphenyls (PCBs) which has several industrial uses or polybrominated diphenyl ethers (PBDEs) which was widely used as flame retardants. Unintentional POPs are produced as unwanted by-products of chemical processes. Such compounds can be polycyclic aromatic hydrocarbons (PAHs), which are made in combustion processes and as a by-product in industrial processing. Other compounds that are unintentionally made and released into the environment are dioxins and dibenzofurans.

A common characteristic of POPs is that they are hydrophilic and lipophilic. This means that POPs are less likely to be found free in water. In aquatic systems they are more likely to partition to solids in order to avoid the aqueous phase. If fat or lipids are present, such as in organisms, POPs are more likely to partition to the lipids. Lipids are often used as storage for energy in organisms, and thus makes it slower to metabolise. This makes

POPs more persistent and more likely to accumulate in the food chain over time.

Many POPs are either volatile or semi-volatile. This makes them susceptible to atmospheric transport. POPs can volatise from soil or water and enter the atmosphere at moderately high temperatures and travel with the air currents at great distances. As the temperature sinks, the POPs will exit the atmosphere and re-deposit in water or soil. Several POPs like PCBs have been found far in the Arctic regions. These compounds do not have a local source in the Arctic, and atmospheric transport is therefore the most likely source of these compounds in the Arctic.

Several measures have been implemented in order to reduce the release of various organic pollutants in the environment. Conventions such as the Stockholm convention works towards restriction and elimination of POPs that especially poses a threat to wildlife and the environment. Though many POPs have been banned through such measures, they still remain in the environment. Even though it has been decades since their ban, due to their persistency those POPs, known as legacy POPs, still remain in the environment. These compounds have been found to accumulate in wildlife despite, their production level being considerably reduced. An example is the accumulation of PCBs in polar bears in the Arctic, where PCBs are accumulated in lipid tissues of polar bears through their high lipid diet. This has caused endocrine disruptions within the polar bears and decrease in bone mineral density.

1.4   Sorption of organic pollutants to microplastics

Sorption of trace organic compounds onto microplastics have been known for decades. Rice et al. tested sorption of 19 different trace organic chemicals onto propylene, and published the paper as early as 1984 (Rice and Gold, 1984). Since then, several cases of microplastics in the environment have been found contaminated with POPs. Sorption of POPs

onto microplastics in the aquatic environment have become an increasing scientific topic of interest. Several studies have investigated POPs adsorbed onto microplastics found in the environment (Endo et al., 2005; Mato et al., 2001; Rios et al., 2007). Mato et al. (2001) found PCBs, DDE and nonylphenols on polypropylene resins collected from Japanese coastal areas. Endo et al. found PCBs on resin pellets collected from a Tokyo beach. Rios et al. (2007) sampled thermoplastic resins and post-consumer fragments from the North Pacific Gyre. The main plastics found were polypropylene and polyethylene. PAHs were found in all samples, while PCBs could be found at beach collected samples.

Laboratory studies done on microplastics have shown that most polymer types readily adsorb POPs. Teuten et al. investigated sorption of phenanthrene onto microplastic (Teuten et al., 2007). Their study showed that polymer type affected the sorption of phenanthrene onto microplastics by more than an order of magnitude. Polyethylene was reported to adsorb a lot more compared with polypropylene and poly vinyl chloride. Polypropylene adsorbed more than polyvinyl chloride. It was also reported that the plastics adsorbed more than two different natural sediments. Rochman et al. (2014) found that polystyrene adsorb PAHs. A comparison they did with other polymer types showed that polystyrene adsorbed a lot more than PAHs then other compounds, probably due to the aromatic group on the polystyrene (Rochman et al., 2014). A study done by Saini et al. (2016) characterised sorption of gaseous PBDEs to cotton and polyester. Their results showed PBDEs concentrations on polyester to be 20-50 times higher than on cotton (Saini et al., 2016).

In order to understand the impacts of sorption of POPs onto microplastics, more knowledge is necessary. Experimental results show that environmental factors such as pH, salinity and temperature affect sorption/desorption of POPs to microplastics. Other factor such as polymer type, additives and degree of weathering could also have an effect on how POPs adsorb organic

pollutants (Ziccardi et al., 2016). Fate of the POPs adsorbed on microplastics should be researched. POPs adsorbed on microplastics have the possibility to transfer from microplastics to organisms. Microplastics can also act as a sink for POPs as most microplastics sink to the sediments.

1.4.1 Microplastics as vector for bioaccumulation of organic pollutants in marine organisms

Microplastics have been suspected to act as vectors for transport of POPs into organisms. Aquatic creatures have been found to ingest microplastics in the environment as they mistake it for food. Whether or not these transported compounds have a toxic effect have been discussed, but studies show that transfer of POPs from microplastics to organisms is possible (Teuten et al., 2009).

Bakir et al. (2004) investigated sorption and desorption of several organic pollutants on polyethylene and polyvinyl chloride. Desorption rates in gut surfactant simulated environment was considerably higher than that in seawater. Rochman et al. (2013) investigated fish exposed to a mixture of complex chemicals, including PAHs, PCBs and PBDEs, sorbed into low density polyethylene (Rochman et al., 2013). Their result show possible bioaccumulation of these compounds after two-month exposure. It must be noted that the fish diet consisted of 10 % plastic and might not be relevant in the environment.

1.5 The aim of this study

This master thesis is part of the SINTEF-lead MICROFIBRE project. The main aim of the MICROFIBRE project is to investigate the fate and effect of the release of microplastic fibres in the environment in order to create mitigation measures to reduce the release of microplastic fibres in the environment investigating the interactions between microplastic fibres and PAHs. The current thesis focuses on investigating the interactions between microplastic fibres and PAHs.

The aim of this master thesis is to study the factors that impact sorption behaviour of organic compounds to microplastics fibres. Sorption behaviour of two PAHs, phenanthrene (PHE) and fluoranthene (FLA), one alkylated PAHs 1-methylphenanthrene (1-MP), and hydroxylated PAHs 9-phenanthrol (POH), to different synthetic fibres (polyester, polyamide and polyacrylonitrile) was investigated. In addition, a natural fibre (wool) is also to be studied in order to compare it with the synthetic fibres. These fibres are used in textile production. Phenanthrene and fluoranthene are listed as a compound of concern by the US environmental protection agency (US EPA), while 1-methylphenanthrene can be found in crude oils and petroleum products. For target compound structure see Figure 1-1.

With phenanthrene as the core compound, sorption to fibres was investigated at 5°C, 10°C and 20°C in seawater and 20°C in freshwater, in order to assess effect of temperature and salinity. 1-methylphenanthrene and fluoranthene was investigated at 20°C in seawater in order to see the effect of less polarity and increase in mass.
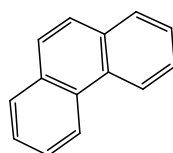
Phenanthrene
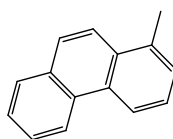
1-methylphenanthrene
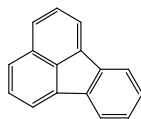
Fluoranthene
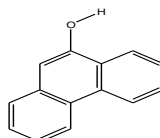
9-phenanthrol

Figure 1-1 Target compounds for this study of PAHs on fibres

2 Theoretical background

2.1 Types of plastics: composition and potential hazards

The term "plastics" is used for a group of synthetic or semi-synthetic organic polymers. These polymers are derived from monomers are derived from monomers that has been extracted from oil or gas (Cole et al., 2011). The properties of the polymers are determined by monomer composition and chain length of the polymers. The chain length of the polymers affects the physical state of a polymer (Andrady, 2017). For instance, when polyethylene chains consist of a few hundred monomers, it is in the form of a viscous liquid or a soft wax. Whereas if the number of monomers is in the hundreds of thousands, then polyethylene is found as a solid plastic. Longer molecular chains allow for stronger intermolecular van der Waals forces between the chains, giving the polymers stronger modulus strength and fracture toughness. As such, the melting points of different plastic polymers are affected by the chain length of the polymers.

Some plastic polymers have a partly crystalline morphology (Andrady, 2017). The polymers will have short crystalline sections in the bulk which have an effect the morphology of the polymers, while the rest consist of randomly oriented amorphous chains. Higher degree of crystallinity in the polymer makes the polymer tougher, while too high degree of crystallinity can make the polymer brittle. The degree of crystallinity can affect different properties of the polymers. Higher degree of crystallinity has a negative correspondence with the buoyancy of the polymer. In addition, the loading of POPs will be relatively lower in higher crystalline plastics. The amorphous section fraction of a semi crystalline polymer has better ability to dissolve POPs compounds. In order to categorise polymers based on their crystallinity the glass transition temperature is often used, which is the temperature which allows limited thermal motion in short segments of the polymer chains (Hüffer and Hofmann, 2016). Non-crystallisable polymers,

which are amorphous in their molecular structure are known as "glassy" polymers while semi-crystalline polymers are known as "rubber" polymers. The degree of crystallisation in a polymer can be changed by physical or thermal treatment. For instance, in spinning textile fibres the plastic is drawn uniaxially to high extensions to encourage very high degrees of crystallization to yield uni-axially strong plastic fibre.

The largest groups in total non-fibre plastics production are polyethylene (36%), polypropylene (21%), and poly vinyl chloride(12%), followed by polyester, polyurethane, and polystyrene (<10% each) (Geyer et al., 2017). Among fibres, polyester (PES) is the most produced polymer. During production, polymers are typically mixed with chemicals known as additives in order to either change the properties of the polymers or to add desired properties to the polymer. Additives can include carbon or silica to strengthen the material, thermal stabilisers or UV stabilisers.

2.1.1   Polyester

The most commonly produced type of polyester is polyethylene terephthalate (PET). This is a product of condensation reactions between ethylene diglycol and terephthalic acid. Commercial polyester fibres generally consist of a mixture of crystalline and non-crystalline regions due to the production method. PES is in general hydrophobic of nature. It is often characterised by low moisture absorption and an ability to accumulate electrostatic charges on the surface (Grishanov, 2011). The structure of polyethylene terephthalate is shown in Figure 2-1.
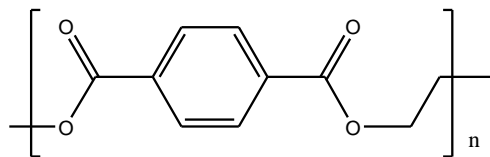
Figure 2-1 Chemical structure of polyethylene terephthalate monomer

2.1.2 Polyamide

Polyamide, more commonly known as nylon, is the name for polymers which are linear structural units linked by an amide functional group. The most commercially common types are known as nylon 6 and nylon 6,6. In nylon 6,6 the monomer units are hexamethylenediamine and adipic acid. The number 6,6 indicates the number of carbon in the diamine and dibasic acid (Grishanov, 2011). The chemical structure of nylon 6,6 is shown in Figure 2-2.

The most important polymeric linkage for all nylons is the amide group, which provide strong intermolecular hydrogen bonds, which results in high melting points, polymer strength and exceptionally high elasticity. The amide group serves as sites for moisture sorption, being reasonably hydrophilic (Rebenfeld, 2002). As such structural properties such as elasticity are affected by moisture due to reduction of the intermolecular hydrogen bonds.
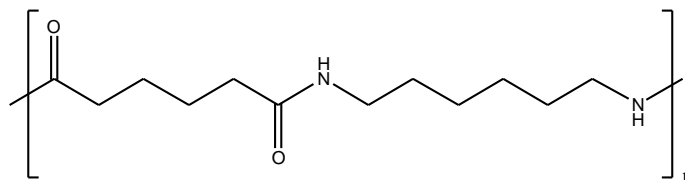
Figure 2-2 Chemical structure of nylon 66 monomer

2.1.3 Acrylic fibres

Most acrylic fibres are based on polyacrylonitrile as a constituent. The most common use of polyacrylonitrile is in the production of bulky fabrics, such as knitwear and blankets as an alternative to wool. It is often produced with other comonomers in addition with acrylonitrile. The sorption properties with water varies with comonomer composition. Chemical structure of acetonitrile is shown by Figure 2-3.
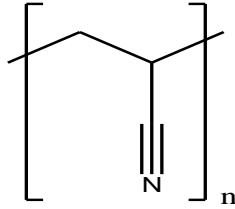
Figure 2-3 Chemical structure of polyacrylonitrile monomer

2.1.4   Wool

Wool is a natural protein-based staple fibre. Most wool types are collected from hair of the body of sheep. Wool consists of a complex structure composed of a class of proteins known as keratins. Structurally, wool is a very complex material. The surface of wool and many other animal fibres has a system that forms overlapping scales. These scales serve to protect the fibres and the animal from the external environment (Rebenfeld, 2002). An interesting feature of wool is that the fibre surface is very hydrophobic, and not readily absorb water. Yet wool fibres are able to absorb water to a high extend. The high moisture absorption is because of the hydrophilic internal proteins in the internal fibre structure. This allows wool to retain water up to 30 % of its dry weight (Grishanov, 2011). The high water absorption is due to porous structure in wool which allows water absorption (B Speakman, 1943).

2.2   Polycyclic aromatic hydrocarbons (PAHs)

Polycyclic aromatic hydrocarbons (PAHs) are a class of chemicals that can exist in more than 100 different combinations (Crawford and Quinn, 2016a). They can be classified into three classes based in their source: biogenic (natural processes), petrogenic (petroleum products) and pyrogenic (incomplete combustion). PAHs are in general produced as a consequence of incomplete combustion of organic materials, such as wood, petroleum and tobacco. As a consequence, biogenic PAHs can be produced from natural sources such as forest fires and volcanic eruptions. Anthropogenic sources such as combustion engines also contribute to release of PAHs in the

environment. Oil extraction and refinement processes can contribute to the release of petrogenic PAHs and their derivatives into the environment (Huang et al., 2017). Such compounds can be 1-methylphenanthrene, which could be found in crude oil from the Deep-Water Horizon incident. Burning of plastics have shown to produce pyrogenic PAHs, with polystyrene producing the highest quantities (Wheatley et al., 1993).

PAHs are structurally composed of two or more fused aromatic benzene rings, constituted by carbon and hydrogen atoms (Bidlack, 2013). PAHs consisting of 4, 5 and 6-rings are in general heavier and less polar and have been found to dominate in sediment samples. PAHs consisting of 2 or 3 rings are more commonly found dissolved in water or air.

In the environment they occur as a ubiquitous pollutant. The US EPA has characterised 16 PAHs as pollutants of concern, due to their toxicity and presence in the environment (see Figure 2-4) (Fähnrich et al., 2002). PAHs have shown to have toxic effects even at low exposure levels. Some have even shown to be carcinogenic and mutagenic.
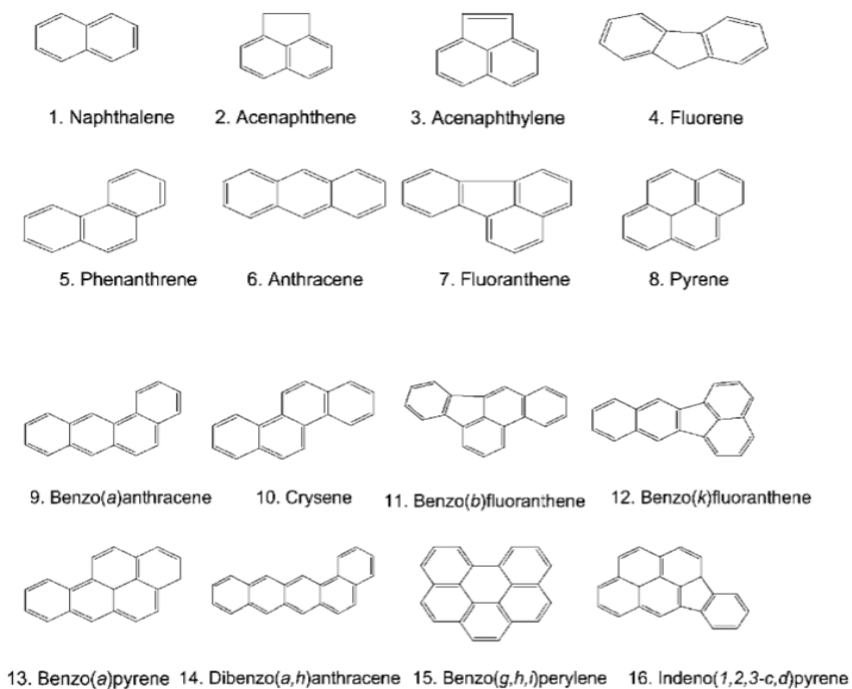
Figure 2-4 PAHs listed of special concern by the US Environmental protection agency

PAHs are very hydrophobic compounds, meaning they are quite water resistant. The hydrophobicity and aromaticity increase with the number of rings added to the structure of PAHs. In the environment, the main routes for transport of PAHs are by atmospheric or water transport. PAHs becomes volatile after high temperature combustion processes, and in the atmosphere, PAHs are found in two phases, vapor phase or solid phase. In the vapour phase, the PAHs are dissolved into aqueous vapour which can be precipitated and deposited further away from the source through wet deposition. PAHs can also be sorbed onto particles in the air, then be deposited through dry deposition. Because of atmospheric transport samples with relatively high amounts of PAHs can be found in very remote areas or contribute to pollution far from its source. PAHs are rarely found in water by itself, but often adsorbed to particulates. PAHs are very hydrophobic and thereby less soluble in the water phase. PAHs can be transported with

ground water, river or ocean currents into bigger lakes or oceans. This makes it possible to sample sediment samples far of the coast with detectable PAHs values and can also be used to get historical data of PAHs emissions.

Standard methods for extraction and detection of PAHs includes liquid-liquid extraction (LLE) and solid phase extraction in combination with HPLC or GC. Detection can be achieved with UV or fluorescent detector, or with techniques such as flame ionisation or mass spectrometry (Poster et al., 2006).

2.3 Interactions between organic compounds and solids

2.3.1 Sorption

Sorption is a process where a compound (sorbate) becomes associated with a solid phase (sorbent) (D'Arcy and Watt, 1970).There are two main sorption processes, adsorption and absorption. Adsorption is a process where a compound sorb onto the surface of a sorbent, while absorption is a process where a compound sorb into the sorbent condensed phase.

The equilibrium conditions of sorption can be explained by the distribution coefficient, K_d, between water-solid interfaces and is given by the ratio:

$$K_d = \frac{q_e}{C_e}$$

where q_e is the amount of sorbate sorbed on the sorbent and C_e is the equilibrium concentration in the aqueous phase.

Sorption occurs when Gibbs free energy of the sorption reaction is negative. Several aspects affect whether or not sorption is favourable process between sorbate and sorbent, such as the sorbate affinity towards the sorbent (von Oepen et al., 1991). External factors can such as temperature, salinity and pH can affect whether or not sorption is favourable.

Several intermolecular forces might be involved in in sorption processes, such as van der Waals interactions, hydrophobic bonding, hydrogen bonding, charge transfer, direct and induced ion dipole and dipole-dipole interactions and chemisorption (von Oepen et al., 1991).

2.3.1.1 Effects of temperature

It is expected that sorption of PAHs onto solids decreases as temperature increases, due to increased solubility of the PAHs (Lamichhane et al., 2016). Hulscher et al. (1996) studied the effect of temperature on the sorption and sorption kinetics of micropollutants. Various effects on the equilibrium sorption was observed. For most compounds, equilibrium sorption decreased with increasing temperatures. Other examples showed increasing equilibrium sorption with increasing temperature, and some examples saw no effect of temperature on sorption concentration. Temperature seems to especially have an effect on sorption into porous materials. At low temperatures, the sorbate might not have sufficient energy to enter the pores on a microporous surface (Dąbrowski, 2001). Little research has been done on effects impact of temperature on sorption of PAHs on microplastic

Hiller et al. (2008) did a study on sorption of PAHs on soil, which showed that PAHs adsorption decreased as temperature was rose (Hiller et al., 2008).

2.3.1.2 Effects of salinity

PAHs sorption capacity has been found to be increased with increasing salinity. The formation of hydration shells by inorganic ions reduces the water solubility of PAHs, which forces more PAHs onto adsorption surfaces (Lamichhane et al., 2016). It was found in a study done by Wang et al. that increased salinity enhanced the sorption capacity of PAHs onto sediments from the Yellow River Delta, due to salting out (Wang et al., 2015). In the study done by Karapanagioti et al. (2008) on plastic pellets showed that salinity affected the diffusion of phenanthrene into polyethylene and polyoxymethylene (Karapanagioti and Klontza, 2008). Otherwise, few

studies has been done on effects of salinity on sorption of PAHs on microplastics.

2.3.1.3 Sorption involving aromatic compounds

Most aromatic compounds are hydrophobic by nature which leads to increased tendency to partition onto solids in an aqueous environment (Hemond and Fechner, 2014). This is favourable for the aromatic compounds energetically due to the hydrophilic nature of water. The main driving force of partitioning is hydrophobic partitioning in from the aqueous environment to a solid that helps stabilise the molecules. Additional interactions that favour sorption are electrostatic Van der Waals interactions.

Aromatic compounds have the possibility to take part in aromatic interactions in which overlaying π-electrons resulting in a more stable configuration. The phenomenon is called π-stacking where overlaying orbitals generate favourable orientations between the aromatic compounds. The rings can be oriented edge-face, offset stacked or face to face stacked (Waters, 2002). Another type of interactions with π-orbitals in aromatics involves delocalisation of electron lone pairs into empty π-orbitals of aromatic compounds (Singh and Das, 2015). The aromatic ring can act as a hydrogen bond acceptor to form a hydrogen bond with lone pair donors such as amides (Tóth et al., 2001). These kinds of interactions have shown to be important in protein structures.

2.3.2 Sorption kinetics and order of reaction

Adsorption kinetics is the measurement of the adsorption uptake with respect to time at constant temperature, and can be used to measure diffusion of adsorbate onto adsorbent (Saha and Grappe, 2016). The kinetics of adsorption is one of the most important characteristics in defining adsorption efficiency. Several kinetics models have been used to determine sorption kinetics (Wu, 2017).

A commonly used model to determine adsorption kinetics is the pseudo first order equation proposed by Lagergren (Ho and McKay, 1998).

$$log(q_e - q(t)) = log(q_e) - \frac{k_1}{2,303}t$$

Where q_e (μg/mg) is the adsorbed amount of adsorbate on the adsorbent at equilibrium, and has to be determined from experimental data, $q(t)$ (μg/mg) is the amount of adsorbate on the adsorbent at time t, and t is the time of sampling. k_1 is the rate constant for the pseudo first order equation.

If the rate is of a second order mechanism, pseudo-second order equation can be used. It has a derived linear form, which was proposed by Ho et al. (1998)

$$\frac{t}{q(t)} = \frac{1}{k_2 q_e^2} + \frac{1}{q_e}t$$

t is the time of sampling, $q(t)$ (μg/mg) is the amount of adsorbate on adsorbent at time t, q_e (μg/mg) is the calculated amount of adsorbate on adsorbent at equilibrium and k_2 is the rate constant for the reaction. An advantage of the pseudo-second order reaction lies in the fact that q_e must not be known.

2.3.3 Adsorption isotherm models and mechanisms

An adsorption isotherm is a graph describing the relationship between q_e and C_e (Dąbrowski, 2001). An isotherm is a graph that is plotted with q_e and C_e at constant pressure or temperature, which describes the macro retention of a compound on a solid. It is commonly used to describe adsorptive behaviour in adsorption processes. In order to create these isotherms, an accurate description of equilibrium conditions must be known, such as equilibrium time, for prediction of adsorption parameters (Gimbert et al., 2008). In environmental studies, adsorption isotherms are often used to describe and predict the mobility of substances in the environment, and helps explain their interactions with solids (Limousin et al., 2007).

The form of the adsorption isotherm can help interpret the adsorption mechanisms of the adsorption process. There are four main categories of isotherm shape that are generally used, the S-curve, the L-curve, the H-curve and the C-curve (Giles et al., 1974). The various shapes are illustrated in Figure 2-5.
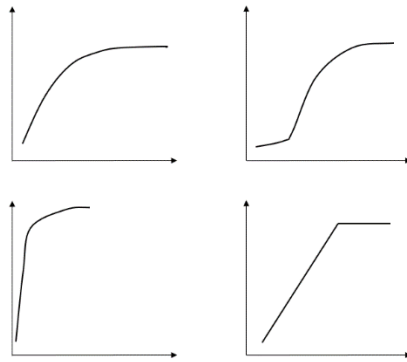
Figure 2-5 General classes of shapes for adsorption isotherms. The top left represents the L-shape, the top right represents the S-shape, the bottom left represents the H-shape and the bottom right represent the C-shape.

The L-curve is characterised by quick initial adsorption, but as adsorption sites are being filled, it becomes increasingly difficult for an adsorbate to find vacant adsorption sites. It is often characterised by a plateau at higher concentrations, indicating sorption capacity. The S-curve is characterised by slow adsorption at initial stages. When concentration rises adsorption becomes easier due to assisted adsorption from the adsorbate at intermediate and higher concentrations it follows the L-curve. The H-curve indicates high affinity between adsorbate and adsorbent. It is a special case of the L-curve in which dilute solutions are completely adsorbed. The C-curve is characterised by constant partitioning between solution and adsorbent until maximum adsorption can occur, which leads to a sudden horizontal shift of the curve. Fundamentally this means that as sorption sites are occupied, more sorption sites are created and can imply that the adsorbate more readily penetrates into the adsorbent.

Adsorption isotherm have been done by a linear and a non-linear approach in selecting the optimal isotherm. They are expressed by equations which describe different parameters in relation with the adsorption process. In this study, adsorption will be modelled using non-linear models with non-linear regression methods for each model. Non-linear models have often resulted in better isotherm parameters for the given model (Kumar and Sivanesan, 2006).

The Langmuir, Freundlich, Redlich-Peterson and Dubinin-Astakov models selected are based on the work done by Emilie Rogers (Rogers, 2018) in her thesis work. These models seemed to give good fit with experimental data, especially the Redlich-Peterson model. The Sips model was added to supplement the Redlich-Peterson model. Both the Sips model and the Redlich-Peterson model combine the Langmuir and Freundlich model, but the Sips model takes into account other parameters such as pH, temperature and concentration (Ayawei et al., 2017). These four isotherm models predict sorption as a layer-by-layer interaction in which a compound adhere to the surface of a solid. The Dubinin-Raduskevich model was added in case the Dubinin-Astakov model proved to be the best fit. These two models predict micropore filling as adsorption mechanisms, but on different types of pore distributions on the surface (Kleineidam et al., 2002). Both models were applied in order to get better precision on pore filling mechanisms. The isotherm models are presented in Table 2-1.

Table 2-1 Isotherm models used to fit in this study experimental data in this study. The equation parameters are explained further down in this section. C_e (μg/L) is the free concentration of PAHs at equilibrium in the sample solution and q_e (μg/mg) is the adsorbed amount of PAHs on the fibres

Model	Equation
Langmuir	$q_e = \dfrac{QK_LC_e}{1+K_LC_e}$
Freundlich	$q_e = K_FC_e1/n$
Redlich-Peterson	$q_e = \dfrac{K_rC_e}{1+a_RC_e^g}$
Sips	$q_e \dfrac{Q_SK_SC_e^{B_S}}{1+K_SC_e^{B_S}}$
Dubinin-Astakov	$\log q_e = \log Q^0 - \left(\dfrac{\varepsilon_S}{E}\right)^b$
Dubinin-Raduskevich	$q_e = (q_s)exp(-k_{ad}\varepsilon^2)$

Hüffer et al (2016) suggests that hydrophobic interactions are of major importance on the adsorption between plastics and non-polar organic compounds (Hüffer and Hofmann, 2016). It is expected that partitioning from the water phase to the solid surface is because of reduced solubility of these compounds in water. Other interactions can also occur such as π-π interactions between aromatic organic compounds and aromatic groups in the monomers.

2.3.3.1 Langmuir isotherm (LM)

The Langmuir isotherm is an empirical model that assumes monolayer adsorption over a homogenous surface. This model implicates limited adsorption sites, where adsorption on an occupied site can't take place. Once a sorption site has been occupied, no further adsorption can take place in that site. This approach assumes no interactions between adsorbate molecules on adjacent site. The L-shape isotherm is based on the shape of

the typical Langmuir isotherm. The non-linear Langmuir equation can be found in Table 2-1.

This model is a two-parameter model, where the Q (µg/mg) parameter expresses the maximum amount of sorbate that can adsorb to per weight unit of adsorbent to complete the monolayer on the surface. The K_L (L/ µg) parameter is the Langmuir constant and is related to the affinity of binding sites on the adsorbent surface (Guechi and Hamdaoui, 2016).

2.3.3.2   Freundlich isotherm (FL)

The Freundlich isotherm describes a non-ideal and reversible adsorption of a single adsorbate in an aqueous solution (Proctor and Toro-Vazquez, 2009). This model can be applied to multilayer adsorption processes with a non-uniform distribution over a heterogenous surface. The flaw in the Freundlich equation lies in the fact that it does not predict adsorption capacities, and as such indicate continuous adsorption at a constant rate till possible saturation. The non-linear Freundlich equation can be found in Table 2-1.

The equation parameters K_F (µg/mg) is used as an indication to describe adsorbent capacity, while 1/n is used to describe the heterogenicity of the surface, becoming more heterogenous as it approaches zero (Haghseresht and Lu, 1998). A *1/n* value below 1 indicates chemisorption, while a value higher than 1 indicates cooperative adsorption.

2.3.3.3   Redlich-Peterson isotherm (RP)

The Redlich-Peterson isotherm is a hybrid isotherm featuring Langmuir and Freundlich isotherms, combining into a three parameter equation (Redlich and Peterson, 2007). This isotherm is considered versatile, due to its ability to be able to describe both homogenous and heterogenous surfaces. At lower concentrations, the model has Langmuir characteristics, while at higher concentration, the model has Freundlich characteristics. The non-linear Redlich-Peterson isotherm can be found in Table 2-1.

K_r (L/mg) and a_r (L/mg) are parameters are Redlich-Peterson isotherm constants (Vijayaraghavan et al., 2006). The parameter g varies between 0 and 1. When g is closer to 1, the model behaviours turn towards that of the Langmuir model, while when g approaches zero the equation becomes more Freundlich (Ng et al., 2002).

2.3.3.4 Sips isotherm

The Sips isotherm is a combination of Langmuir and Freundlich isotherms as well but was modelled to predict better heterogenous adsorption surfaces. At lower concentrations it reduces the Freundlich isotherm, while at higher concentrations it incorporates the monolayer characteristics of the Langmuir isotherm which is described by the K_s parameter (Belhachemi and Addoun, 2011). The non-linear Sips equation can be found in Table 2-1.

The Q_s describes a mono layer adsorption capacity (µg/mg), and K_s is Sips constant related to the energy of adsorption. B_s is the Sips isotherm exponent. B_s values close to 1 returns the equation to the Langmuir isotherm, while deviation from 1 indicates heterogenicity. The parameter of the Sips isotherm model are pH, temperature and concentration dependant (Ayawei et al., 2017).

2.3.3.5 Dubinin-Astakov isotherm (DA)

The Dubinin-Astakov model is a model derived from Polanyi theory of micropore filling and evaluates parameters that characterise the microporous structure of a solid (Inglezakis, 2007). This model assumes an adsorption mechanism of pore filing on a non-homogeneous surface of micropores, rather than layer-by-layer surface coverage as with the previous models. Originally a model for vapour adsorption on solids, it has also been extended to model aqueous systems by including adsorbate solubility in the aqueous phase. This is incorporated in the Polanyi adsorption potential ε_{sw} into the non-linear form of the equation (Kleineidam et al., 2002). The non-linear Dubinin-Astakov equation can be found in Table 2-1

$$\varepsilon_{\text{sw}} = RTln(s_w/C_e)$$

R is the gas constant (8,314*10^-3) T is the temperature and s_w is the solubility of the adsorbate at given conditions. The parameters Q^0 (µg/mg) represents the amount of adsorbate adsorbed on the surface at equilibrium and b is a heterogeneity parameter. E is the energy of adsorption. A big advantage of this model is its temperature dependency.

2.3.3.6 Dubinin-Raduskevich isotherm (DR)

The Dubinin-Raduskevich isotherm is a model used to describe a Gaussian energy distribution onto a heterogenous surface. This isotherm model was derived from Polanyi theory. This model was originally derived for adsorption subcritical vapours onto micropore solids following a pore filling mechanism and can be derived from the Dubinin-Astakov equation by setting the parameter b=2 (Kleineidam et al., 2002). The Polanyi adsorption potential for the Dubinin-Raduskevich equation can be expressed without the maximum solubility of the adsorbent. The non-linear Dubinin-Raduskevich equation can be found in Table 2-1.

$$\varepsilon = RTln\left(1 + \frac{1}{C_e}\right)$$

The equation parameters q_s is the theoretical isotherm saturation capacity (µg/mg) and k_{ad} is an isotherm constant (mol²/kJ²) (A.O, 2012).

2.3.4 Adsorption vs. absorption

It has been suggested that absorption can occur in the form of internal diffusion, where the sorbate penetrates the crystalline network of polymers (D'Arcy and Watt, 1970). This has been suggested as a possible sorption mechanism on a sorption study done by Karapanagioti et al. (2008) (Karapanagioti and Klontza, 2008). They suggested that sorption occurred as an intrapolymer diffusion in polyethylene and polyoxymethylene. As the solvent was able to penetrate the crystalline structure of the polymers, more adsorption site opened up. This kind of behaviour has been explained

through the use of C-curve shapes, in which sorption sites become more available as a result of opening-up or disentanglement of the structure (Giles et al., 1974). Hüffer et al. (2016) suggested that when the Freundlich exponent was approximately equal to 1, it indicates that partitioning occurs as partitioning into the bulk polymer for sorption by rubbery polyethylene.

Endo et al. suggested the use of the ratio between the distribution coefficients of *n*-alkanes and their cyclic homologues (Endo et al., 2008). This was suggested as a possible indication as absorption being the possible main mode of sorption on rubbery polyethylene by Hüffer et al. (2016).

2.4   Coefficient of determination (R^2)

Coefficient of determination (R^2) was calculated in order the express the fitting degree of isotherms and kinetic models with experimental data (Kumar and Sivanesan, 2006). Coefficient of determination is defined by the equation shown below

$$R^2 = \frac{\sum(q_{e,meas} - \overline{q_{e,calc}})^2}{\sum(q_{e,meas} - \overline{q_{e,calc}})^2 + \sum(q_{e,meas} - q_{e,calc})^2}$$

Values range between 0 and 1, and values closer to 1 represents a better fit.

2.5   Error functions

In order to determine the best fit of data for non-linear regression, several error functions have been developed (Foo and Hameed, 2010; Rivas et al., 2006). These error functions make it possible to compare different isotherm fits quantitatively, where the lower error function value often gives the best fit. Due to error models inherent bias towards the diverse form of

parameters, estimation error and fit distortions, several error functions have been used to determine the fit of the isotherm data. Sum of square errors (SSE), mean weighed square errors (MWSE) hybrid fractional error function (HYBRID), average relative error (ARE), Marquadt's percent standard deviation (MPSD) and sum of absolute errors (EABS) has been used to fit the experimental data to the isotherm models. The error functions used in this study are sum of square errors, mean weighed square errors and sum of absolute errors.

2.5.1   Sum square of errors

Sum of square errors (SSE) is one of the most commonly used error functions for non-linear regression (Foo and Hameed, 2010). At higher concentrations ranges of the liquid phase concentrations the magnitude and square of errors tend to increase, making it more suitable for isotherm parameter derivation. The function is given by the equation below.

$$\sum_{i=1}^{N}\left(q_{e,calc} - q_{e,meas}\right)_{i}^{2}$$

2.5.2   Mean weighed square errors

Mean weighed square error (MWSE) has previously been used when fitting isotherms of PAHs to microplastics (Rogers, 2018). This error function has previously been shown to avoid good fits from overparametrisation of model (Wu et al., 2012). The function is given by the equation below.

$$\sum_{i=1}^{N}\left[\frac{1}{N-p}\frac{\left(q_{e,meas} - q_{e,calc}\right)^{2}}{q_{e,meas}^{2}}\right]$$

2.5.3   Sum of absolute errors

This sum of absolute errors (EABS) is similar to sum of square errors, in which it can increase the error in order to get better fitting, leading to a bias towards higher concentration ranges. It has been shown to give good fittings

with good R^2 values (Ng et al., 2002). The function is given by the equation below.

$$\sum_{i=1}^{N} \left| q_{e,meas} - q_{e,calc} \right|$$

3 Materials and Methods

3.1 Chemicals and materials

3.1.1 Chemicals

Filtered MilliQ-Water was supplied by a Millipore filtration system. LC-MS grade acetonitrile (ACN) was supplied by Honeywell (Steinheim, Germany) HPLC grade methanol (MeOH) was supplied by Sigma-Aldrich (Steinheim, Germany). Analytical grade dichloromethane (DCM) was supplied by Rathburn Chemicals (Walkerburn, UK). *N*-hexane was supplied by Fluka Analytical (Steinheim, Germany). 37% Hydrochloric acid (HCl) and sodium sulphate (Na_2SO_4) were purchased from Merck (Darmstadt, Germany).

Standards of phenanthrene, fluoranthene, 1-methylphenanthrene and 9-phenanthrol were purchased from Sigma-Aldrich. Deuterated PAHs for internal standards for GC-MS analysis were supplied by Chiron AS (Norway).

3.1.2 Laboratory equipment

All non-volumetric glass equipment was baked at 450 °C in a ceramic oven before use for 4 hours. Equipment that could not be baked (glass, metal, Teflon and plastic) was rinsed using DCM or MilliQ-water prior to use. Standards and fibres were weighed using a Mettler Toledo (XPE205) scale, with an accuracy of 0,01 mg, which was validated each day before use.

3.1.3 Synthetic and natural fibres

Spools of the different kinds of fibres were acquired from textile producers associated with the MICROFIBRE project. Table 3-1 shows the different fibre types, the supplier, colour and density of the fibres. Density measurements was done by a group in SINTEF Oslo. The chemical structure of the synthetic fibres was confirmed by another master student, Shannen Sait, working on a joint project (Sait, 2019).

Table 3-1 Supplier, colour and density of the different fibre types.

Fibre type	Supplier	Colour(s)	Density* (g/mL)
Polyester (PES)	Helly Hansen	Black (PES-B)	1.387 ± 0.001
		White (PES-W)	1.339 ± 0.009
Polyamide (Nylon 66 (PA))	Pierre Robert Group	White	1.146 ± 0.006
Polyacrylonitrile (PAC)	Varner	Blue	1.178 ± 0.004
Wool	Helly Hansen	White	1.312 ± 0.004

*Determined by displacement of ethanol at 18,5 °C. n=2

3.2   Chemical analysis

3.2.1   HPLC-UV analysis

Analysis using liquid chromatography was done by using high performance liquid chromatography (HPLC) with ultraviolet detection (UV was accomplished using Agilent series 1200. For samples analysed in the initial stages of the period, a diode array detector (Agilent 1260 Infinity II DAD) was used, but later swapped out with a variable wavelength detector (Agilent 1260 Infinity VWD). Detection wavelength for phenanthrene, 1-methylphenanthrene and 9-phenanthrol was 250 nm, while the detection wavelength for fluoranthene was 230 nm. The mobile phase consisted of 70 % acetonitrile and 30 % MilliQ-water at a flow rate of 1,5 mL/minute for phenanthrene, 1-methylphenanthrene and fluoranthene. The mobile phase for 9-phenanthrol was 60 % acetonitrile and 40 % MilliQ-water with a flow rate of 1,5 mL/minute. Retention time for phenanthrene was 1,3 minutes, for 1-methylphenanthrene and fluoranthene was 2,3 minutes and 9-phenanthrol was 0,8 minutes. The analysis data was processed using Chemstation software.

3.2.1.1 Quantification of HPLC-UV data

Calibration using a calibration curve of known concentrations analytes was used for quantification. Initial eight-point calibration was done in order to confirm the linearity of the calibration curve (0,0005 µg/mL, 0,001 µg/mL, 0,005 µg/mL, 0,01 µg/mL, 0,05 µg/mL, 0,1 µg/mL, 0,5 µg/mL and 1 µg/mL PAHs in MeOH and seawater/freshwater). After initial trials for the kinetics experiments, more precise calibration curves were made for each individual PAHs (see Table B 1 in Appendix B). Calibration solutions were prepared freshly before each analysis every day, by dilution of stock solutions in methanol into seawater/freshwater using Eppendorf pipettes.

For quantification of concentration using external calibration, the slope and intercept of the calibration curve is necessary.

$$C_a = \frac{A - Intercept}{Slope} * 1000$$

Ca is the concentration of the analyte, *A* is the area of the analyte peak in the chromatogram, Intercept is the y-axis interception between the calibration curve and the y-axis and Slope is the slope of the calibration curve.

3.2.2 GC-MS analysis

In cases where PAHs concentration were too low to detect in HPLC-UV, extracts if of water samples were analysed with GC-MS. The extracts were extracted using liquid-liquid extraction.

3.2.2.1 Extraction procedure of water samples for GC-MS analysis

For the lowest concentration in the isotherms for phenanthrene in 5 °C, extraction was necessary as concentrations were too low to accurately be determined in the HPLC-UV. The samples in Kimax® tubes (12 mL) were added SIS-A703 surrogate internal standard (100 µL) and a 50/50 mixture of DCM and hexane (1 mL) and capped with a Teflon lined screw cap. The tubes were then vortexed for 30 seconds with an IKA MS 3 basic vortex

and centrifuged for two minutes with a 5804 R Centrifuge set to 2000 rpm and 20 °C.

The organic phase was transferred to Kimax® tubes, with baked sodium sulphate already added to it, using glass pipettes while avoiding transfer of water. After transfer, 1 mL of the 50/50 mixture of DCM and hexane were added again to the original Kimax® tube, but vortexed for 5 second and then centrifuged for 2 minutes at 2000 rpm. This step was done twice. The organic extract in the new Kimax® tubes could be stored in a fridge.

The organic extract in the Kimax® tubes were centrifuged with the salt, then transferred to conical tubes. In order to minimise transfer of water, a drying unit was prepared consisting of a glass pipette with Bilsom cotton added to it and baked sodium sulphate added on top of the Bilsom cotton. The organic extracts were filtered through the glass pipettes and transferred to the conical tubes. The sodium sulphate in the Kimax® tube were three times rinsed with DCM (~0,5 mL) with assistance from a short vortex, and the DCM was transferred to the conical tube.

The combined organic phases (three extractions) were concentrated to 100 µL using a SBH13OD/3 block heater, at 40 °C, under a gentle flow of N2 gas. The concentrated samples were transferred to GC vials, and the conical tubes were rinsed with DCM three times and the DCM was transferred to the GC vial. The volume in the GC vial was adjusted to 300 µL and added RIS-A705 recovery internal standard. The samples were now ready for GC-MS analysis.

Two laboratory blanks were included, which were treated the same way as the real samples.

Table 3-2 shows standard content and their respective concentrations concentration of the SIS-A703 and RIS-A705 standards.

Table 3-2 Chemical content and concentrations for compounds in SIS-A703 and RIS-A-705 surrogate and recovery standards.

	Chemical	Concentration (μg/mL)	Standard ID	Chemical	Concentration (μg/mL)
SIS-A703	Napthalene-*d*8	25,1	RIS-A705	Acenaptene-*d*10	1,6
	Phenanthrene-*d*10	5,00		Fluorene-*d*10	9,84
	Perylene-*d*12	5,08			
	Chrysene-*d*12	4,86			

3.2.3 GC-MS analysis

Chromatographic separation was achieved using an Agilent 7890A GC equipped with a DB5-MS ultra-inert column (30 m long, 0,25 μm film thickness and 0,25 mm i.d.). The GC was coupled with an Agilent 5975 C Mass Selective Detector (MSD). The carrier gas for the analysis was helium at a constant flow of 1 mL/min. Samples were injected at 1 μL in pulsed splitless mode. The inlet was set to 250 °C, the transfer line to 300 °C, the ion source to 230 °C and the quadrupole to 150 °C. The instrument was operated in selected ion monitoring (SIM) mode, and compounds were identified and quantified by the area of their molecular ion.

Chemstation was used to record and integrate the chromatograms.

3.2.4 Quantification of samples from GC-MS analysis

Concentration of analytes using GC-MS was done using internal standard method. For the GC-MS data an eight-point calibration was performed (0,001 μg/mL, 0,01 μg/mL, 0,025 μg/mL, 0,05 μg/mL, 0,10 μg/mL, 0,5 μg/mL, 1,0 μg/mL and 2,5 μg/mL). The standards for calibration were prepared using a stock solution containing a mix of the three chemicals (PAH mix), SIS A681- standard (100 μL) and RIS A690- standard (100 μL).

In order to quantify the concentration of analytes using the internal standard method, the relative response factor (RRF) must be calculated.

$$RRF = \frac{A_{std} * C_{rec}}{A_{rec} * C_{std}}$$

A_{std} is the area of the quantification ion in the internal standard, A_{rec} is the area of the recovery internal standard, C_{std} is the concentration of target chemical in the internal standard and C_{rec} is the concentration of the target chemical in the recovery standard.

The concentration of the analytes C_a can be decided can be decided with the RRF value.

$$C_a = \frac{A * C_{rec}}{V_a * RRF_i * REC}$$

Where C_a is the concentration of the analyte, A is the area of the analyte peak in the chromatogram, C_{rec} is the concentration of the target chemical in the recovery standard, V_a is the sample volume, RRF_i is the average RRF for the analyte and REC is the calculated percentage recovery of the internal standard.

3.3   Preparation of fibres, PAHs and media

3.3.1   Preparation of fibres

Fibres of synthetic (black and white polyester, blue polyacrylonitrile and white polyamide) and wool yarns were prepared at approximately 5 mm in length. Individual fibres were twirled around a spool consisting of two rods for easy removal of twirled fibre (Cole, 2016). The fibre was then removed from the spool and cut into 5 mm pieces using sharp scissors. The cut fibres were collected in a beaker filled with MilliQ-water to allow yarn filaments to separate into individual fibres. Water was removed from the fibres by vacuum filtration through a 0,45 µm Millipore filter. The fibres were collected

in 40 mL vials and put in a 40 °C oven until dry, which took two to three days depending on the amount of fibres cut.

3.3.2 Preparation of PAHs stock solutions

Calibration solutions for quantification using HPLC-UV was prepared by individually weighing and dissolving standards into 10 mL methanol, which were then transferred to 4 mL vials. These standards were stored in a freezer at -18 °C. For concentrations of each PAHs see Table 3-3. The stock solutions of PAHs were further diluted to 100 µg/mL, 10 µg/mL, 1 µg/mL, 0,1 µg/mL and 0,01 µg/mL which were stored in GC vials with screw caps. The diluted stock solutions were used to create calibration curves for HPLC-UV analysis.

Preparation of PAHs for dissolution into seawater and freshwater media was done by weighing dissolving PAHs standards into 10 mL DCM, which were then transferred to 4 mL vials. These solutions were stored in a freezer at 18 °C. For concentrations see Table 3-3. Due to extensive use, several stock solutions of phenanthrene in DCM had to be made, and the concentrations of each are given.

Table 3-3 Concentrations of PAHs in MeOH and DCM stock solutions.

	Concentration in MeOH (µg/mL)	Concentration in DCM (µg/mL)
PHE	1,066	4,949
		5,004
		4,997
1-MP	1,000	5,040
FLA	1,003	1,087
POH	1,062	5,020

3.4   Preparation of seawater and freshwater media

Seawater was collected from an in-house tap, which pumps seawater from the Trondheim fjord outside Trondheim harbour from a depth of 80 meters below the thermocline. The seawater was then sterile filtered using Sterivex cartridge filters (0,22 μm) before use. Filtered seawater was stored in at 4 °C until use.

Freshwater media was prepared according to the OECD guideline for preparation of TG 201 freshwater media.(Organisation for Economic Co-operation and Development., 2011) Deionised water was autoclaved in capped 2 L glass bottles, which were acclimatised to room temperature afterwards. In an empty autoclaved 2 L bottle, dissolved salt mixtures were added in order to achieve proper salinity. Content of the salt mixtures can be found in Appendix H. The content of the bottle was then volume adjusted to 2 L. Lastly the media in the bottles were pH adjusted to pH 8,1±0,1 by addition of HCl or NaOH.

3.5   Dissolving PAHs into seawater and freshwater media

In order to achieve maximum solubility of each PAHs in the media, a so-called "TeflonWAF" method was used (WAF: water accommodated fraction). PAHs stock solution dissolved in DCM were applied to Tetrafluoroethylene and ethylene polymer monofilament (Teflon grid) pads (4x8 cm) produced by FluortexTM, Sefar AG., in Heiden, Switzerland. Application was done using a 1000 μL syringe one drop at the time. For volumes of PAHs applied on the Teflon pads see Table 3-4. PAHs were applied in excess of theoretical solubility in the volume of media to ensure maximum dissolution. The Teflon pads were left to dry for 30 minutes in order to evaporate the DCM of the pads.

Table 3-4 Volume of PAHs dissolved in DCM applied to Teflon pads.

	PHE	1-MP	FLA	POH
Volume applied to Teflon pad for 10 L bottles (mL)	2,6	-	-	-
Volume applied to Teflon pad for 2 L bottles (mL)	0,6	0,2	1	0,6

After the Teflon pads had dried, they were transferred to bottom tap bottles filled with either seawater or freshwater. The media had beforehand been acclimated to the experimental before transferring the Teflon pads. The bottom tap bottles were placed on a magnet stirrer with a magnet in the bottles. The rotation speed of the magnets just slow enough that no visible vortex was observable on the liquid surface. Depending on experimental need, 2 L or 10 L solutions were prepared. On the first preparation of each solution, equilibrium times were investigated by daily sampling.

After equilibration, the Teflon pads were removed, and the bottles were left at stirring for an additional 15 minutes. The stock solutions of PAHs were transferred from the tap bottles using the taps into clean bottles (2L or 1L). The bottled stock solutions were then stored in the dark at the experimental temperature (either 4 °C, 10 °C or 20 °C).

3.6 Experimental procedure for sorption studies

The sorption of PAHs was prepared at different temperatures under simulated ocean movement using shaking tables with horizontal linear movement (motor speed 8 of 10, ~2-3 Hz per second). Experiments were conducted three different temperature (nominally 4 °C, 10 °C and 20 °C). The temperature was monitored using electronic calibrated thermometers throughout the sorption studies.

Experiments were conducted in order to establish equilibrium time and fibre concentration of PAHs on fibres. Equilibrium time was established when there was no difference in the percentage decrease of free PAHs concentration over time. Fibre concentrations had to be determined in order to be able to observe possible sorption. Sufficient fibre concentrations was determined when a minimum of 30 % decrease of free PAHs concentrations were observed. Characterisation of sorption at the initial hours after solution had been added to the fibres was also measured in order to get a better understanding of the sorption kinetics. From these samples, uptake of PAHs in fibres were calculated.

Samples were prepared in 40 mL vials for the kinetics studies and in 22 mL vials for the adsorption isotherm studies. Fibres for the kinetics and adsorption isotherm studies weighed directly into the vials, and the solutions were added at the start of each experiment. The accurate weight of fibres in the kinetics and adsorption isotherm studies can be found in Appendix C

Control samples (no fibres) were added in order to accommodate for possible degradation or wall adsorption. These samples were added to accommodate for potential adsorption of PAHs on the glass wall of the vials and possible degradation of PAHs

3.6.1 Determination of PAHs equilibrium time and appropriate fibre concentrations

The aim of this study was to establish equilibrium time and fibre concentration for PAHs and the fibres. Equilibrium time was achieved when the percentage decrease of PAHs didn't change over the sampling period. Three groups of experiments were necessary to determine these parameters for phenanthrene.

All experiments were conducted with PAHs concentrations at 50 % of solubility (diluting the stock solutions by freshwater or seawater). Sufficient sorption was determined when the free concentration of PAHs in the fibre

samples had decreased by a minimum of 30 % compared to the control samples without fibres. Free concentration of PAHs was analysed using HPLC-UV. Sampling points was done at after 1, 2, 3, 4, 7, 10 and 14 days had passed from when the samples had been prepared.

For 1-methylphenanthrene and fluoranthene only fibre concentration was determined at this stage. Equilibrium time was determined during kinetics studies for these compounds.

3.6.1.1 Determination of fibre concentrations and equilibrium times for phenanthrene

Initially, a set of experiments was conducted to determine appropriate fibre concentrations and equilibrium times between phenanthrene and fibres at different temperatures and salinity. Measured fibre concentrations can be found in Appendix C (Tables C 1-C 3)

Initial kinetics study for phenanthrene was done with all synthetic fibres and wool for seawater in 4 °C and 20 °C. Three control samples without fibres were added to account for possible loss of PAHs other than sorption. Samples were taken after day 1, 2, 3, 4, 7 and 10. Fibre concentrations were kept constant at the beginning. Fibre concentrations for this experiment is are listed in Table 3-5.

Table 3-5 Fibre concentrations for fibres used in uptake kinetics experiment 1 for phenanthrene

	PES-W (mg/L)	PES-B (mg/L)	PA (mg/L)	PAC (mg/L)	Wool (mg/L)
SW 4°C	100	100	100	100	100
SW 20 °C	100	100	100	100	100

Second group of kinetics study for phenanthrene was done with all synthetic fibres and wool for seawater in 4 °C, 10 °C and 20 °C and freshwater in 20

°C. The design of these experiments was conducted based on the initial determination of equilibrium time and fibre concentration experiment. Experiment solution for phenanthrene in freshwater was prepared with 100 % stock solution of phenanthrene. Concentrations were adjusted in order to assess sufficient fibre concentrations. Fibre concentrations for this experiment are listed in .

Table 3-6.

Table 3-6 Fibre concentrations for fibres used in uptake kinetics experiment 2 for phenanthrene

	PES-W (mg/L)	PES-B (mg/L)	PA (mg/L)	PAC (mg/L)	Wool (mg/L)
SW 4 °C	500	500	100	500	200
SW 10 °C	400	400	100	600	250
SW 20 °C	500	500	100	500	200
FW 20 °C	500	500	100	500	250

Third group of the kinetics study was done based on the observations from the second experiment for determination of equilibrium time and fibre concentration. Fibres concentrations were adjusted to give sufficient adsorption of phenanthrene. These experiments were able to run for a full 14-day period, and equilibrium times could be established. Fibre concentrations for this experiment is are listed in Table 3-7.

Table 3-7 Fibre concentrations for fibres used in uptake kinetics experiment 3 for phenanthrene

	PES-W (mg/L)	PES-B (mg/L)	PA-W (mg/L)	PAC-B (mg/L)	Wool (mg/L)
SW 4 °C	400	400	100	-	400
SW 10 °C	400	400	100	-	400
SW 20 °C	400	400	100	-	400
FW 20 °C	400	400	100	600	250

3.6.1.2 Determination of fibre concentrations for1-methylphenanthrene and fluoranthene

This experiment was done in order to determine sufficient fibre concentration for further kinetic and equilibrium time determination. Measured fibre weights can be found in Appendix C (Table 4) Black polyester was not used in the studies involving 1-methylphenanthrene and fluoranthene, as the two colours of polyester had already been investigated with phenanthrene. Samples in 40 mL vials were prepared at 100 mg/mL, 400 mg/mL and 800 mg/ml without replicates.

3.6.2 Sorption kinetics for PAHs and equilibrium time for 1-methylphenanthrene and fluoranthene

The aim of this study was to get a better understanding of sorption kinetics and determine rate constants and order of reaction. Additional sampling points was added at 2, 4 and 6 hours after the samples had been prepared. Sampling was later done the same way as in the first experiments for determination of equilibrium time and fibre concentrations. Sampling for 1-methylphenanthrene and fluoranthene was done in the full 14-day period with same sampling points as in uptake kinetics, while sampling for phenanthrene ended when the samples had reached equilibrium time that

was established for phenanthrene during initial kinetics experiments (1-3). The weight measured for each sample can be found in Appendix C (Tables C 5-C 6).

Preparation of samples were done the same way as in the experiments determination of equilibrium time and fibre concentrations for phenanthrene. Additional sampling points were after 2,4 and 6 hours after the experiment initialised. Experiment were stopped for each fibre after they had reached the equilibrium times established from the uptake kinetics study (see Table 4-5). Fibre concentrations is shown in Table 3-8.

Table 3-8 Fibre concentrations for fibres used in precision kinetics for phenanthrene

	PES-W (mg/L)	PES-B (mg/L)	PA-W (mg/L)	Wool (mg/L)
SW 4 °C	400	400	100	400
SW 10 °C	400	400	100	400
SW 20 °C	400	400	100	400
FW 20 °C	400	400	100	400

Sorption kinetics for 1-methylphenanthrene and fluoranthene was done to investigate early sorption rates of 1-methylphenanthrene and fluoranthene. Since equilibrium time had not been established for 1-methylphenanthrene and fluoranthene, these experiments were run for the 14-day period as in order to determine equilibrium times. Fibre concentrations are shown in Table 3-9.

Table 3-9 Fibre concentrations for fibres used in precision kinetics for 1-methylphenanthrene and fluoranthene

	PES-W (mg/L)	PA-W (mg/L)	PAC-B (mg/L)	Wool (mg/L)
1-MP	400	100	-	400
FLA	400	100	600	400

3.6.3 Adsorption isotherm study

Once equilibrium time and amount of sorbate had been established, isotherm studies for the microplastic fibres and the PAHs could be conducted. Sample solutions were prepared in seven levels of concentrations. Sample solutions for phenanthrene were prepared at 10 %, 25 %, 40 %, 55 %, 70 %, 85 % and 100 % of the maximum solubility stock solution. Sample solutions for 1-methylphenanthrene and fluoranthene were prepared at 40 %, 50 %, 60 %, 70%, 80, %, 90% and 100 % of the maximum solubility stock solution of each individual compound (the lower concentration were skipped due to lower solubility of these compounds).

Each sample for the isotherm study were made in 22 mL vials, with 20 mL PAHs solution and appropriate fibre amounts (see Appendix C, Table C 7 – C 12) in three replicates for each concentration. Fibre concentration that was used in the end were the same for all compounds under all the conditions and can be found in Table 4-4. The fibre concentration for each fibre established from the kinetics study were used for each isotherm at the specific conditions. The samples were left shaking for the longest equilibrium time among the fibres from each kinetic study in order to analyse everything the same day. Results from the kinetics study showed that PAHs were stable even after equilibrium time. Sampling was done after 7 days for phenanthrene in seawater at 5 °C and 10 °C and freshwater at 20 °C, after 10 days for seawater at 20 °C, after 2 days for fluoranthene in seawater at 20 °C and after 3 days for 1-methylphenanthrene in seawater at 20 °C.

Baked glass pipettes were used to take out an aliquot of sample from the vials. The glass pipettes were rinsed with the sample, before transferring the sample to GC-vials for HPLC analysis.

For the lowest concentration of the isotherm study of phenanthrene in seawater in 5 °C, an aliquot of 2 mL of the sample were transferred to Kimax tubes using Eppendorf pipettes. The samples were then added HCl (10 µL, 15 % solution in MilliQ-water) to lower the pH<2 for hindering bacterial growth.

3.7   Data and statistical treatment

Sorting of data, calculations and model fittings was done using Microsoft Excel (version 2018)

3.7.1   Standard deviation

Standard deviation was determined using the equation underneath.

$$s = \sqrt{\frac{1}{N-1} \sum_{i=1}^{N} (x_i - \bar{x})^2}$$

σ is the standard deviation of target analyte

x_i are the observed values for individual sample items

$\bar{x}$ is the mean value if the observations

N is the number of observations

When a value y was calculated using two different data x and z, expanded standard deviation was used.

$$s_y = y * \sqrt{\left(\frac{s_x}{z}\right)^2 + \left(\frac{s_z}{x}\right)^2}$$

s_x is the standard deviation for value x

s_z is the standard deviation for value z

x is the observed value from dataset 1

z is the observed value from dataset 2

3.7.2   Determining percentage decrease in free PAHs concentration

The percentage reduction of PAHs in the solution due to sorption was calculated using the equation shown below.

$$\%decrease = \frac{(\overline{C_{Ctrl}} - C_{free})}{\overline{C_{Ctrl}}} * 100\%$$

%decrease is the percentage reduction of free concentration in PAHs compared to control samples

$\overline{C_{Ctrl}}$ is the average concentration of PAH in the control sample (μg/mL)

C_{free} is the concentration of PAH in the aqueous phase (μg/mL)

3.7.3   Calculating amount of PAHs sorbed to microplastic fibres

The concentration of PAHs sorbed onto the microplastics fibres was determined using the equation shown below.

$$q = (\overline{C_{Ctrl}} - C_{free})\frac{V_s}{M}$$

q is the amount of PAHs in μg sorbed to the fibres in mg (μg/mg)

$\overline{C_{Ctrl}}$ is the average concentration of PAH in the control sample (μg/mL)

C_{free} is the concentration of PAH in the aqueous phase (μg/mL)

V_s is the sample volume

M is the mass of fibres in the sample

3.7.4   Fit of isotherms

Isotherm parameters and fitting of curves to experimental data were calculated using Microsoft Excel (2018) spreadsheets. Isotherm parameters were determined by minimising error functions across the studied

concentration ranges using "Solver" add on available for Microsoft Excel (Kumar et al., 2008). Three criteria were used to determine the best fitted isotherm: the coefficient of determination, the error function values and visual inspection. Visual inspection is necessary to see if there are any overfitting or bias fin fit toward certain concentration ranges. In general, the lowest error function value was determined for each dataset, and the error function values which gave the best R^2 or had the best visual was selected.

4 Results and discussion

4.1 Determination of solubility of PAHs

Equilibrium time for the dissolution of phenanthrene, 1-methylphenanthrene and fluoranthene are shown in Table 4-1. The solubility of phenanthrene in seawater (4 °C, 10 °C and 20 °C) and freshwater, 1-methylphenanthrene in seawater and fluoranthene in seawater are shown in Table 4-2. Concentrations of solutions of phenanthrene, 1-methylphenanthrene and fluoranthene are found in Appendix A. Finally, Table 4-3 shows literature values of phenanthrene, 1-methylphenanthrene and fluoranthene. The experimentally measured solubilities in the current study are very similar to those reported in the literature.

Table 4-1 Equilibrium time, in days, for phenanthrene, 1-methylphenanthrene and fluoranthene in seawater (SW) and freshwater (FW)

	PHE	1-MP	FLA
SW 20 °C	4	5	3
SW 10 °C	4	-	-
SW 5 °C	4	-	-
FW 20 °C	3	-	-

Table 4-2 Maximum solubility (µg/L) of phenanthrene (PHE), 1-methylphenanthrene (1-MP) and fluoranthene (FLA) in seawater (SW) and freshwater (FW).

	PHE	1-MP	FLA
SW 20 °C	697±10	123±1	106±6
SW 10 °C	353±3	-	-
SW 5 °C	309,7±1	-	-
FW 20 °C	1029±49	-	-

Table 4-3 Literature values of solubility (μg/L) of phenanthrene (PHE), 1-methylphenanthrene (1-MP) and fluoranthene (FLA) in seawater (SW) and freshwater (FW). [1] values retrieved from pubchem.ncbi.nlm.nih.gov

	PHE	1-MP	FLA
SW	600 (22 °C)[1]	>1000 (20 °C)[1]	120 (20 °C)[1]
FW	1100(22 °C)[1]	-	-

Preliminary studies with 9-phenanthrol showed reduction in concentration in seawater within few days. There was observed another peak on the chromatogram for 9-phenanthrol that increased in area as the 9-phenanthrol peak decreased. This could indicate degradation of 9-phenanthrol. Since the stock solutions of 9-phenanthrol could not be kept stable, experiments with 9-phenanthrol could not be completed.

4.2 Determination of fibre concentrations and equilibrium times

Calculated concentrations of PAHs are found in Appendix D. The aim of initial experiments was to determine the amount of fibres needed to significantly reduce the PAH concentrations in water. For calculated concentrations for the determination of fibre concentrations, see Appendix D. The first experiments were conducted in seawater at 5 °C and 20 °C with fibre concentrations of 100 mg/mL for all fibres. No significant difference was observed in the free concentration of phenanthrene in the sample solutions for polyester (white and black) and polyacrylonitrile. Wool samples had some reduction of free concentration of phenanthrene (~20 %), but this was determined to be insufficient to proceed with the planned sorption isotherm studies. Polyamide showed sufficient sorption with a >30 % reduction of freely dissolved phenanthrene compared with control samples. As a result, further studies with phenanthrene employed polyamide concentrations of 100 mg/mL, while the fibre concentrations for the polyesters (white and

black), polyacrylate and wool were increased, and the sorption level re-assessed.

Experiments done in seawater at 4 °C and 20 °C and in freshwater at 20 °C did not show any conclusive results. The experiment done in seawater at 10 °C showed sufficient sorption of phenanthrene for the polyesters (white and black) at fibre concentrations of 400 mg/mL. This lead to a reduction of the free concentration of phenanthrene of >30 % relative to the control samples. Polyester concentrations of 400 mg/mL were used for further study. The wool concentration was increased from 100 mg/mL to 250 mg/mL since it already showed some reduction of free concentration of phenanthrene from the first experiment (~27 %). No significant reduction of free concentration of phenanthrene relative to control samples was observed in samples with polyacrylate, even at concentrations as high as 600 mg/mL. As such, polyacrylate was not included in further studies.

The wool concentrations were adjusted from 250 mg/mL to 400 mg/mL for the samples in seawater at 4 °C, 10 °C and 20 °C, but not for freshwater at 20 °C in the third experiment. Sufficient reduction of free concentration of phenanthrene was observed for the samples with wool in seawater at 400 mg/mL relative to the controls. Sufficient reduction of free concentration of phenanthrene in samples with wool and freshwater was later confirmed during sorption kinetics experiments to be at 400 mg/mL. Figure 4-1 shows the reduction of free concentration of phenanthrene in seawater (4 °C, 10 °C and 20 °C) freshwater using the optimised amount of fibre.
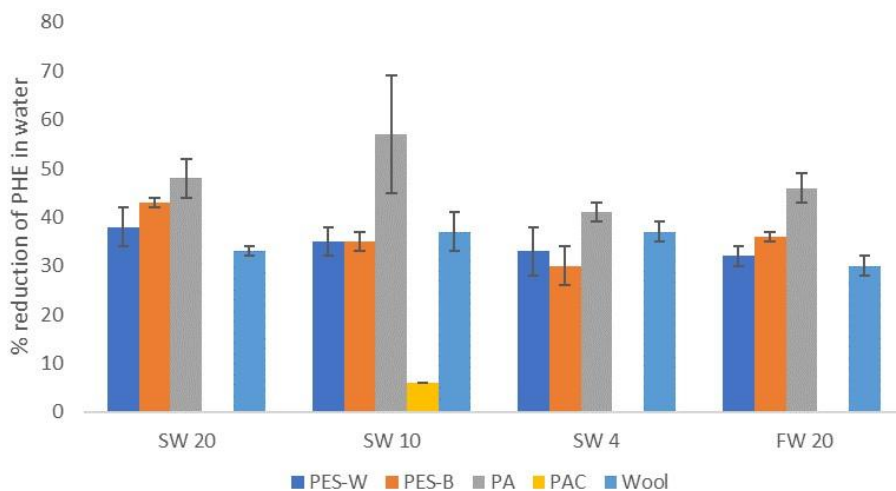
Figure 4-1 Percentage reduction of phenanthrene with fibres in seawater at 4 °C, 10 °C and 20 °C and in freshwater at 20 °C.

Fibre concentrations for 1-methylphenanthrene and fluoranthene were determined testing fibre concentrations of 100 mg/mL, 400 mg/mL and 800 mg/mL. These concentrations were selected based on the work done with phenanthrene, as it was more efficient to cover a bigger concentration range. Sufficient reduction of the free concentration of 1-methylphenanthrene and fluoranthene was observed at 400 mg/mL for polyester, 100 mg/mL for polyamide and 400 mg/mL for wool. No significant reduction of free 1-methylphenanthrene and fluoranthene concentrations was observed for polyacrylate. Table 4-4 summarises the optimised fibre concentrations for sorption of PAHs onto fibres.

Table 4-4 Optimised concentrations of fibres (mg/mL) for the sorption studies of PAHs.

	Concentration (mg/mL)
PES-W	400
PES-B	400
PA	100
Wool	400

4.3 Kinetics and equilibrium times

Once suitable fibre concentrations had been identified, the equilibrium times were determined. Equilibrium time was reached when the reduction of the free concentration of each PAH remained constant relative to the controls. Table 4-5 summarise the equilibrium times for the fibres in their different environments.

Table 4-5 Equilibrium time for PAHs and fibres determined from the kinetics study (d=days, h=hours)

	SW 20 °C PHE	SW 10 °C PHE	SW 4 °C PHE	FW 20 °C PHE	SW 20 °C 1-MP	SW 20 °C FLA
PES-W	10d	7d	7d	7d	3d	2d
PES-B	7d	7d	7d	7d	-	-
PA	2d	2d	7d	2d	3d	1d
PAC	-	-	-	-	-	-
Wool	2h	1d	2d	4h	4h	2h

Wool was the fibre to reach equilibrium quickest, with an equilibrium time of hours for studies done at 20 °C. Equilibrium time increased as temperature was decreased to 10 °C (1 day) and 4 °C for phenanthrene (2 days), which

indicates that sorption rates are temperature dependant. Polyamide had the second quickest equilibrium times. No significant differences in equilibrium time were observed for polyamide and phenanthrene in seawater at 20 °C and 10 °C (2 days), but a big increase to 7 days was observed at 4 °C. The opposite was observed for white polyester, where equilibrium time was longer at 20 °C in seawater. Equilibrium time for fluoranthene was in general shorter than for the other compounds. This is most likely because fluoranthene is more hydrophobic than the other compounds. Equilibrium time for 1-methylphenanthrene was higher for polyamide and wool, but lower for polyester in comparison with phenanthrene in seawater at 20 °C.

4.4   Sorption kinetics for PAHs

4.4.1   Determination of sorption kinetics for phenanthrene

Calculated concentrations of PAHs are found in Appendix E. Figure 4-2 shows the change in free concentrations of phenanthrene in seawater (4 °C, 10 °C and 20 °C) and in freshwater at 20 °C with time. The results show that early interactions between phenanthrene and the synthetic fibres were slower. The interaction between phenanthrene and wool was quick in comparison to synthetic fibres with equilibrium established within a few hours. (see also Table 4-5)
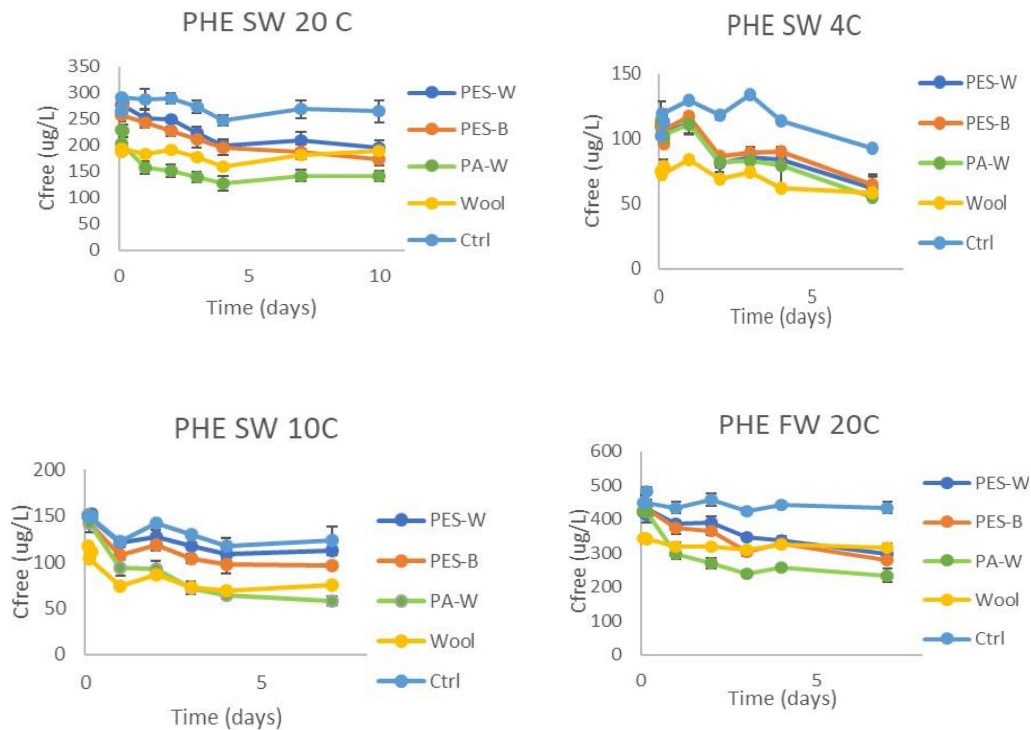
Figure 4-2 Change in free concentration (Cfree) of phenanthrene in solution with fibres till equilibrium time. The top left graph shows change in concentration of phenanthrene in seawater at 20 °C, the top right graph shows change in concentration of phenanthrene in seawater 4 °C, the bottom left graph shows change in concentration of phenanthrene in seawater at 10 °C and bottom left shows change in concentration of phenanthrene in freshwater at 20 °C.

The uptake of phenanthrene onto the fibres (µg/mg) in 50% solubility solutions was calculated and shown in Figure 4-3. Polyamide had much higher uptake of phenanthrene than the other fibres, despite having lower fibre concentrations in the samples at 100 mg/mL compared with 400 mg/mL for the polyesters (white and black) and wool. The polyesters and wool had similar uptake of phenanthrene per mass of fibre. Sorption of phenanthrene onto the fibres increased with both increasing temperature and decreasing salinity.
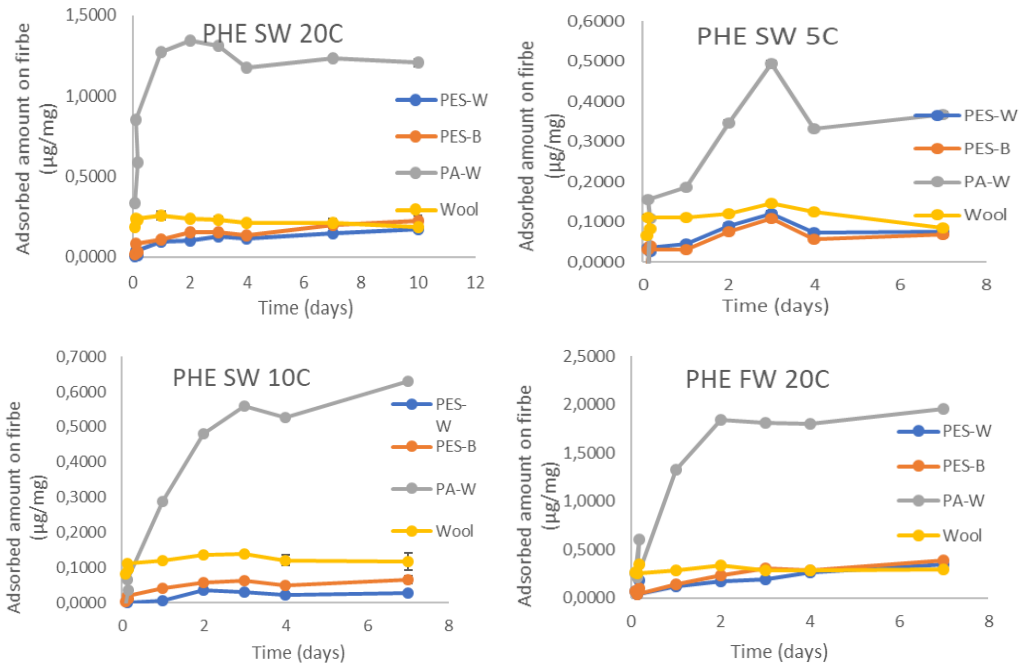
Figure 4-3 Uptake of phenanthrene on the fibres over time from the sorption kinetics experiments The top left graph shows the uptake of phenanthrene in seawater at 20 °C, the top right graph shows the uptake of phenanthrene in seawater 4 °C, the bottom left graph shows the uptake of phenanthrene in seawater at 10 °C and bottom left shows the uptake of phenanthrene in freshwater at 20 °C.

4.4.2 Determination of sorption kinetics for 1-methylphenanthrene and fluoranthene

Figure 4-4 shows the evolution of 1-methylphenanthrene concentration over time (left graph) and the corresponding percentage decrease of 1-methylphenanthrene (right graph). The results show that interactions between 1-methylphenanthrene and polyester is fastest and that interactions with polyamide and wool are slower. The interaction with wool was quick in comparison with the synthetic fibres, with equilibrium time established within a few hours (see Table 4-5).
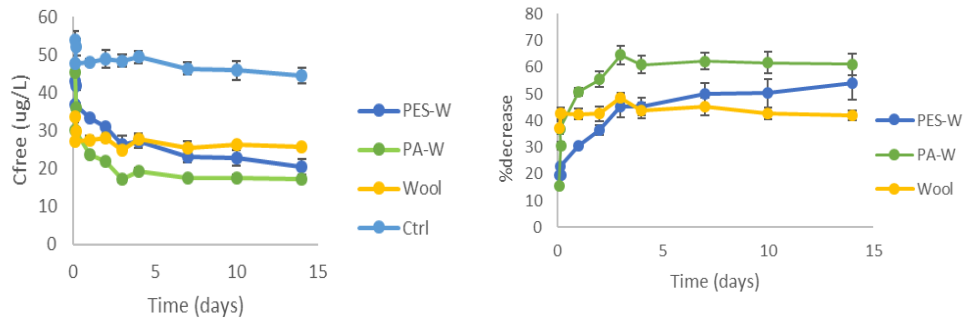
Figure 4-4 Precision kinetics for 1-methylphenanthrene. The left graph shows the change in free concentration (Cfree) of 1-MP over time, and the right graph shows the percentage decrease of 1-methylphenanthrene over time.

Figure 4-5 shows the uptake of 1-methylphenanthrene on the fibres (µg/mg) over time. Polyamide have higher adsorption of 1-methylphenanthrene than polyester and wool, which had similar uptake concentrations on the fibres.
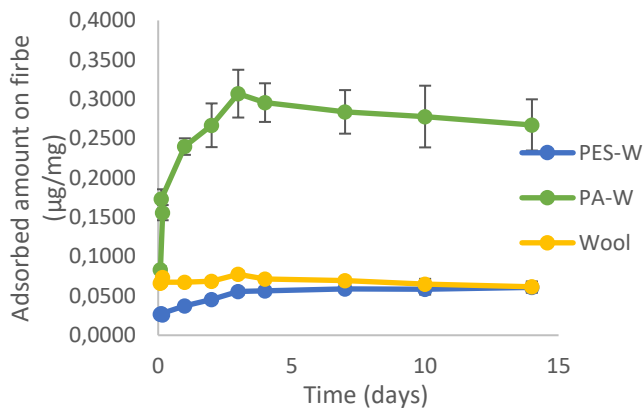
Figure 4-5 Uptake of 1-methylphenanthrene on fibres over time.

Figure 4-6 shows the change in free concentration of fluoranthene (left graph) and the corresponding percentage decrease of fluoranthene (right graph). Interactions with wool was quick in comparison with the synthetic fibres, with equilibrium time established within a few hours (see Table 4-5).
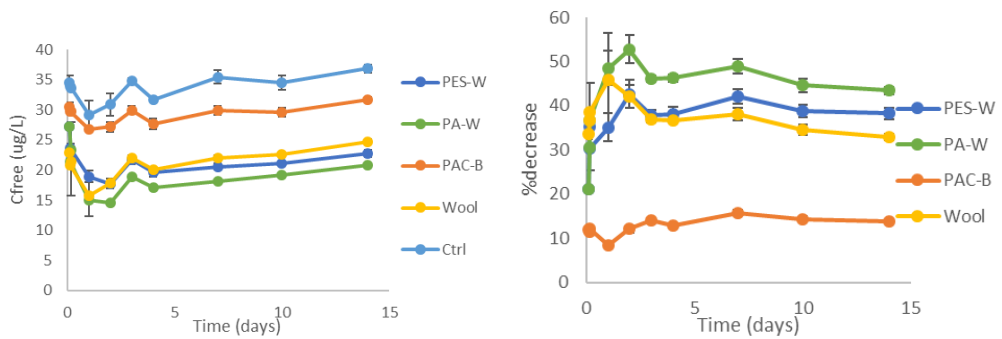
Figure 4-6 The left graph shows the change in free concentration (Cfree) of fluoranthene over time, and the right graph shows the percentage decrease of fluoranthene over time.

Figure 4-7 shows the uptake of 1-methylphenanthrene on the fibres (µg/mg) over time. Polyamide had much higher uptake of fluoranthene than the other fibres. Polyester and wool show similar amounts of adsorption. Polyacrylonitrile show little uptake of fluoranthene at high fibre concentrations.
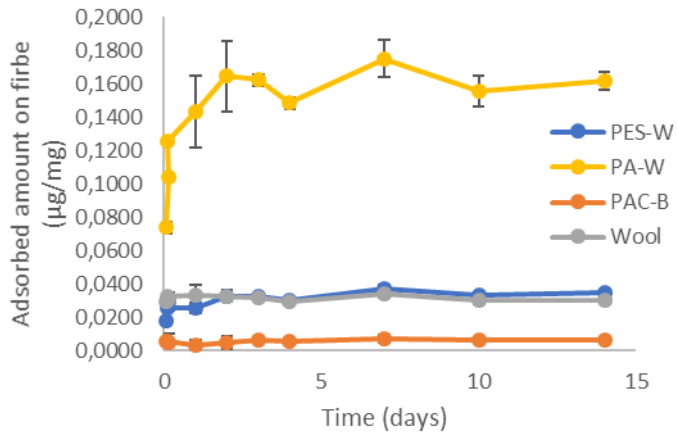
Figure 4-7 Uptake of FLA on fibres over time.

4.4.3 Summary of sorption equilibrium results

Polyamide had the highest amount of sorption of PAHs with exception of 1-methylphenanthrene. Polyamide was present in the samples at fibre concentrations (100 mg/mL) lower than polyester (400mg/mL) and wool (400 mg/mL), which indicates stronger interactions between polyamide and the PAHs phenanthrene and fluoranthene. Polyester and wool had similar sorption amount of PAHs onto the fibres. Wool had quicker equilibrium time than the synthetic fibres (see Table 4-5), with equilibrium achieved within a few hours. Polyamide had the second quickest equilibrium times and polyester was the slowest to reach equilibrium time. Decreased salinity gave increased sorption of phenanthrene onto fibres, while increasing temperature gave increased sorption of phenanthrene onto fibres.

It is expected that sorption of PAHs on solid decreases as temperature increases due to the increased solubility of the PAHs in the solutions (Lamichhane et al., 2016). In this study, the opposite was observed, where increasing temperature gave increasing sorption. The same observations have been found in a study done with naphthalene, acenaphthylene and phenanthrene from wastewater, which found higher sorption in higher temperatures (Balati et al., 2015). Higher sorption capacity could be expected for the compounds whose solubility decreases with temperature (Kipling, 1965). The effect of temperature on sorption capacity could be a combined contribution of both sorption and solubility, meaning that the properties of the solids has to be taken into account (Lamichhane et al., 2016). Multi-layered interactions between phenanthrene and the fibres could also occur.

It should be expected that the sorption of phenanthrene onto fibres in seawater should be higher than in freshwater. Inorganic ions bind water molecules into tight hydration shells, reducing the water concentration of phenanthrene (Lamichhane et al., 2016). The solubility of phenanthrene in freshwater is also higher (see Table 4-2) than in seawater. Little literature is

available explaining this, but as with the effect of temperature, increased sorption at lower salinity could be explained as a combined contribution of solubility and sorption onto the solids.

1-methylphenanthrene and fluoranthene had shorter equilibrium time with polyester than phenanthrene. This consistent with their respective solubilities in water (see Table 4-2), where phenanthrene would be more susceptible for sorption onto hydrophobic surfaces. It was observed that uptake of phenanthrene, 1-methylphenanthrene and fluoranthene onto polyamide was much higher than polyester and wool. This indicates strong interactions between polyamide and the PAHs. No differences were observed in the equilibrium times of 1-methylphenanthrene and fluoranthene on wool.

Polyacrylonitrile was tested for sorption at concentrations up to 800 mg/mL for fluoranthene but was discontinued for further studies as insufficient sorption occurred relative to control samples.

4.4.4   Determination of order of reaction

Order of reaction and rate constants for the sorption process of PAHs onto fibres could not be properly calculated due to there being too few sampling points during the equilibrium period which result in uncertainties in the eligibility of the fitting into the pseudo first order and pseudo second order equations. Additionally, the sampling points are quite spread out during the sampling period, which won't accommodate for change in sorption processes during the sorption period. To better determine the order of reaction and rate constants, more sampling points would be necessary during the equilibrium time.

4.5   Adsorption isotherms

For calculated concentrations from the adsorption isotherm studies, see Appendix F. All calculated parameters for isotherm fitting can be found in Appendix G. Fitted isotherm graphs are added as a supplementary to this master thesis.

The experimental data was fitted with the isotherm models, with the error function, R^2 value and visual inspection as the criteria to determine most suitable isotherm model. The Redlich-Peterson, Sips and Dubinin-Astakov models gave the best fit to the experimental data after evaluating all the fit criteria's. The Redlich-Peterson and Sips models are similar in that they are both a combination of the Langmuir and the Freundlich models. This combination results in better fits at higher and lower concentrations than Langmuir and Freundlich separately. Dubinin-Astakov has been found to describe adsorption into pores with good success (Inglezakis, 2007).

Optimizing isotherms by use of the sum of square errors (SSE) gave better calculated data that was closer to the experimental data when compared with the mean weighed square error (MWSE) and sum of absolute errors (SAE) error functions. This was true in all cases with the exception of 1-methylphenanthrene and wool, which had the MWSE as the most suitable error function. In this case MWSE gave higher R^2 values than all the other calculations and had very good visual fit between experimental and calculated data. Visually, the graphs retrieved using the mean weighed square error gave poorer fits with the experimental data. The SAE function gave a similar fit as SSE in many cases, but generally produced fitted data with worse R^2 values. As a result, it was chosen to focus on the data calculated using the SSE error function. Calculated parameters fitted with SSE can be found in Tables 4-6 – 4-9.

Table 4-6 Calculated parameters of the adsorption isotherms for phenanthrene (PHE), 1-methylphenanthrene (1-MP) and fluoranthene (FLA) fitted with SSE for modelling of adsorption on white polyester fibres

Langmuir	Q	K_L		R^2	SSE
PHE SW 20 °C	0,546535	0,005973		0,762185	0,123763
PHE SW 10 °C	0,289517	0,02202		0,725041	0,044068
PHE SW 4 °C	0,465437	0,005402		0,941067	0,005017
PHE FW 20 °C	0,982551	0,002664		0,852963	0,114761
1-MP SW 20 °C	0,001544	0,972942		0,510783	2,89E-06
FLA SW 20 °C	0,103065	0,075514		0,578435	0,003395

Freundlich	K_f	1/n		R^2	SSE
PHE SW 20 °C	0,023197	0,469184		0,744102	0,136438
PHE SW 10 °C	0,036948	0,35072		0,663256	0,058967
PHE SW 4 °C	0,00651	0,696324		0,941425	0,004981
PHE FW 20 °C	0,013267	0,604738		0,833165	0,133332
1-MP SW 20 °C	8,31E-05	0,797088		0,723426	1,15E-06
FLA SW 20 °C	0,029561	0,257609		0,558544	0,003682

Redlich-Peterson	K_r	a_r	g	R^2	SSE
PHE SW 20 °C	0,002038	2,38E-05	1,791033	0,768294	0,119689
PHE SW 10 °C	0,00342	5,39E-05	1,983219	0,837137	0,022607
PHE SW 4 °C	0,147323	21,97789	0,30763	0,897717	0,011034
PHE FW 20 °C	0,002155	0,000121	1,440224	0,86296	0,10571
1-MP SW 20 °C	0,001935	10,3161	0,418192	0,701711	1,28E-06
FLA SW 20 °C	0,003229	5,9E-05	2,495008	0,684208	0,002151

Sips	Q_s	K_s	B_s	R^2	SSE
PHE SW 20 °C	0,490107	1,183229	0,00305	0,763198	0,123078
PHE SW 10 °C	0,235201	2,579774	9,11E-05	0,783724	0,032047
PHE SW 4 °C	0,936119	0,813731	0,00493	0,897171	0,011101
PHE FW 20 °C	0,755513	1,318968	0,000782	0,857152	0,110943
1-MP SW 20 °C	0,004308	1,257159	0,00566	0,728483	1,12E-06
FLA SW 20 °C	0,081784	5,936402	2,4E-08	0,68475	0,002147

Dubinin-Astakov	Q^0	b	E	R^2	SSE
PHE SW 20 °C	0,414962	1,837174	8,964517	0,765024	0,121835
PHE SW 10 °C	0,233248	3,956298	7,272893	0,786588	0,031506
PHE SW 4 °C	0,321978	1,11278	7,705199	0,941736	0,004954
PHE FW 20 °C	0,626614	1,890982	7,966617	0,858845	0,10941
1-MP SW 20 °C	0,003119	1,03268	8,212635	0,709815	1,23E-06
FLA SW 20 °C	0,081464	10,23174	4,513673	0,691439	0,002079

Dubinin-Raduskevich	q_s	k_{ad}		R^2	SSE
PHE SW 20 °C	0,390563	1128,448		0,736738	0,142632
PHE SW 10 °C	0,235172	148,8839		0,77469	0,033777
PHE SW 4 °C	0,197595	289,1098		0,883402	0,010635
PHE FW 20 °C	0,555162	2362,651		0,79936	0,168375
1-MP SW 20 °C	0,001505	1,004155		0,503095	2,98E-06
FLA SW 20 °C	0,089083	36,62545		0,616073	0,002903

Table 4-7 Calculated parameters of the adsorption isotherms for phenanthrene (PHE) fitted with SSE for modelling of adsorption on black polyester fibres.

Langmuir	Q	K_L		R^2	SSE
PHE SW 20 °C	10,09666	0,000199		0,8894	0,125998
PHE SW 10 °C	0,982551	0,002664		0,852963	0,114761
PHE SW 4 °C	0,465437	0,005402		0,941067	0,005017
PHE FW 20 °C	0,001544	0,972942		0,510783	2,89E-06
Freundlich	K_f	1/n		R^2	SSE
PHE SW 20 °C	0,003561	0,888471		0,892626	0,121688
PHE SW 10 °C	0,013267	0,604738		0,833165	0,133332
PHE SW 4 °C	0,00651	0,696324		0,941425	0,004981
PHE FW 20 °C	8,31E-05	0,797088		0,723426	1,15E-06
Redlich-Peterson	K_r	a_r	g	R^2	SSE
PHE SW 20 °C	0,018227	4,306968	0,122712	0,768294	0,119689
PHE SW 10 °C	0,002155	0,000121	1,440224	0,86296	0,10571
PHE SW 4 °C	0,147323	21,97789	0,30763	0,897717	0,011034
PHE FW 20 °C	0,001935	10,3161	0,418192	0,701711	1,28E-06
Sips	Q_s	K_s	B_s	R^2	SSE
PHE SW 20 °C	580,3927	0,888963	6,12E-06	0,763198	0,123078
PHE SW 10 °C	0,755513	1,318968	0,000782	0,857152	0,110943
PHE SW 4 °C	0,936119	0,813731	0,00493	0,897171	0,011101
PHE FW 20 °C	0,004308	1,257159	0,00566	0,728483	1,12E-06
Dubinin-Astakov	Q^0	b	E	R^2	SSE
PHE SW 20 °C	78,25252	0,212015	0,055492	0,913107	0,096239
PHE SW 10 °C	0,626614	1,890982	7,966617	0,858845	0,10941
PHE SW 4 °C	0,321978	1,11278	7,705199	0,941736	0,004954
PHE FW 20 °C	0,003119	1,03268	8,212635	0,709815	1,23E-06
Dubinin-Raduskevich	q_s	k_{ad}		R^2	SSE
PHE SW 20 °C	0,077124	5000		0,661635	0,698796
PHE SW 10 °C	0,555162	2362,651		0,79936	0,168375
PHE SW 4 °C	0,197595	289,1098		0,883402	0,010635
PHE FW 20 °C	0,001505	1,004155		0,503095	2,98E-06

Table 4-8 Calculated parameters of the adsorption isotherms fitted for phenanthrene (PHE), 1-methylphenanthrene (1-MP) and fluoranthene (FLA)with SSE for modelling of adsorption on polyamide fibres.

Langmuir	Q	K_L		R^2	SSE
PHE SW 20 °C	294,7366	4,02E-05		0,93445	1,842303
PHE SW 10 °C	2,146745	0,015499		0,798563	,279326
PHE SW 4 °C	0,59802	0,00734		0,949456	0,008326
PHE FW 20 °C	9,778431	0,000944		0,91037	2,006862
1-MP SW 20 °C	52,75523	6,77E-06		0,759498	4,36E-05
FLA SW 20 °C	1056,872	2,72E-05		0,82225	0,074503
Freundlich	**K_f**	**1/n**		**R^2**	**SSE**
PHE SW 20 °C	0,009979	1,030206		0,93507	1,82406
PHE SW 10 °C	0,009367	0,717844		0,938044	0,010332
PHE SW 4 °C	0,147319	0,462748		0,736759	1,810808
PHE FW 20 °C	0,023818	0,786593		0,910396	2,006089
1-MP SW 20 °C	1,65E-05	1,948894		0,902185	1,49E-05
FLA SW 20 °C	0,009335	1,38981		0,869024	0,051826
Redlich-Peterson	**K_r**	**a_r**	**g**	**R^2**	**SSE**
PHE SW 20 °C	0,066504	4,654956	0	0,934807	1,831522
PHE SW 10 °C	0,019229	3,52E-07	2,942744	0,944293	0,299619
PHE SW 4 °C	0,003552	3,8E-05	2,003956	0,958863	0,00671
PHE FW 20 °C	0,0132	0,055071	0,48119	0,910562	2,002005
1-MP SW 20 °C	0,001304	2,650482	0	0,75956	4,36E-05
FLA SW 20 °C	0,032983	0,14781	0	0,822349	0,074452
Sips	**Q_s**	**K_s**	**B_s**	**R^2**	**SSE**
PHE SW 20 °C	13,02992	1,249516	0,000296	0,927948	2,041502
PHE SW 10 °C	1,538748	2,576846	7,36E-05	0,867895	0,7711
PHE SW 4 °C	0,311673	1,955425	0,000548	0,960498	0,006437
PHE FW 20 °C	17,51932	0,888592	0,000875	0,910799	1,996184
1-MP SW 20 °C	0,016705	4,391232	8,74E-07	0,913947	1,291E-05
FLA SW 20 °C	0,707296	5,432833	5,42E-07	0,945311	0,019893
Dubinin-Astakov	**Q^0**	**b**	**E**	**R^2**	**SSE**
PHE SW 20 °C	172,5232	0,329211	0,441934	0,947106	1,466581
PHE SW 10 °C	1,518697	3,834039	7,094462	0,868023	0,770163
PHE SW 4 °C	0,290061	3,005265	6,776541	0,958279	0,006818
PHE FW 20 °C	4,849839	1,123065	7,242724	0,910813	1,995834
1-MP SW 20 °C	0,017742	4,676485	4,720619	0,91387	1,3E-05
FLA SW 20 °C	0,717207	8,19486	5,509147	0,94278	0,020869
Dubinin-Raduskevich	**q_s**	**k_{ad}**		**R^2**	**SSE**
PHE SW 20 °C	3,616088	2227,314		0,83866	5,128032
PHE SW 10 °C	1,546044	191,5401		0,850109	0,894442
PHE SW 4 °C	0,278611	212,1289		0,948255	0,008554
PHE FW 20 °C	3,122118	3800,801		0,813887	4,713711
1-MP SW 20 °C	0,024561	124,8326		0,913569	1,3E-05
FLA SW 20 °C	1,061002	44,82385		0,924048	0,028262

Table 4-9 Calculated parameters of the adsorption isotherms fitted for phenanthrene (PHE), 1-methylphenanthrene (1-MP) and fluoranthene (FLA)with SSE for modelling of adsorption on wool fibres.

Langmuir	Q	K_L	Wool	R^2	SSE
PHE SW 20 °C	3,992706	0,000323		0,885242	0,079582
PHE SW 10 °C	0,364009	0,009318		0,665574	0,098002
PHE SW 4 °C	0,640456	0,00426		0,898796	0,01314
PHE FW 20 °C	1,646576	0,000769		0,824844	0,120211
1-MP SW 20 °C	0,007559	0,007644		0,794914	1,12E-06
FLA SW 20 °C	121,1396	2,91E-05		0,848348	0,002451
Freundlich	K_f	1/n		R^2	SSE
PHE SW 20 °C	0,001501	0,955262		0,883831	0,080676
PHE SW 10 °C	0,017035	0,495796		0,631094	0,11392
PHE SW 4 °C	0,005391	0,772502		0,886813	0,014895
PHE FW 20 °C	0,002661	0,828695		0,818267	0,125717
1-MP SW 20 °C	1,17E-05	1,369611		0,908948	4,34E-07
FLA SW 20 °C	0,001694	1,217681		0,866839	0,002104
Redlich-Peterson	K_r	a_r	g	R^2	SSE
PHE SW 20 °C	0,001245	9,81E-08	2,284049	0,888121	0,07735
PHE SW 10 °C	0,002255	7,05E-07	2,631309	0,7637	0,061754
PHE SW 4 °C	0,002292	4,7E-08	3,233433	0,930815	0,008683
PHE FW 20 °C	0,007557	2,090889	0,199787	0,818481	0,125537
1-MP SW 20 °C	0,000638	13,20361	0	0,859865	7,08E-07
FLA SW 20 °C	0,013222	2,753591	0	0,848472	0,002449
Sips	Q_s	K_s	B_s	R^2	SSE
PHE SW 20 °C	0,974691	1,456486	0,000146	0,8898	0,07602
PHE SW 10 °C	0,247672	3,528007	2,96E-07	0,723731	0,074457
PHE SW 4 °C	0,247931	2,761929	1,36E-05	0,936126	0,007984
PHE FW 20 °C	0,696153	1,712509	4,73E-05	0,83338	0,113212
1-MP SW 20 °C	0,008595	1,720849	0,000477	0,919333	3,8E-07
FLA SW 20 °C	0,132805	5,064045	1,84E-07	0,94323	0,000824
Dubinin-Astakov	Q^0	b	E	R^2	SSE
PHE SW 20 °C	0,621542	1,428111	5,691037	0,89003	0,075841
PHE SW 10 °C	0,244604	3,964596	5,169247	0,724976	0,074012
PHE SW 4 °C	0,24081	3,319675	5,669381	0,933366	0,008352
PHE FW 20 °C	0,574034	1,782733	6,137942	0,833234	0,113311
1-MP SW 20 °C	0,002476	4,503216	4,137671	0,960442	0,004192
FLA SW 20 °C	0,132326	6,288358	4,654498	0,94091	0,00086
Dubinin-Raduskevich	q_s	k_{ad}		R^2	SSE
PHE SW 20 °C	0,545381	5123,348		0,842624	0,115631
PHE SW 10 °C	0,250316	415,7932		0,922193	0,009883
PHE SW 4 °C	0,261325	596,5499		0,708777	0,080133
PHE FW 20 °C	0,552229	7805,698		0,803174	0,139929
1-MP SW 20 °C	0,003403	185,1825		0,954246	2,08E-07
FLA SW 20 °C	0,18333	91,19268		0,923545	0,001134

4.5.1 Adsorption isotherms for polyester

Modelled isotherms for white polyester (PES-W) are shown in Figure 4-8. For PES-W with phenanthrene in seawater at 20 °C, the best fitted isotherm was determined to be the Redlich-Peterson model. Visually this model had a better fit at higher concentrations, as well as the best R^2. The R^2 value was rather low (R^2=0,77) for this fitting. The spread of the isotherm data makes it difficult to assess the isotherm models effectively, but the Redlich-Peterson model had the lowest SSE value. The curve shows a L-curve shape, indicating that adsorption capacity had been reached at higher concentrations. Owing to the generally bad fitting of the isotherm models, it is hard to properly determine the adsorption mechanisms. The Freundlich, Sips and Dubinin-Astakov models gave similar R^2 values with the SSE as the Redlich-Peterson model, but the Redlich-Peterson model had better visual fitting at higher concentration ranges. Because of the low R^2 value, adsorption mechanisms could not be properly determined, but the best fitted models indicate that adsorption happens on a heterogenous surface seems to happen, most likely by layer-by-layer interaction, though pore filling mechanisms may be possible as predicted by the Dubinin-Astakov model.
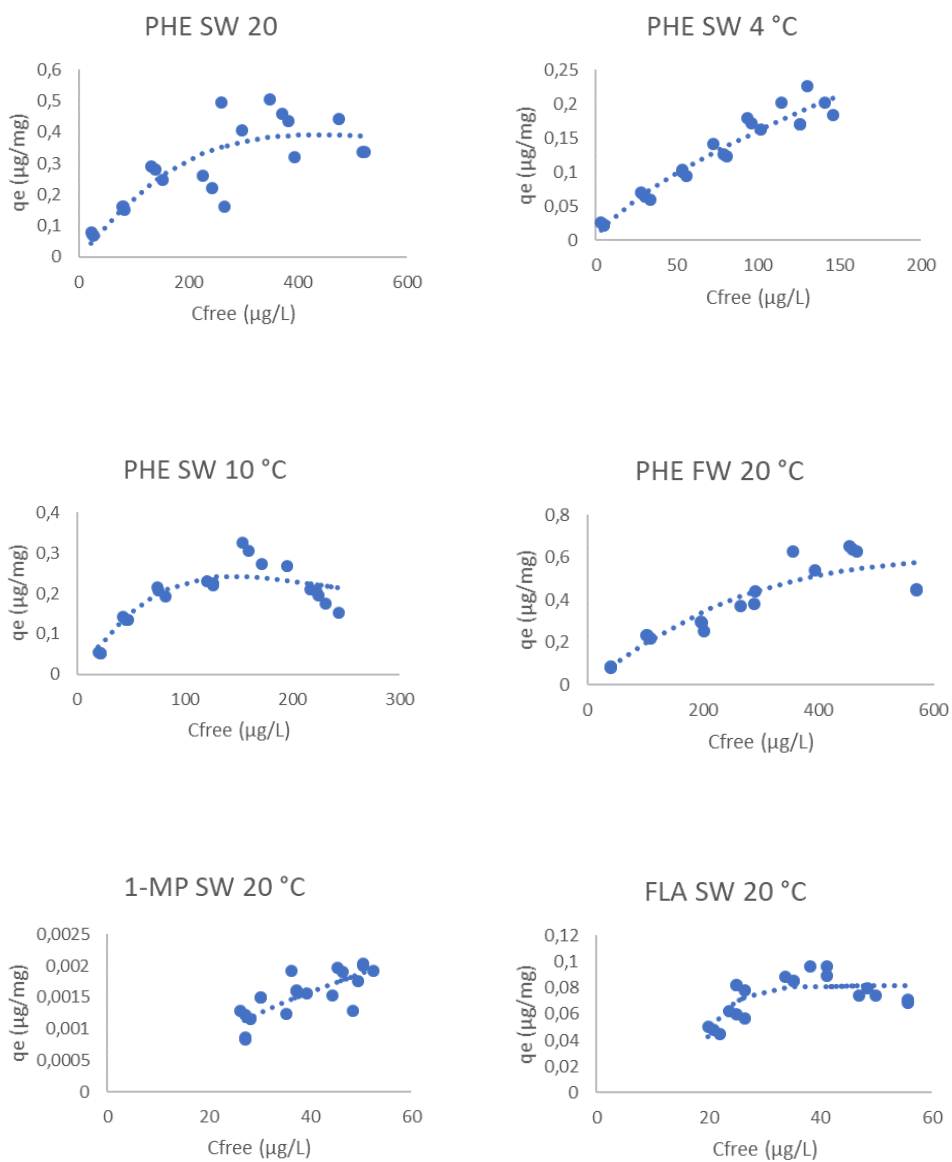
Figure 4-8 Best fitted isotherms for PAH sorption onto white polyester. The top left shows the Redlich-Peterson isotherm for phenanthrene (PHE) in seawater at 20 °C, top right shows Redlich-Peterson isotherm of PHE in seawater at 4 °C, middle left shows the Redlich-Peterson isotherm for PHE in seawater at 10 °C, middle right shows the Redlich-Peterson isotherm for PHE in freshwater at 20 °C, bottom left shows the Sips isotherm for 1-methylphenanthrene (1-MP) in seawater at 20 °C and bottom right shows the Dubinin-Astakov isotherm for fluoranthene (FLA) in seawater at 20 °C.

For adsorption of phenanthrene on PES-W at 4 °C in seawater, the Freundlich, Redlich-Peterson, Sips and Dubinin-Astakov models gave similar graphs with fitting parameters that were comparable to each other. For this data set, the Redlich-Peterson model was chosen based on its versatility among adsorption in fitting isotherms. It had the second lowest SSE and the second highest R^2 (R^2=0,898). The shape of the curve seems to be close to linear, but the curve flattens out at higher concentrations, indicating L-curve type shape and implying that the isotherm is reaching sorption capacity. The adsorption process happens on a heterogenous surface as predicted by the isotherm models. The Redlich-Peterson model predicts layer-by-layer type adsorption, but because the Dubinin-Astakov model gave similar fit, other adsorption mechanisms such as pore filling could also be occurring.

For adsorption of phenanthrene on PES-W at 10 °C in seawater, the Redlich-Peterson model gave the best fit of isotherms, with the highest R^2 values (R^2=0,83) and the lowest SSE value. The graph shows a L-curve type, indicating that sorption capacity has been reached. From the isotherm model, it can be predicted that adsorption occurs on a heterogenous surface on PES-W. The model also predicts that the main mode of sorption is layer-by-layer type of sorption.

For adsorption of phenanthrene on PES-W at 20 °C in freshwater, the Redlich-Peterson model also gave the best fit for the isotherm. The model gave best fit at higher concentrations among the other isotherm models, while also having the lowest SSE value. The graph shows L-curve type graph which indicates that there is a sorption capacity. From the isotherm model, it can be predicted that adsorption occurs on a heterogenous surface on PES-W. The model also predicts that the main mode of sorption is layer-by-layer type of sorption.

For adsorption of 1-methylphenanthrene on PES-W in seawater at 20 °C, the Sips model gave the best fit for the isotherms although the data was quite scattered and resulted in a rather low R^2 value (R^2=0,72). This model

also gave the lowest SSE value. Due to the generally poor fitting of data, it is hard to determine the shape of this isotherm, but the curvature indicates that it is reaching sorption capacity. It could be assumed that adsorption occurs onto a heterogenous surface based on the Sips model.

For adsorption of fluoranthene on PES-W in seawater at 20 °C, the Dubinin-Astakov model gave the best fitting of isotherms. The Redlich-Peterson and Sips models also gave similar fittings, but the Dubinin-Astakov seems to give a better fit. The data was quite scattered, which also gave a low R^2 value (R^2=0,69). As such, no definite conclusions could be drawn from this isotherm, although it could be assumed that adsorption onto a heterogenous surface is most likely to occur based on the models

Modelled isotherms for black polyester (PES-B) can be found in Figure 4-9. For PES-B at 20 °C in seawater, the Freundlich isotherm was chosen. It had good visual fit and the best and the second best R^2 value (R^2=0,89). The Dubinin-Astakov model had better R^2 value (R^2=0,91), but the data appeared to have been overfitted, which is apparent from the high Q^0 parameter calculated for this model and from a visual inspection of the graph. As such, the Freundlich model was chosen based on the best R^2 value, as it also had a relatively low SSE. The curve of the graph appears to be linear, which indicates C-curve type. This means that the number of sorption sites remains constant until the fibre has been saturated. This could also mean that other processes other than adsorption could be present, such as absorption.
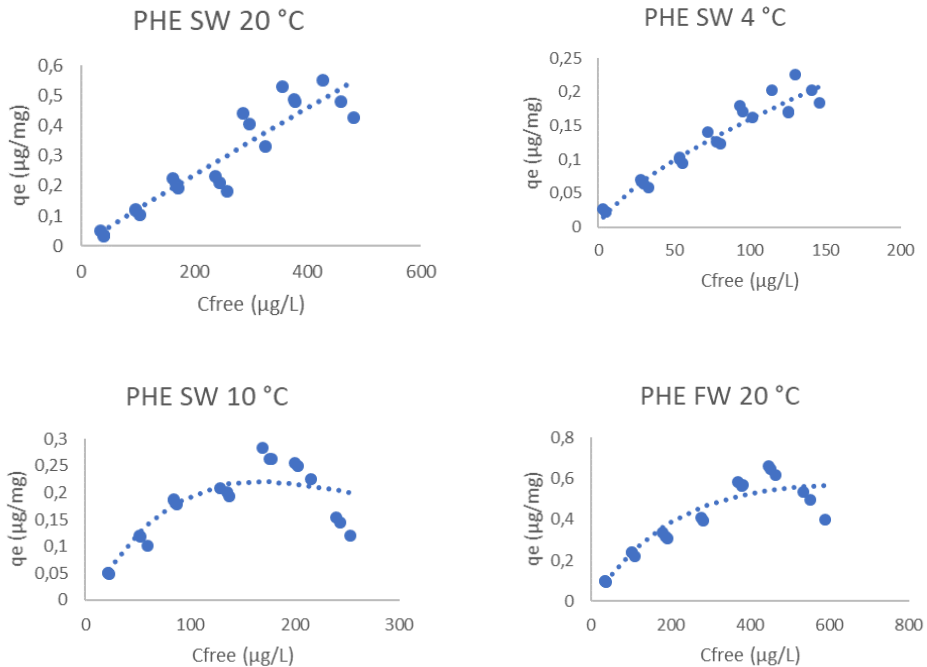
Figure 4-9 Best fitted isotherms for PES-B. The top left shows the Redlich-Peterson isotherm for phenanthrene in seawater at 20 °C, top right shows the Freundlich isotherm of phenanthrene in seawater at 4 °C, bottom left shows the Redlich-Peterson isotherm for phenanthrene in seawater at 10 °C and bottom right shows the Redlich-Peterson isotherm for phenanthrene in freshwater at 20 °C.

For PES-B at 4 °C in seawater, the best fitted isotherm is the Dubinin-Astakov, but the Freundlich isotherm also fitted quite well. The Redlich-Peterson and Sips models also had good fitting parameters and visual fitting. As a result, the Freundlich model was chosen to represent these conditions, due to its general description of adsorption onto a heterogenous surface. The shape of the graph is that of a L-curve, indicating it has reached sorption capacity.

For PES-B at 10 °C in seawater, the Redlich-Peterson model gave the best fit, with the highest R^2 value (R^2=0,84). Visually, this isotherm also curved better at higher concentrations. This implies that the adsorption is most likely

onto a heterogenous surface with a layer-by-layer mode of sorption. The shape of the isotherm is of L-shape, that is declining at higher concentration points. This indicates that sorption capacity had been reached.

For PES-B at 20 °C in freshwater, the Redlich-Peterson model was chosen. This model had the highest R^2 value (R^2=0,88), and better visual fitting towards the higher concentration areas. It had the second lowest SSE value, Dubinin-Astakov model gave the lowest, but the Redlich-Peterson model gave better R^2 and visual fitting towards higher concentrations. Based on the models, adsorption onto a heterogenous surface is more likely to occur. Since the Redlich-Peterson model gave better fit at higher concentrations, it can be assumed that the mode of sorption is layer-by-layer sorption with high Freundlich characteristics based on the low *g* parameter calculated from the model (*g*=0,34). The shape of the curve is that of a L-curve, indicating a definite sorption capacity.

The Redlich-Peterson isotherm was the model that gave the best overall fit with the experimental data for sorption of phenanthrene onto polyester. The Dubinin-Astakov also gave a good fit with several of the data sets, which indicates that pore filling may also be occurring. Similar adsorption curves were found for phenanthrene in seawater at 4 °C and 10 °C and in freshwater at 20 °C between PES-W and PES-B. For experiments in seawater at 20 °C, a clear difference was shown in the shape of the graphs, where it seems like PES-W has reached sorption capacity, while for PES-B sorption capacity had not been reached at higher concentrations. This could indicate different properties on the fibres due to differences in manufacturing. For 1-methylphenanthrene and fluoranthene, it is indicated that sorption occurs onto a heterogenous surface. The curvature of the graphs indicates that sorption capacity had been reached for these compounds.

4.5.2   Adsorption isotherms for polyamide

Figure 4-10shows the best fitted isotherms for polyamide. For phenanthrene in seawater at 20 °C the Dubinin-Astakov model gave the best fit with the

highest R^2 and lowest SSE. Looking at the calculated parameters, the fitting had probably over-fit the data at the higher concentration areas, which gives a much higher Q^0 value for the Dubinin-Astakov value than expected. Because of this, the Redlich-Peterson model was chosen to represent these this isotherm. It had the second highest R^2 value (0,93) and the second lowest SSE value. The isotherm also fits well with the graph visually. In this case the g value equalled to zero from the calculations. This indicates high Freundlich characteristics of the adsorption process, which means that sorption happens onto a heterogenous surface with possibilities of multi-layered adsorption. The shape of the graph appears to be linear, which fits the C-curve type isotherm. As such, multi-layered adsorption could be a possibility as the sorption sites appear to be constant.
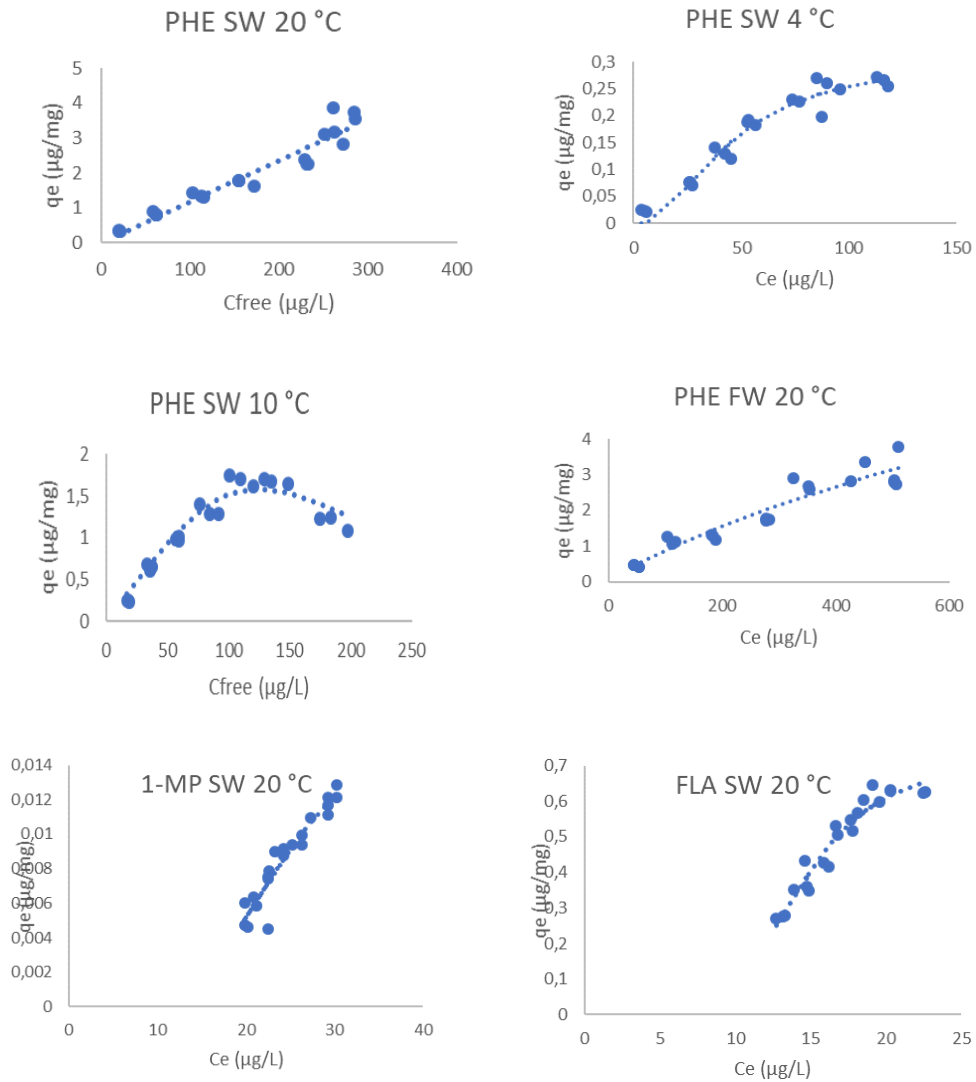
Figure 4-10 Best fitted isotherms for polyamide (PA). The top left shows the Sips isotherm for PHE in seawater at 20 °C, top right shows the Sips isotherm of phenanthrene (PHE) in seawater at 4 °C, middle left shows the Redlich-Peterson isotherm for PHE in seawater at 10 °C, middle right shows the Sips isotherm for PHE in freshwater at 20 °C, bottom left shows the Sips isotherm for 1-methylphenanthrene (1-MP) in seawater at 20 °C and bottom right shows the Sips isotherm for fluoranthene (FLA) in seawater at 20 °C.

For phenanthrene in seawater at 4 °C, the Sips model gave the best fit of data. The Sips model gave the highest R^2 value (R^2=0,96), and also the

lowest SSE value. Visual inspection shows that the graph curves well with the experimental data. This indicates that adsorption in higher concentrations has Freundlich characteristics and Langmuir characteristics at lower concentrations. The adsorption surface also appears to be heterogenous. The shape of the curve seems to be of L-curve type, indicating sorption capacity.

For phenanthrene in seawater at 10 °C, the Redlich-Peterson model gave the best fit of with experimental data. The Redlich-Peterson model gave the lowest SSE values, and the highest R^2 values (R^2=0,94). Visually, this model gave the best overall fit. This indicates that sorption at higher concentrations has Freundlich characteristics and Langmuir characteristics at lower concentrations, and that sorption occurs onto a heterogenous surface.

For phenanthrene in freshwater at 20 °C, the Dubinin-Astakov model had better SSE and R^2 values (R^2=0,9108), but the Sips model had very similar SSE and R^2 values (R^2=0,9107). Visual inspection showed that the Sips model gave better fit at higher concentration and was then chosen. Owing to the similarities in fitting of the Sips and Dubinin-Astakov models, it is hard to determine how sorption occurs, but the models strongly predicts that it occurs onto a heterogenous surface.

For adsorption of 1-methylphenanthrene, the Sips model gave the best fit of isotherms. It has the highest R^2 value (R^2=0,91) and the lowest SSE value. The shape of the graph is of L-curve type isotherm, as concentrations flattens out. For adsorption of fluoranthene, the Sips model gave the best fit of isotherms. It has the highest R^2 value (R^2=0,94) and the lowest SSE value. The graph also appears to fit well visually. The curve of the graph seems to be of L-curve type, which indicates that it is reaching sorption capacity. The Sips model fitted for 1-methylphenanthrene and fluoranthene indicates that sorption occurs as layer-by-layer mode, with Freundlich characteristics at higher concentrations and Langmuir characteristics at lower concentrations.

The best fitted isotherms for polyamide was the Sips isotherm model. Like the Redlich-Peterson model, the Sips isotherm is a hybrid between Langmuir and Freundlich models, but the Sips model indicates more adsorption onto a heterogenous surface than the Redlich-Peterson model. The heterogenous surface of polyamide could be due to differences in crystallinity of the polymer structure from the production process. Sips isotherm was best fitted for experiments done in seawater at 4 °C and 10 °C and for experiments done with 1-methylphenanthrene and fluoranthene. The Dubinin-Astakov model had some good fitting for phenanthrene at 20 °C in seawater and freshwater. This could indicate that pore filling also might happen as a mode of sorption. At higher temperatures, higher sorption capacity was observed for phenanthrene.

4.5.3   Adsorption isotherms for wool

Fitted isotherms for wool are shown in Figure 4-11. In general, wool was best fitted with the Sips model. Adsorption isotherm for phenanthrene on wool at 20 °C in seawater was best fitted with the Dubinin-Astakov model. It showed the best SSE, and the highest R^2 value (R^2=0,89). Visually, this model gave the best fit at higher concentration areas. The shape of the curve seems to be that of a L-curve, as is seems to flatten out at higher concentrations. The Freundlich, Redlich-Peterson and Sips models gave quite similar fitting parameters and visual shapes, but the Dubinin-Astakov had better SSE and R^2 values. The different surface of wool, in which the surface consists of overlapping scale, might have pores in which phenanthrene can permeate, as such pore filling as sorption mechanism can occur.
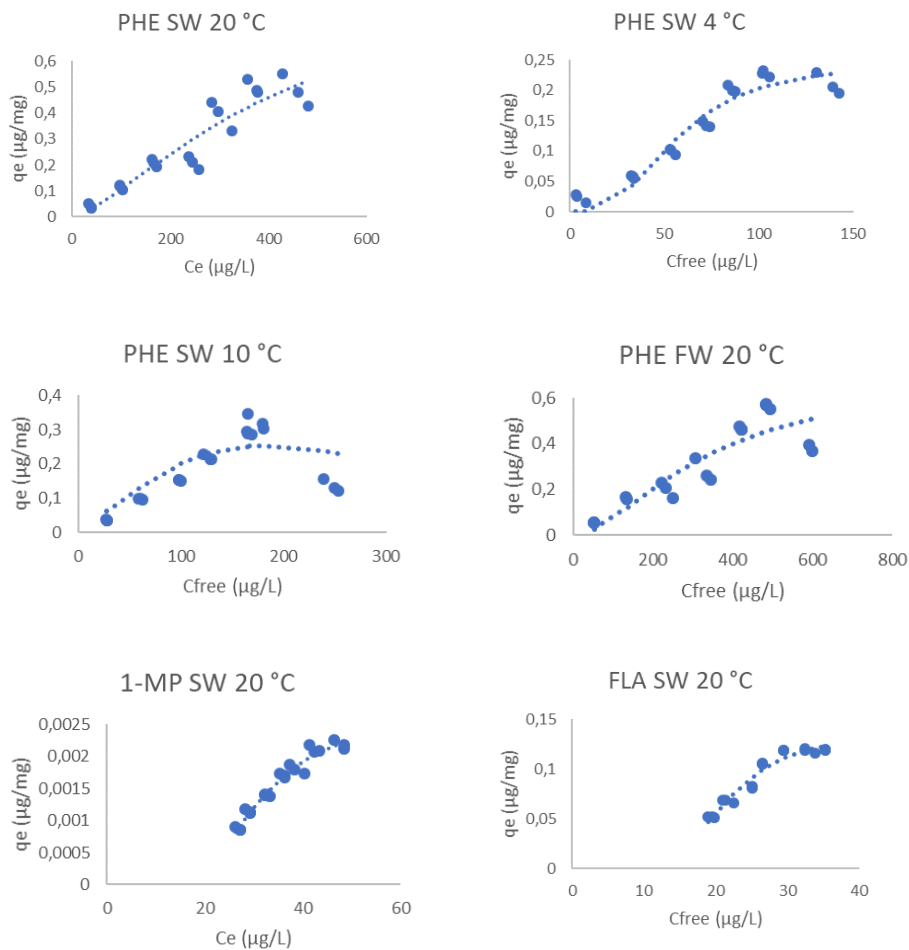
Figure 4-11 Best fitted isotherms for wool. The top left shows the Dubinin-Astakov isotherm for phenanthrene (PHE) in seawater at 20 °C, top right shows the Sips isotherm of PHE in seawater at 4 °C, middle left shows the Redlich-Peterson isotherm for PHE in seawater at 10 °C, middle right shows the Sips isotherm for PHE in freshwater at 20 °C, bottom left shows the Dubinin-Astakov isotherm for 1-methylphenanthrene (1-MP) in seawater at 20 °C and bottom right shows the Sips isotherm for fluoranthene (FLA) in seawater at 20 °C.

For phenanthrene in seawater at 4 °C, the Sips model was the best fitted model. It did not have the best fit visually for the lowest concentration point, but it had the lowest SSE and the highest R^2 (R^2=0,936), and a general better fit at the for the rest of the concentration points. This indicates that adsorption occurs as layer-by-layer mode onto a heterogenous surface. The Dubinin-Astakov model also gave good fitting parameters, but not as good

as the Sips model. This could imply that possible pore filling is less apparent at lower temperatures the curve shows a L-curve type isotherm, which indicates that a definite sorption capacity.

For phenanthrene in seawater at 10 °C, the Redlich-Peterson model gave the best fit. It had the highest R^2 value (R^2=0,76) and had the best fit visually. In general, the adsorption models used provided bad fitting for the experimental data, especially for the highest concentration point. This could be because of the reduction of phenanthrene uptake for the highest concentration point that was observed. As such mechanism of adsorption can't be predicted with certainty, but they indicate adsorption on a heterogenous surface.

For phenanthrene in freshwater, the best fitted isotherm was the Sips model. It had the lowest SSE and the highest R^2 (R^2=0,8333). In general, it had the best visual fit over the concentration ranges. Though the SSE, R^2 value (R^2=0,8332) and the visual fit is quite close to that of the Dubinin-Astakov model. This indicates sorption onto a heterogenous surface. As with phenanthrene and wool in seawater at 20 °C, pore filling mechanisms can be possible on the surface of wool. The shape of the curve is the of a L-curve type, indicating a definite sorption capacity.

For adsorption of 1-methylphenanthrene was best fitted using the Dubinin-Astakov model. The best fit was achieved using the mean weighed square errors error function which gave the highest R^2 (R^2=0,96) and also had good visual fit as well. This indicates that mode of adsorption for 1-methylphenanthrene is by pore filling mechanisms onto a heterogenous surface. The shape of the curve is that of a L-curve, but this might not be entirely true, as S-curve type could occur at the lower concentrations. At higher concentrations it seems to have reached equilibrium.

For adsorption of fluoranthene, the Sips model gave the best fitting of the experimental data. It had the lowest SSE and the highest R^2 value

(R^2=0,943). It also has good visual fit across the concentration range and the lowest SSE value. The visual fit is quite close to that of the Dubinin-Astakov model, but it has worse SSE and R^2 value (R^2=0,941). This indicates adsorption onto a heterogenous surface, by layer-by-layer mode of adsorption. It might be that due to the size of this molecule that it does not diffuse into pores as well as phenanthrene and 1-methylphenanthrene. This may reduce the Dubinin-Astakov model and rather favour the Sips model as it explains another mode of sorption. The shape of the curve is that of a L-curve, but this might not be entirely true, as S-curve type could occur at the lower concentrations. At higher concentrations it seems to have reached equilibrium.

Both the Sips model and Dubinin-Astakov model gave good fit with the experimental data. This was especially apparent for phenanthrene in freshwater and seawater at 20 °C and 1-methylphenanthrene experiments. More differences occurred at lower temperatures in seawater, where at 10 °C the Redlich-Peterson model gave best fit and at 4 °C the Sips model gave best fit. This could be an indication that if pore filling does occur, it is less likely in lower temperatures. Sorption of fluoranthene gave better fit towards the Sips, which could be due to the size of the molecule, which makes diffusion in pores less likely. At higher temperatures, higher sorption capacity was observed for phenanthrene.

4.5.4 Summary of isotherm results

The best fitted isotherm models from the adsorption isotherm study are summarised in Table 4-10.

Table 4-10 Best fitted isotherms for phenanthrene (PHE), 1-methylphenanthrene (1-MP) and fluoranthene (FLA) in seawater and freshwater (FW) in various temperatures. RP=Redlich-Peterson, DA=Dubinin-Astakov and FM=Freundlich.

	SW 20 °C PHE	SW 10 °C PHE	SW 5 °C PHE	FW 20 °C PHE	1-MP	FLA
PES-W	RP	RP	RP	RP	Sips	DA
PES-B	RP	RP	FM	RP	-	-
PA-W	Sips	RP	Sips	Sips	Sips	Sips
Wool	DA	RP	Sips	Sips/DA	DA	Sips/DA

4.6 General discussion of results as a whole

Polymeric composition has shown to have an effect on the sorption capacity and equilibrium time of phenanthrene, 1-methylphenanthrene and fluoranthene on synthetic fibres (white and black polyester and polyamide) and wool (see Table 4 5 & Figure 4 1). A common trend is that polyamide adsorbed more phenanthrene, 1-methylphenanthrene and fluoranthene under all conditions, as indicated from the sorption kinetics and the adsorption isotherm studies. In contrast, wool and polyester exhibit similar sorption capacities for all PAHs. The isotherm models offering the best fit for all fibre types were Redlich-Peterson, Sips & Dubinin-Astakov. These three models suggest sorption onto a heterogenous surface. Looking at the manufacturing process of polymers, this is to be expected (Andrady, 2017). The Redlich-Peterson model and the Sips model predicts sorption as a layer-by-layer interaction, which means that sorption occur as the PAHs adhere to the surface of the fibres. These models gave the best fit with the synthetic fibres. Dubinin-Astakov on the other hand assumes that sorption

happens as PAHs diffuse into micropores. This model gave good fit with wool, indicating that sorption happened into the pores of wool.

Kinetics studies indicated that the sorption of PAHs onto polyester had the longest equilibrium time of all the fibres. Polyester is quite hydrophobic in nature (Grishanov, 2011), which should imply that PAHs readily sorb onto polyester, but this process is slow in comparison with polyamide and wool. As stated later in this chapter, polyamide and wool has mechanisms which allow them to interact with water. Polyester, being hydrophobic, repels water which could indicate that the interface between the water and the surface of polyester is less available for the PAHs. The crystallinity of a material also influences the number of possible sorption sites (Andrady, 2017). Polyester production involves a varying degree of crystalline areas in the polymer based on the production method. Fibres are often produced to be highly crystalline and as such have a reduced number of sorption sites compared with non-crystalline materials of the same polymer. It could be that more potential sorption sites on the polyester fibres became available as mixing continued.

The polyester was best characterised by adsorption models that predict layer-by-layer as mode of adsorption (e.g. Redlich-Peterson). It is most likely that adsorption occurs due to the hydrophobic character of polyester. Another interaction that can occur is with the aromatic benzene rings in the polyester monomers. Aromatic compounds can interact with each other through the π-stacking phenomenon (Waters, 2002). This interaction involves overlap of π-orbitals in the aromatic systems which has been found to be favourable. In layer-by-layer interactions, this process may take part in stabilising the PAHs on the polyester surface via the aromatic groups.

Two types of polyester were used in the study for phenanthrene, one white and one black. No significant difference in isotherm modelling could be observed for the samples in 4 °C and 10 °C and in freshwater at 20 °C (see Table 4-10). A difference occurred for the samples in seawater at 20 °C.

White polyester reached sorption capacity of phenanthrene at higher concentrations ranges of phenanthrene, but black polyester exhibited linear behaviour indicating that sorption capacity had not been reached. The linear behaviour indicates constant partitioning of phenanthrene to PES-B, which means that the number of sorption sites remained constant. Such linear behaviour could also indicate that other processes might be present on the sorption of phenanthrene such as absorption (Hüffer and Hofmann, 2016). This may be a reflection in any differences in morphology or additives resulting from the manufacturing of the two different polyester fibres (Andrady, 2017). For example, the black polyester contains a significant quantity of dye, which could indicate that the observed sorption was due to the presence or absence of such additives.

Polyamide showed much higher sorption capacities for phenanthrene,1-methylphenanthrene and fluoranthene in this study than the other fibres. The difference is especially notable at the studies done at 10 °C and 20 °C. An important polymeric linkage in polyamide is the strong intermolecular hydrogen bonds between the amide groups (Rebenfeld, 2002). As polyamide comes in contact with water, these intermolecular hydrogen bonds weaken, which has been demonstrated to cause a change in elasticity of polyamide when it gets wet. Due to weakened hydrogen bonds, the amide groups becomes more exposed and could serve as sites for moisture sorption. This can help explain why adsorption with polyamide reached equilibrium faster than polyester. Interactions with naphthalene and amides have been found to be favourable in water (Cheng et al., 2017). These interactions are explained as delocalisation of lone pair electrons into empty π-orbitals of aromatic compounds. Naphthalene being a PAHs, implies that such interactions could also occur with the amide groups on polyamide and the PAHs used in this study, and help explain the increased sorption of PAHs onto polyamide

Interactions between aromatic compounds such as PAHs and the amide groups may occur, where the aromatic ring can act as a hydrogen bond acceptor and the amide acts as a lone pair donor (Singh and Das, 2015). In combination with the hydrophobic nature of the PAHs, it is more likely that such interactions will occur. The polyamide used in this study was nylon 6,6, which has an alkane carbon chain of 6 carbons between each amide group. These carbons are also hydrophobic in nature and can help promote sorption of PAHs onto this polymer type. In general, the best fitted isotherm for polyamides was the Sips isotherm, which describes adsorption of Langmuir characteristics at low concentrations and Freundlich characteristics at higher concentrations. The main mode of PAH adsorption to polyamide is therefore best explained by layer-by-layer sorption onto a heterogenous surface.

Wool exhibited similar sorption capacities as the polyesters (white and black), but the kinetics studies showed that wool reached equilibrium much faster than the other fibres under all conditions. Wool has a hydrophobic surface layer and a hydrophilic inner layer (Grishanov, 2011). The hydrophilic inner layer allows for a high degree of absorption of water, which could lead to less surface tension between water and the hydrophobic surface of the wool. Absorption of water into wool has been shown to be quick, which could make it easier for the dissolved PAHs to come in contact with the hydrophobic surface of wool.

Based on the isotherm fittings for wool, it would seem that the mechanisms of sorption are a mixture of layer-by-layer and pore filling as mode of sorption. The surface of wool also consists of overlapping scales, adding to the complexity of the structure of wool (Rebenfeld, 2002). Potential pores on the wool surface can emerge, acting as a sorption site for PAHs, unlike the synthetic fibres where layer-by-layer mode of sorption seems to be the dominating mode of sorption as predicted by their isotherm models. It has been proposed that water adsorption in wool can take place in capillary

pores in the wool structure (B Speakman, 1943). Pores on the wool surface have been characterised and shown to expand in the presence of water of water (J.B Speakman, 1923). The Dubinin-Astakov models predict sorption into pores as adsorption mechanisms, and it would therefore be expected that the model provides a better fit for porous wool. For phenanthrene in seawater and 1-methylphenanthrene at 20 °C, the Dubinin-Astakov model did give the best fit. However, Sips gave the best fit for phenanthrene in freshwater and fluoranthene in seawater, although both the differences could be considered negligible. As such, it is most likely that pore filling do occurs as a sorption mechanism on wool, but good fit with the Sips isotherm also indicates some layer-by-layer interactions.

The acrylic fibre used in this study, polyacrylonitrile, showed little to no adsorption of PAHs for in this study. The functional group in the polymer, nitrile, is quite polar and hydrophilic, and can therefore act as a repellent to the hydrophobic PAHs. Fluoranthene showed some adsorption to polyacrylonitrile, but this was at very high fibre concentrations, and as such was dismissed for further study.

4.6.1   Effect of temperature on adsorption of phenanthrene

The effect of temperature on sorption of PAHs to synthetic fibres and wool was investigated with phenanthrene as a model compound in seawater. The solubility of phenanthrene decreased with decreasing temperature. It is expected that more sorption will occur at lower temperatures because of decreased solubility of PAHs (Lamichhane et al., 2016). Yet highest sorption was observed at 20 °C for all fibres. This could be explained by describing the effect of temperature as a combination of sorption and solubility, in which the surface properties of the fibres has to be considered. Similar trends were observed by Balati et. Al (2015) where increasing temperature increased sorption capacity (Balati et al., 2015). The fitted isotherms shows that there was little differences in the sorption mechanisms of phenanthrene onto the fibres. The isotherm models best fitted were the Redlich-Peterson model and

the Sips model. Both are a combination of the Langmuir and Freundlich model, which predicts sorption onto a heterogenous surface.

For white polyester it would seem that decreasing temperature leads to decreased sorption capacity on the fibres see Figure 4-8. This is characterised by the L-curve type isotherms for the samples done in 4 °C and 10 °C. Similar trends can also be seen on the black polyester samples. Especially for the black polyester samples that were done in 20 °C, which has a C-curve, and which indicates that partitioning to black polyester remains constant as the number of sorption sites remains constant due to the formation of new ones. In contrast, the samples for black polyester done in 4 °C and 10 °C had L-curve shapes. Temperature did not seem to have a big effect on the equilibrium times for the polyesters. A difference was seen for the coloured polyesters in seawater at 20 °C, where white polyester had longer equilibrium time than black polyester. This could be due to different manufacturing and additives, where the latter may influence the chemical properties of the final material (Andrady, 2017).

For polyamide, temperature seemed to have a big effect on the sorption capacity of phenanthrene. At 20 °C in seawater, polyamide had C-curve type isotherm, which indicates that the number of adsorption sites remained constant due to the formation of new sorption sites. This could also be explained by multi-layered adsorption, in which several PAHs can occupy one sorption spot. This is also accompanied by polyamide having the highest sorption amounts registered. At 10 °C, polyamide showed higher sorption capacities of phenanthrene than the other fibres at the same temperature, but the isotherm was of L-curve type, which indicates that temperature had a limiting effect on sorption. Interestingly, adsorption of phenanthrene on polyamide from the adsorption isotherm study which occurred at 4 °C was in similar amounts as with the other fibres, unlike at 20 °C and 10 °C where sorption was significantly higher than the other fibres (see Figure 4-3). The isotherm also showed L-curve type at lower concentrations, which indicates

that sorption capacity had been reached for polyamide in 4 °C. The solubility of phenanthrene in seawater at 4 °C and 10 °C are very similar (see Table 4-2), so the effect of temperature is more apparent here.

At lower temperatures, the water might not be able to unravel the polymer matrix. It is predicted that interactions between the aromatic PAHs and the amide groups on the polyamide contribute to sorption (Rebenfeld, 2002). These amide groups are usually bound to each other in the polymer matrix by intramolecular hydrogen bonds. Manas et al. (2000) found that lowering temperature strengthened hydrogen bonds between amide groups (Manas et al., 2000). Within polyamide, this could imply that water won't be able to break down the hydrogen bonds between the amide groups, and thereby making them less accessible for the phenanthrene. Other sorption mechanisms must then be dominant, seeing as interactions between amides and PAHs are less likely to occur. Hydrophobic partitioning would most likely be one of the main interactions between phenanthrene and polyamide in seawater at 4 °C. This could also explain why polyamide had longer equilibrium time in 4 °C (7 days) than in 10 °C (2 days) and 20 °C (days), seeing as interactions with the amide group is less likely to occur. At higher temperatures, the matrix might also soften, making the interior of the polymer more easily accessible.

Wool also showed decreased sorption capacity at lower concentrations. At 20 °C in seawater, wool has a C-curve type isotherm. This indicates that as sorption sites are occupied, new sorption sites emerge keeping the amount of sorption types constant. Isotherms at both 4 °C and 10 °C are L-curve type isotherms, indicating that that the fibres had reached sorption capacity, which is lower than in samples at 20 °C. Samples at 4 °C also had lower sorption capacity than at 10 °C, despite similar solubilities. This could be because the surface properties of wool could be different at lower temperatures. The isotherm modelling of wool indicates that pore filling could be a possible sorption mechanism, especially at 20 °C, but this characteristic

seems to be less apparent at lower temperatures, where layer-by-layer models are better predicted (Redlich-Peterson and Sips models). This could indicate that temperature has an influence on the pore sizes in wool which can affect diffusion of phenanthrene into wool. It has already been found that pores in wool expand in the presence of water (J.B Speakman, 1923). This expansion could be temperature dependant, but no available literature have been found.

4.6.2 Effect of salinity on adsorption of phenanthrene

The effect of salinity on sorption of PAHs to microplastics fibres and wool was investigated with phenanthrene as a model compound, at 20 °C. Salinity did not have a big impact on the adsorption of phenanthrene to the different fibres. For the polyesters, the Redlich-Peterson model was determined to be the best isotherm model, indicating similar adsorption mechanics in both seawater and freshwater. The most noticeable difference is that sorption capacity in black polyester is higher in seawater than in freshwater based on the isotherm modelling (see Figure 4-9). In fact, it does not seem like the material has reached sorption capacity in seawater based on the curve of the graph. However, this behaviour could not be seen for white polyester, indicating that production method could have an effect on the sorption properties of the material. For polyamide and wool salinity did not seem to have a large effect on adsorption, as the isotherms seems to go to the same saturation points. Furthermore, salinity did not have any significant effect on the equilibrium time between phenanthrene and any of the fibres (see Table 4-5).

4.6.3 Effect of PAHs

1-methylphenanthrene (123 µg/L) and fluoranthene (106 µg/L) had lower solubilities than phenanthrene in seawater at 20 °C (676 (µg/L). Based on the physicochemical properties of the three compounds, it is expected that the degree of sorption to the different fibres will also vary. In general, phenanthrene had higher sorption capacity than fluoranthene, which had

higher adsorption capacity than 1-methylphenanthrene. Phenanthrene had much higher solubility than 1-methylphenanthrene and fluoranthene, and sorption in the experiments would be more likely to occur because of the presence of higher concentrations of phenanthrene. It is important to note that the concentrations applied in the current study are well above what is considered environmentally relevant under normal circumstances and was chosen in order to study the fundamental principles affecting sorption of these compounds to synthetic and natural fibres.

1-methylphenanthrene and fluoranthene had faster equilibrium time than phenanthrene onto polyester. Both compounds are less soluble and less polar than phenanthrene, making them more susceptible to sorb onto a hydrophobic surface, such as polyester. The compounds might possibly have such higher affinity towards the polyester that it is easier for them to penetrate through the interface between the seawater and the polyester. For sorption onto both polyamide and wool, 1-methylphenanthrene and fluoranthene had similar equilibrium times as phenanthrene.

Sorption isotherms showed that there was no difference in the predicted sorption mode between phenanthrene, 1-methylphenanthrene and fluoranthene onto polyamide fibres. All three compounds were best predicted with the Sips model, which indicates layer-by-layer mode of sorption on the surface onto a heterogenous. Adsorption on a heterogenous surface was best predicted from the isotherm models for polyester. Bad fitting of the data gave inconclusive answer on mode of sorption, but layer-by-layer is most likely. Sorption of PAHs onto wool was characterised by a combination of pore filling and layer-by-layer sorption modes for phenanthrene, 1-methylphenanthrene and fluoranthene due to good fit with both the Sips and Dubinin-Astakov model.

4.7   Implications for the environment

In this study phenanthrene, 1-methylphenanthrene and fluoranthene have been shown to sorb onto a range of synthetic and natural wool fibres. This can have an effect on the mobility of PAHs in the environment, and also the bioavailability of such compounds. Two possible scenarios can occur with synthetic and natural fibres. The first case scenario is where sorption of PAHs occurs on fibres and the fibres are ingested by marine organisms. The fibres might act as vectors for the PAHs in the transport of PAHs to the marine organism. Once in the organisms, the PAHs may desorb from the fibres and taken into tissues. The organisms may be affected by the fibres themselves, by the uptake of PAHs or a combination of both.

The second case scenario is where the fibres acts as a sink for the PAHs, significantly reducing the mobility of PAHs in the water, and decreasing the free concentration of PAHs. This means that the PAHs are less available for the organisms in the water, reducing their bioavailability. The fibres have shown to have higher density than water, which means that they can potentially sink to the seafloor where they will remain. Though this might have some implications for benthic bottom feeders.

The results of this study suggest that synthetic and wool act in a similar fashion in aqueous environment. To the tested synthetic fibres (polyester and polyamide) as well as wool showed high sorption of the PAHs in this study. This might not only be limited to PAHs. Other POPs are also present in the marine environment and also have the potential to sorb onto the fibres.

Polyacrylonitrile did not show significant sorption of PAHs. This is most likely due to the polar nitrile group on the monomers. Despite little to no sorption of PAHs, it should not be disregarded as sorption or interactions with more polar organic pollutants might occur. Compounds of special interests are emerging pollutants that are polar in nature.

5 Conclusion

In this study, sorption of PAHs (phenanthrene, 1-methylphenanthrene and fluoranthene) to synthetic (polyester, polyamide and polyacrylonitrile) and wool fibres was investigated under a range of different environmental conditions. Sorption of phenanthrene to the different fibre materials was studied at 4 °C, 10 °C and 20 °C in seawater and at 20 °C in freshwater to assess effect of temperature and salinity. In addition, 1-methylphenanthrene, fluoranthene and 9-phenanthrol was assessed in 20 °C in seawater to study the influence of PAH properties on sorption processes.

The degree of sorption of phenanthrene, 1-methylphenanthrene and fluoranthene to polyamide was found to be higher than to the polyester materials (white and black) and wool, even at lower fibre concentrations. This suggests that there are strong interactions between polyamide and these two compounds, like interactions between the amide group and the aromatic rings on the PAHs. The degree of sorption of PAHs onto wool and polyester was about the same amount under all temperature and salinity conditions tested. No significant sorption of any PAH was observed onto polyacrylonitrile fibres.

Equilibrium times for the sorption of PAHs was affected by the temperature, but no significant differences were observed in samples of different salinity. Decreasing temperature increased the equilibrium times for wool and polyamide. White polyester had higher equilibrium time at 20 °C, than the black polyester. For phenanthrene, wool had the quickest equilibrium times (ranging between 2 hours to 2 days), followed by polyamide with equilibrium times between (2 days to 7 days), and finally the polyesters with the slowest with equilibrium times (7 to 10 days). 1-methylphenanthrene and fluoranthene had shorter equilibrium times on white polyester compared with phenanthrene. No significant differences were found on the equilibrium times between 1-methylphenanthrene and fluoranthene on to wool fibres. These

observations can be explained by the properties of the different polymer structures of the fibres, as it changes under different environmental conditions.

Non-linear isotherm models were fitted to experimental data to evaluate and understand the sorption mechanisms of PAHs onto synthetic fibres and wool. For this purpose, several isotherms and error functions were tested. The sum of absolute error proved to be the most suitable error function, giving higher R^2 values and better visual fit of calculated data with experimental data. For the synthetic fibres, the Redlich-Peterson and the Sips models typically gave the best fit. These models indicate that sorption on synthetic fibres mainly happens as layer-by-layer interactions onto a heterogenous surface, with a monolayer sorption occurring at low concentrations and possible multi-layered sorption occurring as the PAH concentration rises. The best fitted isotherms for PAHs onto wool were in some cases the Dubinin-Astakov model and in other cases the Sips model. Both models predict adsorption on a heterogenous surface, but by different modes of sorption (sorption into micropores and layer-by-layer sorption, respectively). Given the structure porous structure of wool, pore filling appears likely to happen based on the good fit with the Dubinin-Astakov model. The Sips gave similar fit as the Dubinin-Astakov model, so layer-by-layer mode can also occur, as indicated by experiments done in 4 °C where the Sips isotherm gave the overall best fit. There is a possibility that both types of interactions are co-occurring when PAHs sorb to wool fibres. The study indicates that water temperature and salinity do not appear to have a large effect on the sorption mechanisms of PAHs on synthetic fibres and wool, with exception of wool at lower temperatures, as discussed.

Overall, polyester, polyamide and wool showed significant sorption of PAHs. This can have an effect on the mobility of these compounds in the environment and determine their fates. The fibres may increase the bioavailability of PAHs to biota as transport vectors, or they may act as a

sink for PAHs by reducing the free concentration in water. The latter requires more investigation.

6 Future work

Experiments conducted in this thesis simplify the complexity of the marine environment. Advantages are that environmental parameters can be modified individually to better study their influence on PAH sorption to polymers. However, this laboratory approach might not produce realistic representations of these processes in the marine environment. Biota and other particulates are present in water which could influence sorption of PAHs onto synthetic fibres and wool.

The order of reaction and rate constants could not be established in this study. It could be beneficial to determine these to get a better understanding of sorption kinetics. It would be really interesting for white polyester and black polyester since they are made of the same material, but with different additives. The investigation of sorption of the same materials that have been produced differently is also worth investigating to see the effects of crystallinity, morphology and additives.

Investigation of sorption of other compounds than PAHs onto fibres should also be investigated. Polar compounds, such as 9-phenanthrol, might have interact very differently with the fibres. This might especially be the case with polyacrylonitrile, which has a polar surface because of nitrile groups on the polymer chains. Interactions between polar compounds and polar groups on polymers should be investigated. In addition, emerging pollutants should also be investigated.

The bioavailability and toxicity of PAHs and other organic pollutants to marine organisms when sorbed to synthetic fibres and wool also demands investigation. We do know that PAHs sorb onto synthetic fibres and wool and that organisms ingest these fibres. However, there is still debate within the

scientific community about whether or not these compounds will be bioavailable and transported into the tissues, or if they will remain on the fibres.

7 References

A.O, D., 2012. Langmuir, Freundlich, Temkin and Dubinin–Radushkevich Isotherms Studies of Equilibrium Sorption of Zn 2+ Unto Phosphoric Acid Modified Rice Husk. IOSR J. Appl. Chem. https://doi.org/10.9790/5736-0313845

Andrady, A.L., 2017. The plastic in microplastics: A review. Mar. Pollut. Bull. https://doi.org/10.1016/j.marpolbul.2017.01.082

Andrady, A.L., 2011. Microplastics in the marine environment. Mar. Pollut. Bull. https://doi.org/10.1016/j.marpolbul.2011.05.030

Ayawei, N., Ebelegi, A.N., Wankasi, D., 2017. Modelling and Interpretation of Adsorption Isotherms. J. Chem. https://doi.org/10.1155/2017/3039817

B Speakman, B.J., 1943. AN ANALYSIS OF THE WATER ADSORPTION ISOTHERM O F WOOL, 133. Speakman, Trans. Faraday SOC.

Balati, A., Shahbazi, A., Amini, M.M., Hashemi, S.H., 2015. Adsorption of polycyclic aromatic hydrocarbons from wastewater by using silica-based organic–inorganic nanohybrid material. J. Water Reuse Desalin. https://doi.org/10.2166/wrd.2014.013

Barnes, D.K.A., Galgani, F., Thompson, R.C., Barlaz, M., 2009. Accumulation and fragmentation of plastic debris in global environments. Philos. Trans. R. Soc. B Biol. Sci. https://doi.org/10.1098/rstb.2008.0205

Belhachemi, M., Addoun, F., 2011. Comparative adsorption isotherms and modeling of methylene blue onto activated carbons. Appl. Water Sci. https://doi.org/10.1007/s13201-011-0014-1

Bidlack, W.R., 2013. Casarett & Doull's Toxicology: The Basic Science of Poisons, 6th ed., Journal of the American College of Nutrition. https://doi.org/10.1080/07315724.2002.10719223

Browne, M.A., Crump, P., Niven, S.J., Teuten, E., Tonkin, A., Galloway, T., Thompson, R., 2011. Accumulation of Microplastic on Shorelines Woldwide: Sources and Sinks. Environ. Sci. Technol. 45, 9175–9179. https://doi.org/10.1021/es201811s

Cheng, X., Shkel, I.A., O'Connor, K., Henrich, J., Molzahn, C., Lambert, D., Record, M.T., 2017. Experimental Atom-by-Atom Dissection of Amide-Amide and Amide-Hydrocarbon Interactions in H2O. J. Am. Chem. Soc. https://doi.org/10.1021/jacs.7b03261

Cole, M., 2016. A novel method for preparing microplastic fibers. Sci. Rep. https://doi.org/10.1038/srep34519

Cole, M., Lindeque, P., Halsband, C., Galloway, T.S., 2011. Microplastics as contaminants in the marine environment: A review. Mar. Pollut. Bull. https://doi.org/10.1016/j.marpolbul.2011.09.025

Cózar, A., Echevarría, F., González-Gordillo, J.I., Irigoien, X., Ubeda, B., Hernández-León, S., Palma, A.T., Navarro, S., García-de-Lomas, J., Ruiz, A., Fernández-de-Puelles, M.L., Duarte, C.M., 2014. Plastic debris in the open ocean. Proc. Natl. Acad. Sci. U. S. A. https://doi.org/10.1073/pnas.1314705111

Crawford, C.B., Quinn, B., 2016a. The interactions of microplastics and chemical pollutants, in: Microplastic Pollutants. https://doi.org/10.1016/b978-0-12-809406-8.00006-2

Crawford, C.B., Quinn, B., 2016b. Microplastics, standardisation and spatial distribution, in: Microplastic Pollutants. https://doi.org/10.1016/b978-0-12-809406-8.00005-0

D'Arcy, R.L., Watt, I.C., 1970. Analysis of sorption isotherms of non-homogeneous sorbents. Trans. Faraday Soc. https://doi.org/10.1039/TF9706601236

Dąbrowski, A., 2001. Adsorption - From theory to practice. Adv. Colloid Interface Sci. https://doi.org/10.1016/S0001-8686(00)00082-8

Derraik, J.G.B., 2002. The pollution of the marine environment by plastic debris: a review. Mar. Pollut. Bull.

Dris, R., Gasperi, J., Saad, M., Mirande, C., Tassin, B., 2016. Synthetic fibers in atmospheric fallout: A source of microplastics in the environment? Mar. Pollut. Bull. 104, 290–293. https://doi.org/10.1016/J.MARPOLBUL.2016.01.006

El-Shahawi, M.S., Hamza, A., Bashammakh, A.S., Al-Saggaf, W.T., 2010. An overview on the accumulation, distribution, transformations, toxicity and analytical methods for the monitoring of persistent organic pollutants. Talanta 80, 1587–1597. https://doi.org/10.1016/J.TALANTA.2009.09.055

Endo, S., Grathwohl, P., Schmidt, T.C., 2008. Absorption or adsorption? Insights from molecular probes n-alkanes and cycloalkanes into modes of sorption by environmental solid matrices. Environ. Sci. Technol. https://doi.org/10.1021/es702470g

Endo, S., Takizawa, R., Okuda, K., Takada, H., Chiba, K., Kanehiro, H., Ogi, H., Yamashita, R., Date, T., 2005. Concentration of polychlorinated biphenyls (PCBs) in beached resin pellets: Variability among individual particles and regional differences. Mar. Pollut. Bull. https://doi.org/10.1016/j.marpolbul.2005.04.030

Fähnrich, K.A., Pravda, M., Guilbault, G.G., 2002. Immunochemical detection of polycyclic aromatic hydrocarbons (PAHs). Anal. Lett. https://doi.org/10.1081/AL-120006666

Foo, K.Y., Hameed, B.H., 2010. Insights into the modeling of adsorption isotherm systems. Chem. Eng. J. 156, 2–10. https://doi.org/10.1016/j.cej.2009.09.013

Geyer, R., Jambeck, J.R., Law, K.L., 2017. Production, use, and fate of all plastics ever made.

Giles, C.H., Smith, D., Huitson, A., 1974. A general treatment and classification of the solute adsorption isotherm. I. Theoretical. J. Colloid Interface Sci. https://doi.org/10.1016/0021-9797(74)90252-5

Gimbert, F., Morin-Crini, N., Renault, F., Badot, P.M., Crini, G., 2008. Adsorption isotherm models for dye removal by cationized starch-based material in a single component system: Error analysis. J. Hazard. Mater. https://doi.org/10.1016/j.jhazmat.2007.12.072

Grishanov, S., 2011. Structure and properties of textile materials, in: Handbook of Textile and Industrial Dyeing: Principles, Processes and Types of Dyes. https://doi.org/10.1533/9780857093974.1.28

Guechi, E.K., Hamdaoui, O., 2016. Sorption of malachite green from aqueous solution by potato peel: Kinetics and equilibrium modeling using non-linear analysis method. Arab. J. Chem. https://doi.org/10.1016/j.arabjc.2011.05.011

Haghseresht, F., Lu, G.Q., 1998. Adsorption characteristics of phenolic compounds onto coal-reject-derived adsorbents. Energy and Fuels. https://doi.org/10.1021/ef9801165

Hartline, N.L., Bruce, N.J., Karba, S.N., Ruff, E.O., Sonar, S.U., Holden, P.A., 2016. Microfiber Masses Recovered from Conventional Machine Washing of New or Aged Garments. Environ. Sci. Technol. https://doi.org/10.1021/acs.est.6b03045

Hemond, H.F., Fechner, E.J., 2014. Chemical Fate and Transport in the Environment: Third Edition, Chemical Fate and Transport in the Environment: Third Edition. https://doi.org/10.1016/C2011-0-09677-1

Hiller, E., Jurkovič, L., Bartal, M., 2008. Effect of temperature on the distribution of polycyclic aromatic hydrocarbons in soil and sediment. Soil Water Res.

Ho, Y.S., McKay, G., 1998. A Comparison of Chemisorption Kinetic Models Applied to Pollutant Removal on Various Sorbents. Process Saf. Environ. Prot. 76, 332–340. https://doi.org/10.1205/095758298529696

Huang, M., Mesaros, C., Hackfeld, L.C., Hodge, R.P., Blair, I.A., Penning, T.M., 2017. Potential Metabolic Activation of Representative Alkylated Polycyclic Aromatic Hydrocarbons 1-Methylphenanthrene and 9-Ethylphenanthrene Associated with the Deepwater Horizon Oil Spill in Human Hepatoma (HepG2) Cells. Chem. Res. Toxicol. https://doi.org/10.1021/acs.chemrestox.7b00232

Hüffer, T., Hofmann, T., 2016. Sorption of non-polar organic compounds by micro-sized plastic particles in aqueous solution. Environ. Pollut. https://doi.org/10.1016/j.envpol.2016.04.018

Inglezakis, V.J., 2007. Solubility-normalized Dubinin-Astakhov adsorption isotherm for ion-exchange systems. Microporous Mesoporous Mater. 103, 72–81. https://doi.org/10.1016/j.micromeso.2007.01.039

J.B Speakman, 1923. The Micelle Structure of the Wool Fibre, Proc. Roy. Soc.,' B.

Jambeck, J.R., Geyer, R., Wilcox, C., Siegler, T.R., Perryman, M., Andrady, A., Narayan, R., Law, K.L., 2015. Marine pollution. Plastic waste inputs from land into the ocean. Science 347, 768–71. https://doi.org/10.1126/science.1260352

Karapanagioti, H.K., Klontza, I., 2008. Testing phenanthrene distribution properties of virgin plastic pellets and plastic eroded pellets found on Lesvos island beaches (Greece). Mar. Environ. Res. https://doi.org/10.1016/j.marenvres.2007.11.005

Kipling, J.J. (John J., 1965. Adsorption from solutions of non-electrolytes. Academic Press.

Kleineidam, S., Schüth, C., Grathwohl, P., 2002. Solubility-normalized combined adsorption-partitioning sorption isotherms for organic pollutants. Environ. Sci. Technol. https://doi.org/10.1021/es010293b

Kooi, M., Reisser, J., Slat, B., Ferrari, F.F., Schmid, M.S., Cunsolo, S., Brambini, R., Noble, K., Sirks, L.A., Linders, T.E.W., Schoeneich-Argent, R.I., Koelmans, A.A., 2016. The effect of particle properties on the depth profile of buoyant plastics in the ocean. Sci. Rep. https://doi.org/10.1038/srep33882

Kumar, K.V., Porkodi, K., Rocha, F., 2008. Comparison of various error functions in predicting the optimum isotherm by linear and non-linear regression analysis for the sorption of basic red 9 by activated carbon. J. Hazard. Mater. https://doi.org/10.1016/j.jhazmat.2007.09.020

Kumar, K.V., Sivanesan, S., 2006. Isotherm parameters for basic dyes onto activated carbon: Comparison of linear and non-linear method. J. Hazard. Mater. https://doi.org/10.1016/j.jhazmat.2005.08.022

Lamichhane, S., Bal Krishna, K.C., Sarukkalige, R., 2016. Polycyclic aromatic hydrocarbons (PAHs) removal by sorption: A review. Chemosphere. https://doi.org/10.1016/j.chemosphere.2016.01.036

LI, W.C., TSE, H.F., FOK, L., 2016. Plastic waste in the marine environment: A review of sources, occurrence and effects. Sci. Total Environ. 566–567, 333–349. https://doi.org/10.1016/J.SCITOTENV.2016.05.084

Limousin, G., Gaudet, J.-P., Charlet, L., Szenknect, S., Barthès, V., Krimissa, M., 2007. Sorption isotherms: A review on physical bases, modeling and measurement. Appl. Geochemistry 22, 249–275. https://doi.org/10.1016/J.APGEOCHEM.2006.09.010

Lusher, A.L., Welden, N.A., Sobral, P., Cole, M., 2017. Sampling, isolating and identifying microplastics ingested by fish and invertebrates. Anal. Methods. https://doi.org/10.1039/c6ay02415g

Manas, E.S., Getahun, Z., Wright, W.W., Degrado, W.F., Vanderkooi, J.M., 2000. Infrared spectra of amide groups in α-helical proteins: Evidence for hydrogen bonding between helices and water. J. Am. Chem. Soc. https://doi.org/10.1021/ja001782z

Mato, Y., Isobe, T., Takada, H., Kanehiro, H., Ohtake, C., Kaminuma, T., 2001. Plastic resin pellets as a transport medium for toxic chemicals in the marine environment. Environ. Sci. Technol. https://doi.org/10.1021/es0010498

Ng, J.C.Y., Cheung, W.H., Mckay, G., 2002. Equilibrium Studies of the Sorption of Cu(II) Ions onto Chitosan. J. Colloid Interface Sci. 255, 64–74. https://doi.org/10.1006/jcis.2002.8664

Organisation for Economic Co-operation and Development., 2011. Test no. 201: freshwater alga and cyanobacteria, growth inhibition test. OECD.

PlasticsEurope, 2018. Plastics – the Facts 2018.

Poster, D.L., Schantz, M.M., Sander, L.C., Wise, S.A., 2006. Analysis of polycyclic aromatic hydrocarbons (PAHs) in environmental samples: A critical review of gas chromatographic (GC) methods. Anal. Bioanal. Chem. https://doi.org/10.1007/s00216-006-0771-0

Proctor, A., Toro-Vazquez, J.F., 2009. The Freundlich Isotherm in Studying Adsorption in Oil Processing, in: Bleaching and Purifying Fats and Oils: Theory and Practice. https://doi.org/10.1016/B978-1-893997-91-2.50016-X

Rebenfeld, L., 2002. Chapter VI Fibers and fibrous materials, in: Textile Science and Technology. https://doi.org/10.1016/S0920-4083(02)80009-3

Redlich, O., Peterson, D.L., 2007. A Useful Adsorption Isotherm. J. Phys. Chem. https://doi.org/10.1021/j150576a611

Rice, M.R., Gold, H.S., 1984. Polypropylene as an Adsorbent for Trace Organics in Water. Anal. Chem. https://doi.org/10.1021/ac00272a052

Rios, L.M., Moore, C., Jones, P.R., 2007. Persistent organic pollutants carried by synthetic polymers in the ocean environment. Mar. Pollut. Bull. 54, 1230–1237. https://doi.org/10.1016/J.MARPOLBUL.2007.03.022

Rivas, F.J., Beltrán, F.J., Gimeno, O., Frades, J., Carvalho, F., 2006. Adsorption of landfill leachates onto activated carbon: Equilibrium and kinetics. J. Hazard. Mater. 131, 170–178. https://doi.org/10.1016/J.JHAZMAT.2005.09.022

Rochman, C.M., Hoh, E., Kurobe, T., Teh, S.J., 2013. Ingested plastic transfers hazardous chemicals to fish and induces hepatic stress. Sci. Rep. https://doi.org/10.1038/srep03263

Rochman, C.M., Lewison, R.L., Eriksen, M., Allen, H., Cook, A.-M., Teh, S.J., 2014. Polybrominated diphenyl ethers (PBDEs) in fish tissue may be an indicator of plastic contamination in marine habitats. Sci. Total Environ. 476–477, 622–633. https://doi.org/10.1016/J.SCITOTENV.2014.01.058

Rogers, E., 2018. Investigation of polycyclic aromatic hydrocarbons (PAH) absorption from seawater to model microplastic particles. NTNU.

Saha, D., Grappe, H.A., 2016. Adsorption properties of activated carbon fibers, in: Activated Carbon Fiber and Textiles. https://doi.org/10.1016/B978-0-08-100660-3.00005-5

Saini, A., Rauert, C., Simpson, M.J., Harrad, S., Diamond, M.L., 2016. Characterizing the sorption of polybrominated diphenyl ethers (PBDEs) to cotton and polyester fabrics under controlled conditions. Sci. Total Environ. https://doi.org/10.1016/j.scitotenv.2016.04.099

Sait, S., 2019. No Title. NTNU.

Singh, S.K., Das, A., 2015. The n → π∗ interaction: A rapidly emerging non-covalent interaction. Phys. Chem. Chem. Phys. https://doi.org/10.1039/c4cp05536e

Teuten, E.L., Rowland, S.J., Galloway, T.S., Thompson, R.C., 2007. Potential for plastics to transport hydrophobic contaminants. Environ. Sci. Technol. https://doi.org/10.1021/es071737s

Teuten, E.L., Saquing, J.M., Knappe, D.R.U., Barlaz, M.A., Jonsson, S., Björn, A., Rowland, S.J., Thompson, R.C., Galloway, T.S., Yamashita, R., Ochi, D., Watanuki, Y., Moore, C., Viet, P.H., Tana, T.S., Prudente, M., Boonyatumanond, R., Zakaria, M.P., Akkhavong, K., Ogata, Y., Hirai, H., Iwasa, S., Mizukawa, K., Hagino, Y., Imamura, A., Saha, M., Takada, H., 2009. Transport and release of chemicals from plastics to the environment and to wildlife. Philos. Trans. R. Soc. Lond. B. Biol. Sci. 364, 2027–45. https://doi.org/10.1098/rstb.2008.0284

Tóth, G., Watts, C.R., Murphy, R.F., Lovas, S., 2001. Significance of aromatic-backbone amide interactions in protein structure. Proteins Struct. Funct. Genet. https://doi.org/10.1002/prot.1050

Van Sebille, E., Wilcox, C., Lebreton, L., Maximenko, N., Hardesty, B.D., Van Franeker, J.A., Eriksen, M., Siegel, D., Galgani, F., Law, K.L., 2015. A global inventory of small floating plastic debris. Environ. Res. Lett. https://doi.org/10.1088/1748-9326/10/12/124006

Vijayaraghavan, K., Padmesh, T.V.N., Palanivelu, K., Velan, M., 2006. Biosorption of nickel(II) ions onto Sargassum wightii: Application of two-parameter and three-parameter isotherm models. J. Hazard. Mater. https://doi.org/10.1016/j.jhazmat.2005.10.016

von Oepen, B., Kördel, W., Klein, W., 1991. Sorption of nonpolar and polar compounds to soils:

Processes, measurements and experience with the applicability of the modified OECD-Guideline 106. Chemosphere. https://doi.org/10.1016/0045-6535(91)90318-8

Wang, J., Wang, C., Huang, Q., Ding, F., He, X., 2015. Adsorption of PAHs on the Sediments from the Yellow River Delta as a Function of Particle Size and Salinity. Soil Sediment Contam. https://doi.org/10.1080/15320383.2014.920292

Waters, M.L., 2002. Aromatic interactions in model systems. Curr. Opin. Chem. Biol. https://doi.org/10.1016/S1367-5931(02)00359-9

Wheatley, L., Levendis, Y.A., Vouros, P., 1993. Exploratory Study on the Combustion and PAH Emissions of Selected Municipal Waste Plastics. Environ. Sci. Technol. https://doi.org/10.1021/es00049a032

Wu, W., Chen, W., Lin, D., Yang, K., 2012. Influence of surface oxidation of multiwalled carbon nanotubes on the adsorption affinity and capacity of polar and nonpolar organic compounds in aqueous phase. Environ. Sci. Technol. https://doi.org/10.1021/es3004848

Wu, Y., 2017. Investigation of Adsorption and Absorption Mechanisms During Copper (II) Removal by Periphyton, in: Periphyton. https://doi.org/10.1016/b978-0-12-801077-8.00013-2

Zhang, S., Wang, J., Liu, X., Qu, F., Wang, Xueshan, Wang, Xinrui, Li, Y., Sun, Y., 2019. Microplastics in the environment: A review of analytical methods, distribution, and biological effects. TrAC - Trends Anal. Chem. https://doi.org/10.1016/j.trac.2018.12.002

Ziccardi, L.M., Edgington, A., Hentz, K., Kulacki, K.J., Kane Driscoll, S., 2016. Microplastics as vectors for bioaccumulation of hydrophobic organic chemicals in the marine environment: A state-of-the-science review. Environ. Toxicol. Chem. 35, 1667–1676. https://doi.org/10.1002/etc.3461

Appendix

Appendix A: TeflonWAF solubilities

Table A 1 Determination of solubility of phenanthrene (PHE) in seawater at 4 °C, 10 °C and 20 °C. Concentrations are given in μg/L

	Days			
	6	7	8	Average
Phe 4°C 1	323,031	328,3182	308,9402	309,7
Phe 4°C 2	334,5932	332,3706	309,9733	±0,7
Phe 4°C 3	329,7445	330,5286	310,3176	
Phe 10°C 1	352,8688	365,1589	354,0506	353
Phe 10°C 2	363,685	365,1589	349,9183	±3
Phe 10°C 3	359,5823	370,685	356,1167	
Phe 20°C 1	723,9763	717,7248	685,3187	697
Phe 20°C 2	721,3655	731,7242	700,4703	±10
Phe 20°C 3	728,8249	724,3561	703,9138	

Table A 2 Determination of solubility of phenanthrene (PHE) in freshwater at 20 °C. Concentrations are given in μg/L

	1	2	3	Average
Phe FW 1	1022,103	1068,994	999,6719	1029
Phe FW 2	1031,339	1076,809	968,359	±49
Phe FW 3	1066,152	1071,836	960,3642	

Table A 3 Determination of solubility of 1-methylphenanthrene in seawater at 20 °C. Concentrations are given in μg/L

	1	2	3	4	Average
1-MP 1	125,2926	122,3949	124,7228	121,3719	123
1-MP 2	121,6352	121,2981	124,7228	123,5116	±3
1-MP 3	120,4161	123,4917	133,9723	114,9529	

Table A 4 Determination of solubility of fluoranthene in seawater at 20 °C. Concentrations are given in μg/L

	1	2	3	4	Average
FLA 1	103,5133	103,6358	120,3343	101,5598	106
FLA 2	105,1105	109,6553	111,139	101,5598	±5
FLA 3	103,5133	114,17	105,0088	98,42933	

Appendix B: Calibration calculations for kinetics and adsorption studies

Table B 1 show concentrations of standards used for calibration curve of phenanthrene, 1-methylphenanthrene, fluoranthene and 9-phenanthrol

Table B 1 Concentrations for calibration curves for quantification. Concentrations are given in µg/mL

PHE	1-MP	FLA	POH
1,066	1	1,003	1,062
0,533	0,5	0,5015	0,531
0,4264	0,1	0,1003	0,1062
0,2132	0,05	0,05015	0,0531
0,1066	0,04	0,04012	0,01062
0,0533	0,02	0,02006	0,00531
0,01066	0,01	0,01003	0,001062
0,00533	0,005	0,005015	0,000531
0,001066	0,001	0,001003	
0,000533	0,0005	0,0005015	

Tables B 2– B 5 shows the calculated calibration parameters for determining solubilities with the TeflonWAF method.

Table B 2 Calculated slope, intercept and R² value for calibration of TeflonWAF solutions for phenanthrene in seawater at 4 °C, 10 °C and 20 °C.

	6	7	8
Slope	268,1164	271,4386	290,3992
Intercept	1,89008	1,881762	1,584013
R^2	0,997537	0,997116	0,996871

Table B 3 Calculated slope, intercept and R² value for calibration of TeflonWAF solutions for phenanthrene in freshwater

	1	2	3
Slope	140,7504	140,7504	-96,2833
Intercept	-1,56129	-1,56129	72,51189
R^2	0,997275	0,997275	0,410718

Table B 4 Calculated slope, intercept and R² value for calibration of TeflonWAF solutions for 1-methylphenanthrene in seawater.

	1	2	3	4
Slope	82,02623	91,17476	97,30241	93,47175
Intercept	-0,87728	-1,55933	-1,23583	-1,04485
R^2	0,997821	0,993567	0,996183	0,995669

Table B 5 Calculated slope, intercept and R² value for calibration of TeflonWAF solutions for fluoranthene in seawater.

	1	2	3	4
Slope	62,61015	66,45033	65,25075	63,88821
Intercept	-0,58098	-0,88663	-1,3519	-0,58847
R^2	0,997875	0,996267	0,966463	0,999807

Tables B 6-B 12 show the calculated calibration parameters for the determination of fibre concentrations and equilibrium times for PAHs and fibres.

Table B 6 Calculated slope, intercept and R^2 value for calibration of phenanthrene in seawater at 4 °C and 20 °C for initial determination of fibre concentrations.

	1d	2d	3d	4d	7d	10d
Slope	156,9049	168,4613	165,2908	173,9489	127,72756	363,951
Intercept	2,160606	2,724242	1,01	-0,62606	-5,3757576	1,860606
R^2	0,99695	0,992809	0,998536	0,997581	0,9886773	0,999655

Table B 7 Calculated slope, intercept and R^2 value for calibration of phenanthrene in seawater at 4 °C and 20 °C with adjusted fibre concentrations (see table 3-6)

	1d	2d
Slope	370,1687	297,9471
Intercept	-3,93357	7,274971
R^2	0,997859	0,989013

Table B 8 Calculated slope, intercept and R^2 value for calibration of phenanthrene in seawater at 10 °C with adjusted fibre concentrations (see table 3-6)

	1d	2d	3d	4d	7d	10d	14d
Slope	325,1558	383,2508	377,3351	150,2833	163,4594	122,3195	121,791
Intercept	3,873073	-2,40566	-3,37523	-3,82593	-0,76638	-0,55991	-2,75913
R^2	0,993366	0,999874	0,999111	0,993052	0,996751	0,999434	0,99491

Table B 9 Calculated slope, intercept and R^2 value for calibration of phenanthrene in freshwater at 20 °C with adjusted fibre concentrations (see table 3-6)

	1d	2d	3d
Slope	364,7242	381,9016	318,7560407
Intercept	-6,81515	-9,34848	-12,90606061
R^2	0,997777	0,997319	0,989874441

Table B 10 Calculated slope, intercept and R² value for calibration of phenanthrene in seawater at 4 °C and 20 °C with final adjusted fibre concentrations (see table 3-7)

	1d	2d	3d	4d	7d	10d	14d
Slope	111,5908	106,423	104,1026	101,148	121,5171	150,8723	166,7565
Intercept	-2,86685	-1,87841	-2,29183	-2,5301	-3,18649	-1,1487	-2,80525
R^2	0,995522	0,997321	0,993184	0,994501	0,990548	0,9991	0,996963

Table B 11 Calculated slope, intercept and R² value for calibration of phenanthrene in seawater at 10 °C with final adjusted fibre concentrations (see table 3-7)

	1d	2d	3d	4d	7d	10d	14d
Slope	127,579	140,7047	162,6007	161,0627	167,1984	152,7393	156,38235
Intercept	-1,58729	-2,93876	-3,81221	-2,02553	-1,98235	-1,35095	-3,166703
R^2	0,997676	0,99508	0,996567	0,998438	0,99864	0,998852	0,9954124

Table B 12 Calculated slope, intercept and R² value for calibration of phenanthrene in freshwater at 20 °C with final adjusted fibre concentrations (see table 3-7)

	1d	2d	3d	4d	7d	10d	14d
Slope	368,5711	367,9943	325,0544	142,1396	164,8703	130,8369	97,81965
Intercept	-0,00141	0,18477	1,653666	-2,72684	-2,42471	-1,84805	-0,71932
R^2	0,999944	0,999939	0,999049	0,995	0,993781	0,998334	0,998976

Table B 13 Calculated slope, intercept and R² value for calibration of 1-methylphenanthrene for determination of fibre concentrations

	1d	2d	3d	
Slope		99,64108	95,41258	81,76656
Intercept		-1,50707	-1,16834	-0,77216
R^2		0,994291	0,99532	0,996902

Table B 14 Calculated slope, intercept and R² value for calibration of fluoranthene for determination of fibre concentrations

	1d	2d	3d	
Slope		66,23031	64,1123	49,00224
Intercept		-0,84905	-0,74319	-0,08781
R^2		0,99721	0,997295	0,999404

Tables B 15- B 20 show the calculated calibration parameters for determination of free PAHs concentration from the sorption kinetics study.

Table B 15 Calculated slope, intercept and R² value for calibration of phenanthrene in seawater at 20 °C for sorption kinetics study

	2t	4t	6t	1d	2d	3d	4d	7d	10d
Slope	146,1564	146,1564	146,1564	134,474	143,3096	155,2596	154,8691	148,6002	148,2972
Intercept	-2,15414	-2,15414	-2,15414	-1,59451	-1,72369	-2,64785	-2,38122	-2,47047	-2,61777
R^2	0,996298	0,996298	0,996298	0,997122	0,9973	0,994474	0,996459	0,998036	0,996711

Table B 16 Calculated slope, intercept and R² value for calibration of phenanthrene in seawater at 10 °C for sorption kinetics study

	2t	4t	6t	1d	2d	3d	4d	7d
Slope	150,3381	150,3381	150,3381	139,224	149,423	141,1623	139,2512	147,6829
Intercept	-2,93999	-2,93999	-2,93999	-2,00563	-2,47379	-0,70186	-0,76382	-0,78862
R^2	0,995592	0,995592	0,995592	0,997387	0,996636	0,999238	0,996067	0,999465

Table B 17 Calculated slope, intercept and R² value for calibration of phenanthrene in seawater at 4 °C for sorption kinetics study

	2t	4t	6t	1d	2d	3d	4d	7d
Slope	132,4182	132,4182	132,4182	135,9696	145,2413	131,1979	117,1746	151,3195
Intercept	-0,83656	-0,83656	-0,83656	-4,13464	-2,7792	-2,4395	-1,58213	-2,84618
R^2	0,998684	0,998684	0,998684	0,974039	0,993427	0,993226	0,987735	0,990759

Table B 18 Calculated slope, intercept and R² value for calibration of phenanthrene in freshwater at 20 °C for sorption kinetics study

	2t	4t	6t	1d	2d	3d	4d	7d
Slope	140,7504	140,7504	140,7504	148,0333	145,3016	138,6978	132,7722	139,7391
Intercept	-1,56129	-1,56129	-1,56129	-1,3131	-1,98117	-0,76807	-1,99216	-1,80983
R^2	0,997275	0,997275	0,997275	0,99845	0,996351	0,99981	0,996151	0,997365

Table B 19 Calculated slope, intercept and R² value for calibration 1-methylphenanthrene in seawater for sorption kinetics study

	2t	4t	6t	1d	2d	3d	4d	7d	10d	14d
Slope	94,62422	94,62422	94,62422	99,6214	102,5247	91,03244	97,30241	90,49613	93,48557	100,1601
Intercept	-1,2196	-1,2196	-1,2196	-1,38461	-1,44939	-0,83887	-1,23583	-1,06323	-1,05533	-1,18578
R^2	0,996985	0,996985	0,996985	0,995342	0,992428	0,996639	0,996183	0,995035	0,995684	0,997232

Table B 20 Calculated slope, intercept and R² value for calibration fluoranthene in seawater for sorption kinetics study

	2t	4t	6t	1d	2d	3d	4d	7d	10d	14d
Slope	146,1564	146,1564	146,1564	134,474	143,3096	155,2596	154,8691	148,6002	148,2972	150,3381
Intercept	-2,15414	-2,15414	-2,15414	-1,59451	-1,72369	-2,64785	-2,38122	-2,47047	-2,61777	-2,93999
R^2	0,996298	0,996298	0,996298	0,997122	0,9973	0,994474	0,996459	0,998036	0,996711	0,995592

Table 21 show the calculated calibration parameters for the adsorption isotherm studies of phenanthrene, 1-methylphenanthrene and fluoranthene.

Table B 21 Calculated slope, intercept and R² value for calibration of PAHs for the adsorption isotherm studies

	PHE SW 20 °C	PHE SW 10 °C	PHE SW 4 °C	PHE FW 20 °C	PHE FW 20 °C	1-MP	FLA
Slope	131,896367	132,683522	132,757578	139,759769	139,7391	99,2774641	68,5727084
Intercept	-0,3528073	-1,0515197	-1,0074124	-0,9072040	-1,8098324	-1,3067031	-0,6198653
R^2	0,99440387	0,99646433	0,99841266	0,99922983	0,99736474	0,99353977	0,99785936

Appendix C: Fibre weights

Tables C 1 – C 3 show fibre amounts (mg) used in Uptake kinetics for PHE.

Table C 1 Fibre weight of Uptake kinetics 1 in mg for PHE in milligram

	Replicate				Replicate		
SW 20C PHE	1	2	3	SW 5C PHE	1	2	3
PES-W	4,02	4,05	4,08	PES-W	3,99	4,02	4,02
PES-B	4,02	4,03	4,12	PES-B	4,02	4,03	3,93
PAC-B	3,89	3,97	4,16	PAC-B	3,96	4,11	4
PA-W	4,2	4,02	3,97	PA-W	4,13	4,16	4,1
Wool	3,91	4,06	3,95	Wool	3,95	4,14	3,98

Table C 2 Fibre weight of Uptake kinetics 2 in mg for PHE in milligram

	Replicate				Replicate		
SW 20C PHE	1	2	3	SW 5C PHE	1	2	3
PES-W	20,36	20,58	19,95	PES-W	20,07	20,33	19,75
PES-B	19,67	20,38	19,52	PES-B	20,63	20,52	20,42
PAC-B	20,87	20,16	20,01	PAC-B	19,66	20,52	19,64
PA-W	3,91	3,81	4,06	PA-W	4,06	4,04	4,1
Wool	8,13	7,89	7,82	Wool	7,95	7,96	7,87
	Replicate				Replicate		
SW 10C PHE	1	2	3	FW 20C PHE	1	2	3
PES-W	19,76	20,15	20,02	PES-W	16,16	16,05	15,98
PES-B	19,58	20,37	19,87	PES-B	16,06	16,23	16,25
PAC-B	20,16	20,6	19,66	PAC-B	24,02	24,2	23,81
PA-W	4,14	4,16	4,2	PA-W	3,92	4,12	4,04
Wool	8,23	8,24	8,19	Wool	10,04	9,87	9,95

Table C 3 Fibre weight of Uptake kinetics 3 in mg for PHE in milligram

SW 20C PHE	Replicate			SW 5C PHE	Replicate		
	1	2	3		1	2	3
PES-W	15,98	16,03	16,1	PES-W	16,04	15,88	16,05
PES-B	16	15,93	16,04	PES-B	16,01	15,84	15,99
PAC-B	-	-	-	PAC-B	-	-	-
PA-W	4,16	4,12	4,16	PA-W	3,92	3,93	4,07
Wool	16,05	16,06	15,92	Wool	16,1	16,14	16,26

SW 10C PHE	Replicate			FW 20C PHE	Replicate		
	1	2	3		1	2	3
PES-W	16,2	16,27	16,21	PES-W	16,25	15,99	15,94
PES-B	15,97	15,9	16,03	PES-B	16,07	16,03	15,94
PAC-B	-	-	-	PAC-B	24,05	23,92	23,85
PA-W	3,9	4,08	4,12	PA-W	4,08	3,88	4,18
Wool	16,2	16,03	16,1	Wool	10,26	9,91	9,96

Table C 4 show fibre amounts (mg) used in Uptake kinetics for 1-MP and FLA.

Table C 4 Fibre weight of Uptake kinetics in mg for 1-MP and FLA in milligram

1-MP	100 mg/mL	400 mg/mL	800 mg/mL	FLA	100 mg/mL	400 mg/mL	800 mg/mL
PES-W	3,9	16,1	32,32	PES-W	4,02	16,03	31,98
PAC-B	3,99	16,26	32,15	PAC-B	4,01	15,7	32,55
PA-W	4,07	16,14	32,43	PA-W	3,85	15,8	31,93
Wool	4,13	16,02	32,42	Wool	4,17	15,92	32,11

Table C 5 show fibre amounts (mg) used in precision kinetics for PHE.

Table C 5 Fibre weight of Precision kinetics in mg for PHE in milligram

SW 20C PHE	Replicate			SW 5C PHE	Replicate		
	1	2	3		1	2	3
PES-W	16,08	16,22	16,06	PES-W	16,09	15,93	16,18
PES-B	16,01	16,23	16,06	PES-B	16,05	16,24	16,2
PA-W	3,96	4,07	4,04	PA-W	4,17	3,91	4,06
Wool	16,06	15,96	15,94	Wool	16,16	16,07	16,07

SW 10C PHE	Replicate			FW 20C PHE	Replicate		
	1	2	3		1	2	3
PES-W	15,94	15,75	15,95	PES-W	15,77	16,15	16,15
PES-B	16,28	15,98	16,03	PES-B	15,92	15,97	15,97
PA-W	3,93	3,8	3,91	PA-W	4,16	4,05	4,05
Wool	15,95	16,02	16,01	Wool	16,13	16,17	16,13

Table C 6 show fibre amounts (mg) used in precision kinetics for 1-MP and FLA.

Table C 6 Fibre weight of Precision kinetics in mg for PHE in milligram

1-MP	Replicate			FLA	Replicate		
	1	2	3		1	2	3
PES-W	16,27	16,03	15,86	PES-W	16,25	16,06	16,03
PAC-B	-	-	-	PAC-B	32,14	31,64	31,89
PA-W	4,12	4,02	4,03	PA-W	3,9	3,98	4
Wool	16,11	16,18	16,24	Wool	16,02	15,82	16,02

Tables C 8 – C 13 shows the fibre amounts used for isotherms of PHE in seawater at 20 C, 10 C and 5 C, PHE in freshwater at 20 C, 1-MP in seawater at 20 C and FLA in seawater at 20 C

Table C 7 amount of fibre used for adsorption isotherm PHE at 20 C in seawater in milligram

	Replicate				Replicate		
PES-W	1	2	3	PES-B	1	2	3
10 %	7,89	7,96	7,84	10 %	7,95	7,84	8,12
25 %	7,94	8,15	8,10	25 %	8,17	8,01	8,14
40 %	7,84	8,07	7,92	40 %	7,85	8,09	7,83
55 %	7,94	7,88	7,87	55 %	8,12	7,93	8,01
70 %	7,96	7,99	8,08	70 %	8,05	7,96	7,89
85 %	7,84	8,05	8,03	85 %	7,94	8,15	7,99
100 %	7,98	7,89	7,98	100 %	8,08	8,14	7,84
	Replicate				Replicate		
PA-W	1	2	3	Wool	1	2	3
10 %	2,01	1,91	2,04	10 %	7,95	8,07	8,11
25 %	2,06	2,12	1,96	25 %	7,89	8,04	8,06
40 %	2,04	2,08	2,07	40 %	8,07	8,12	7,87
55 %	1,97	1,95	1,98	55 %	8,02	7,94	7,85
70 %	2,03	2,01	1,95	70 %	7,97	8,02	7,90
85 %	2,09	2,05	1,93	85 %	7,92	7,96	8,02
100 %	1,97	2,02	2,05	100 %	7,97	7,95	8,11

Table C 8 amount of fibre used for adsorption isotherm PHE at 10C in seawater in milligram

PES-W	Replicate 1	2	3	PES-B	Replicate 1	2	3
10 %	7,98	8,18	7,89	10 %	8,12	8,09	8,00
25 %	7,86	8,03	7,99	25 %	7,96	7,95	7,87
40 %	8,13	7,96	8,12	40 %	8,16	8,17	7,98
55 %	8,05	7,84	8,10	55 %	7,88	7,93	8,16
70 %	8,08	8,11	7,88	70 %	8,14	8,02	8,03
85 %	8,01	7,97	8,18	85 %	7,89	8,19	8,13
100 %	8,06	7,99	7,97	100 %	8,08	8,08	8,04

PA-W	Replicate 1	2	3	Wool	Replicate 1	2	3
10 %	2,01	2,06	1,99	10 %	8,05	7,96	8,01
25 %	1,91	1,95	2,09	25 %	8,14	7,91	7,94
40 %	2,09	2,08	1,98	40 %	8,15	8,16	7,91
55 %	1,92	1,98	2,03	55 %	8,08	7,96	8,03
70 %	2,09	2,01	2,03	70 %	7,93	8,17	8,09
85 %	2,07	2,03	1,90	85 %	7,89	8,18	8,04
100 %	1,90	2,08	1,92	100 %	7,96	7,93	8,08

Table C 9 amount of fibre used for adsorption isotherm PHE at 5C in seawater in milligram

PES-W	Replicate 1	2	3	PES-B	Replicate 1	2	3
10 %	7,92	8,06	7,97	10 %	8,06	7,90	7,97
25 %	8,05	7,85	8,16	25 %	8,18	8,14	7,83
40 %	8,04	7,97	8,14	40 %	7,87	8,07	8,08
55 %	7,88	8,05	8,07	55 %	7,99	8,14	8,13
70 %	8,18	7,87	8,08	70 %	8,14	8,05	7,86
85 %	8,08	7,96	8,08	85 %	8,13	8,15	7,97
100 %	8,02	7,84	7,86	100 %	8,04	8,11	7,92

PA-W	Replicate 1	2	3	Wool	Replicate 1	2	3
10 %	1,92	1,9	1,98	10 %	7,86	7,97	8,14
25 %	2,06	1,93	2,01	25 %	7,89	8,15	8,01
40 %	2,1	1,9	1,96	40 %	8,01	8,02	8,17
55 %	1,98	1,94	2,05	55 %	8,01	8,16	7,96
70 %	2,05	1,94	2,01	70 %	7,86	7,88	7,97
85 %	1,91	2,05	2,07	85 %	7,98	8,17	8,08
100 %	1,99	2,02	2,04	100 %	7,94	7,90	8,05

Table C 10 amount of fibre used for adsorption isotherm PHE at 20C in freshwater in milligram

PES-W	Replicate			PES-B	Replicate		
	1	2	3		1	2	3
10 %	7,87	8,06	7,99	10 %	8,01	7,96	8,07
25 %	8,09	8,00	8,16	25 %	7,94	8,03	8,02
40 %	7,90	8,95	7,97	40 %	8,01	8,01	8,13
55 %	7,98	7,89	8,12	55 %	7,96	8,01	7,89
70 %	7,94	8,14	8,00	70 %	8,11	8,03	8,10
85 %	7,87	7,95	7,96	85 %	8,10	8,16	8,13
100 %	8,06	7,98	8,01	100 %	8,10	8,02	7,98

PA-W	Replicate			Wool	Replicate		
	1	2	3		1	2	3
10 %	2,08	1,93	2,06	10 %	8,02	8,03	8,01
25 %	1,92	1,93	2,09	25 %	8,04	8,11	7,95
40 %	1,95	1,95	2,04	40 %	8,09	8,15	7,97
55 %	1,97	2,01	2,07	55 %	8,00	8,08	7,92
70 %	1,96	1,96	1,90	70 %	8,02	8,07	8,01
85 %	1,91	2,02	1,97	85 %	8,09	8,04	8,04
100 %	2,08	2,03	2,06	100 %	8,14	8,08	8,14

Table C 11 amount of fibre used for adsorption isotherm 1-MP at 20C in seawater in milligram

PES-W	Replicate			PA-W	Replicate		
	1	2	3		1	2	3
40 %	8,10	7,99	8,21	40 %	2,09	1,93	2,09
50 %	7,98	8,09	8,19	50 %	1,95	2,12	2,08
60 %	8,12	8,08	8,15	60 %	1,92	2,05	2,02
70 %	8,11	8,15	7,86	70 %	2,09	2,00	2,08
80 %	7,88	8,18	7,99	80 %	2,06	1,95	2,11
90 %	7,97	8,05	8,02	90 %	1,99	2,10	1,90
100 %	8,04	8,20	8,14	100 %	1,90	2,02	2,05

Wool	Replicate		
	1	2	3
40 %	7,95	7,97	8,00
50 %	8,05	7,96	8,01
60 %	7,87	7,99	8,13
70 %	8,01	7,89	8,03
80 %	7,95	7,91	8,06
90 %	7,93	8,14	7,94
100 %	7,96	7,91	8,13

Table C 12 amount of fibre used for adsorption isotherm FLA at 20C in seawater in milligram

PES-W	Replicate			PA-W	Replicate		
	1	2	3		1	2	3
40 %	8,09	8,06	7,98	40 %	1,93	1,96	2,04
50 %	7,94	7,92	8,13	50 %	1,95	2,00	1,90
60 %	7,97	7,93	7,97	60 %	2,00	1,99	1,95
70 %	7,88	7,87	7,90	70 %	2,06	1,98	1,97
80 %	8,00	7,97	7,97	80 %	2,08	2,06	1,97
90 %	7,89	8,05	8,09	90 %	1,89	2,04	1,89
100 %	8,11	7,84	7,90	100 %	1,96	2,01	1,94

Wool	Replicate		
	1	2	3
40 %	8,15	7,91	7,89
50 %	8,02	8,06	7,98
60 %	7,84	8,06	7,99
70 %	7,99	7,98	8,09
80 %	7,91	7,96	7,96
90 %	8,03	7,90	7,99
100 %	8,06	8,09	8,07

Appendix D: Concentrations from samples from determination of equilibrium time and fibre concentrations experiments

Tables D 1-D 2 show the free concentration of phenanthrene from the initial determination of fibre concentrations.

Table D 1 Initial investigation of fibre concentrations of phenanthrene in seawater at 4 °C. All fibre weights were 100 mg/mL. Concentrations are given in µg/L

	1d	2d	3d	4d	7d	10d
PES-W 1	91,38909	86,52286	116,7034	101,1565	140,81345	57,80832
PES-W 2	120,7062	111,4544	86,45369	89,02651	150,5999	53,96165
PES-W 3	110,5089	91,27172	81,61373	85,23229	157,1764	55,88499
PES-B 1	118,1569	78,80596	84,03371	82,35788	143,86682	47,36735
PES-B 2	123,2555	104,3311	108,8385	97,3048	161,63902	47,91688
PES-B 3	94,57573	97,80141	111,8635	102,4787	140,73516	44,34497
PAC-B 1	125,8048	115,6096	107,6285	99,60433	165,00556	67,15024
PAC-B 2	123,2555	117,9841	89,47866	110,5271	148,25115	46,26831
PAC-B 3	85,65313	112,048	111,8635	92,70575	156,39348	53,13736
PA-W 1	62,07196	63,96576	62,49591	46,14034	96,891837	18,79208
PA-W 2	76,0932	58,62328	54,99398	52,46404	96,891837	22,08922
PA-W 3	38,4908	63,37215	52,9975	53,6138	90,628505	18,51731
Wool 1	34,66682	85,33564	74,9588	91,55599	126,64266	45,16926
Wool 2	100,3117	99,58223	79,19376	82,35788	129,0697	38,57496
Wool 3	84,37847	97,2078	78,58876	75,4593	147,7814	43,24592
Ctr 1	88,20244	116,7969	93,71362	92,13087	165,00556	56,98404
Ctr 2	86,29046	119,1713	93,10863	86,95694	190,9201	42,6964
Ctr 3	104,773	109,6736	96,1336	91,78594	168,13723	50,11498
Blank	-12,7887	-15,3996	-3,50897	4,633894	42,90975	-4,72758

Table D 2 Initial investigation of fibre concentrations of phenanthrene in seawater at 20 °C. All fibre weights were 100 mg/mL. Concentrations are given in µg/L

	1d	2d	3d	4d	7d	10d
PES-W 1	223,3161	233,144	186,8827	167,4404	258,1726	102,0451
PES-W 2	185,7137	231,9568	203,8226	177,7882	306,7134	95,72552
PES-W 3	214,3935	266,3861	191,7227	197,3342	299,5889	98,7479
PES-B 1	165,9566	240,2673	180,8328	207,6821	332,3931	119,3551
PES-B 2	227,1401	236,1121	201,4026	183,537	309,8451	118,5308
PES-B 3	197,1857	219,491	173,9964	183,537	306,7134	102,0451
PAC-B 1	176,1538	272,3222	168,1279	215,1555	359,9517	139,9622
PAC-B 2	209,9322	264,6053	188,0927	201,3584	358,3859	130,8951
PAC-B 3	171,0552	266,9797	183,8578	205,9574	273,8309	107,2655
PA-W 1	85,65313	129,2626	83,42872	88,68158	158,7422	43,79544
PA-W 2	137,9141	141,7284	87,66368	96,72992	199,4539	64,40262
PA-W 3	104,1357	95,42698	76,77378	77,75883	138,3864	25,9359
Wool 1	110,5089	231,9568	136,0632	205,3825	312,9768	-5,11224
Wool 2	175,5165	237,8929	166,3129	178,938	282,443	-5,11224
Wool 3	173,6045	223,0527	169,3379	204,5777	262,0872	-5,11224
Ctr 1	164,0446	244,4226	182,6478	207,6821		-5,11224
Ctr 2	206,1083	185,0618	177,2028	201,9333	295,7526	-5,11224
Ctr 3	199,735	205,2445	182,0428	208,2569	278,5284	-5,11224
Blank	-13,1966	-10,9476	3,690465	3,714083	43,65352	-5,11224

Tables D 3 – D 6 shows the free concentration phenanthrene with adjusted fibre concentrations.

Table D 3 Initial investigation of fibre concentrations of phenanthrene in seawater at 4 °C with adjusted fibre weights (see Table 3-6). Concentrations are given in µg/L

	1	2	3
PES-W 1	163,066	143,5219	130,9514
PES-W 2	165,7792	144,0654	
PES-W 3	164,1512	145,9676	136,1198
PES-B 1	164,9652	151,9459	
PES-B 2	167,6784	147,8698	137,9656
PES-B 3	167,4071	148,685	
PAC-B 1		187,5443	
PAC-B 2	195,0815	189,4465	
PAC-B 3	194,2676	190,5335	
PA-W 1	123,1822	62,54236	101,3564
PA-W 2	117,7559	83,73834	104,4328
PA-W 3	115,8566	79,39044	97,04939
Wool 1	162,5233	106,0213	159,1928
Wool 2	162,7947	84,55357	157,9623
Wool 3	160,3528	121,5107	155,1935
Ctr 1		139,9892	189,9569
Ctr 2	191,5544	150,3155	188,4187
Ctr 3	195,3528	128,8477	190,5722
Blank	0,356533	-0,25753	-5,08735

Table D 4 Initial investigation of fibre concentrations of phenanthrene in seawater at 20 °C with adjusted fibre weights (see Table 3-6). Concentrations are given in µg/L

	1	2
PES-W 1	189,4638	143,3538
PES-W 2	192,1653	140,7638
PES-W 3	182,9803	162,6347
PES-B 1	185,6818	156,5914
PES-B 2	187,5728	158,6059
PES-B 3	212,4263	178,4623
PAC-B 1	248,626	248,1039
PAC-B 2	244,5738	248,3917
PAC-B 3	241,8724	239,4707
PA-W 1	148,6716	120,6195
PA-W 2	155,6954	116,8785
PA-W 3	140,8373	107,9574
Wool 1	188,3832	197,4555
Wool 2	211,6159	209,8298
Wool 3	205,4025	212,7076
Ctr 1	238,6306	226,8086
Ctr 2	245,9246	224,2186
Ctr 3	257,811	231,413
Blank	10,75339	0,847519

Table D 5 Initial investigation of fibre concentrations of phenanthrene in seawater at 10 °C with adjusted fibre weights (see Table 3-6). Concentrations are given in µg/L

	1d	2d	3d	4d	7d	10d	14d
PES-W 1	97,88208	91,33877	85,26965	83,34878	46,90084	55,26434	57,13998
PES-W 2	98,49717	90,55599	83,14951	81,35255	46,28907	56,8994	54,67674
PES-W 3	92,65382	88,20766	81,82443	82,68337	46,90084	54,44681	53,85566
PES-B 1	88,96328	85,33747	83,94456	80,02173	48,12439	56,08187	57,13998
PES-B 2	94,80663	89,77321	88,71486	84,01419	53,63034	62,62212	70,27724
PES-B 3	103,7254	87,6858	92,6901	85,34501	46,90084	60,98706	66,17185
PAC-B 1	118,18	112,9956	118,6617	112,6268	78,10125	107,5863	118,7209
PAC-B 2	116,0272	114,5612	117,0716	113,9577	76,87771	96,95842	116,2577
PAC-B 3	114,7971	116,3876	114,4215	109,2998	81,16012	105,1337	112,1523
PA-W 1	83,42747	66,28989	63,5383	68,70976	37,11248	40,54878	53,03458
PA-W 2	78,8143	67,85545	60,3581	62,72107	32,83007	39,73125	52,21351
PA-W 3	81,88975	69,68193	8,944916	60,72484	35,88893	41,36631	53,85566
Wool 1	86,81047	88,99043	8,944916	89,33747	56,68921	72,43249	83,41451
Wool 2	84,35011	86,6421	8,944916	89,33747	60,35984	72,43249	81,77235
Wool 3	102,8028	83,77192	8,944916	84,6796	62,19516	76,52015	86,69882
Ctr 1	126,4838	118,9969	8,944916	121,2772	78,71302	111,674	109,689
Ctr 2	129,2517	126,8247	8,944916	117,2847	86,66607	110,0389	115,4366
Ctr 3	127,7139	124,4763	8,944916	119,9463	81,77189	109,2214	115,4366
Blank	-11,7269	6,590085	8,944916	25,63111	4,878172	4,691873	22,82709

Table D 6 Initial investigation of fibre concentrations of phenanthrene in freshwater at 20 °C with adjusted fibre weights (see Table 3-6). Concentrations are given in µg/L

	1d	2d	3d
PES-W 1	315,6225	224,5303	195,7800093
PES-W 2	260,5124	260,9271	162,5257375
PES-W 3	308,4938	261,4508	177,8979952
PES-B 1	298,8975	24,47878	185,1135448
PES-B 2	290,9463	24,47878	40,48883459
PES-B 3	299,7201	24,47878	256,9553205
PAC-B 1	385,2642	24,47878	40,48883459
PAC-B 2	394,0379	24,47878	40,48883459
PAC-B 3	355,9269	24,47878	40,48883459
PA-W 1	250,6419	24,47878	177,2705561
PA-W 2	251,4644	24,47878	202,6818393
PA-W 3	247,6259	24,47878	200,1720829
Wool 1	310,6873	24,47878	267,9355046
Wool 2	320,5577	24,47878	257,5827596
Wool 3	327,4122	24,47878	234,6812328
Ctr 1	388,8285	24,47878	40,48883459
Ctr 2	350,1692	24,47878	40,48883459
Ctr 3	366,6199	24,47878	40,48883459
Blank	19,01478	24,47878	40,48883459

Tables D 7 – D 10 shows the free concentration phenanthrene with final adjustment of fibre concentrations.

Table D 7 Initial investigation of fibre concentrations of phenanthrene in seawater at 20 °C with adjusted fibre weights (see Table 3-7). Concentrations are given in μg/L

	1d	2d	3d	4d	7d	10d	14d
PES-W 1	20,6	18,5	14,4	13,6	18,1	20	16,7
PES-W 2	21,4	16,6	15,7	13,9	17,8	19,5	16,9
PES-W 3	22,7	18,1	16,6	15,8	20,3	23,7	19,9
PES-B 1	21,7	17,7	15,7	15,7	18,2	19,7	17,4
PES-B 2	20,1	17	15,1	8,5	17,7	19,3	18
PES-B 3	15,4	11,3	9,3	8,3	9,2	9,7	7,9
PA-W 1	15	12,6	10,2	10,9	13,7	16,7	14,8
PA-W 2	14,8	13,1	11,4	9,9	14,4	15,6	16,1
PA-W 3	15,1	11,4	9,6	12,4	13,9	16,6	15,9
Wool 1	16,5	15,4	16,1	16,9	13,2	23,5	21,6
Wool 2	15,7	15	15,7	16,3	17,4	20,6	21,1
Wool 3	15,8	14	14,6	18,1	19,4	22,7	
Ctr 1	28,1	23,3	22,4	17,2	31,4	34,5	34,9
Ctr 2	22,7	23,9	22,6	26,3	32,5	34,3	33,4
Ctr 3	24,1	24,4	22,2	25,3	25,8	35,9	31,7
Blank	0,024	0,051	0,06	0,04	0,104	0,12	0,17

Table D 8 Initial investigation of fibre concentrations of phenanthrene in seawater at 4 °C with adjusted fibre weights (see Table 3-7). Concentrations are given in µg/L

	1d	2d	3d	4d	7d	10d	14d
PES-W 1	103,6542	93,76176	89,25647	100,1513	96,17153	87,15121	81,58751
PES-W 2	98,27738	84,3653	81,57175	81,36694	91,23396	71,24371	65,99592
PES-W 3	98,27738	91,88247	84,45352	85,32155	87,11931	73,89496	70,19366
PES-B 1	92,90059	82,486	78,68997	67,52584	61,60851	67,92965	64,79657
PES-B 2	96,48512	82,486	82,53234	82,35559	92,87982	71,90652	70,79333
PES-B 3	95,58899	84,3653	80,61116	75,43504	73,12951	67,92965	64,79657
PA-W 1	88,41993	74,96883	69,08406	61,59394	64,07729	47,38247	46,20659
PA-W 2	89,31607	75,90848	69,08406	59,61664	56,67093	46,71966	45,60692
PA-W 3	86,62767	65,57237	69,08406	71,48044	68,19194	45,39403	46,20659
Wool 1	92,00446	65,57237	65,2417	57,63934	69,01487	57,32465	58,20012
Wool 2	90,2122	66,51201	66,20229	47,75283	62,43144	57,32465	59,39948
Wool 3	73,1857	63,69307	65,2417	65,54854	75,5983	54,6734	58,20012
Ctr 1	114,4077	112,5547	112,3107	109,0492	134,8492	109,6868	103,1759
Ctr 2	113,5116	107,8565	107,5077	110,0378	127,4428	103,7215	96,57943
Ctr 3	115,3039	114,434	103,6653	110,0378	126,6199	111,0124	106,7739
Blank	26,0223	18,22358	22,3321	25,12263	33,7935	8,037931	17,03832

Table D 9 Initial investigation of fibre concentrations of phenanthrene in seawater at 10 °C with adjusted fibre weights (see Table 3-7). Concentrations are given in μg/L

	1d	2d	3d	4d	7d	10d	14d
PES-W 1	14,6	13,9	10,1	14,6	14,3	11,3	9,4
PES-W 2	14,4	13,1	15,4	14,5	13,7	13	11
PES-W 3	15	12,5	15,8	16,1	12,5	12,2	10,6
PES-B 1	14,7	13	16,5	15	13,2	12,9	12,1
PES-B 2	14,2	12,8	16,1	12,2	13,3	12,2	10,8
PES-B 3	14,2	14	16,4	14,7	13,5	9,8	
PA-W 1	11,5	7,7	10,6	9,7	8,5	5,4	5,5
PA-W 2	12	9,7	6	9,4	8,1	7,7	6,9
PA-W 3	10,2	8	6,9	5	5,7	6,4	4,8
Wool 1	10,2	9,8	12,8	12,6	12,5	13,1	11,5
Wool 2	10,4	10,8	12,8	12,5	12,8	9,6	11,9
Wool 3	9,7	10,5	12,1	12,5	12,3	9,6	11,1
Ctr 1	16,2	17,5	23,1	18,7	20,9	20,3	20,1
Ctr 2	16,7	17,7	23,6	21,1	21,2	21,4	18,4
Ctr 3	16,9	18	22,3	23,2	23	20,4	19,9
Blank	0,005	0,009	0,07	0,09	0,066	0,032	

Table D 10 Initial investigation of fibre concentrations of phenanthrene in freshwater at 20 °C with adjusted fibre weights (see Table 3-7). Concentrations are given in µg/L

	1d	2d	3d	4d	7d	10d	14d
PES-W 1	163,066	143,5219	130,9514	119,7896	88,70432	95,90603	95,27043
PES-W 2	165,7792	144,0654		116,2719	94,16315	98,19896	93,22585
PES-W 3	164,1512	145,9676	136,1198	116,2719	90,52393	98,96327	93,22585
PES-B 1	164,9652	151,9459		121,1966	94,16315	95,90603	94,24814
PES-B 2	167,6784	147,8698	137,9656	142,3026	92,95008	96,67034	100,3819
PES-B 3	167,4071	148,685		133,8602	95,98277	110,4279	103,4487
PAC-B 1		187,5443		180,2934	143,2927	152,465	172,9644
PAC-B 2	195,0815	189,4465		176,7758	146,3254	153,2293	168,8753
PAC-B 3	194,2676	190,5335		183,1076	144,5058	157,0509	167,853
PA-W 1	123,1822	62,54236	101,3564	106,4224	74,14742	85,97	97,31501
PA-W 2	117,7559	83,73834	104,4328	102,9047	80,81933	85,20569	89,13669
PA-W 3	115,8566	79,39044	97,04939	98,68355	77,1801	78,32689	81,98067
Wool 1	162,5233	106,0213	159,1928	138,0814	109,9331	129,5357	143,318
Wool 2	162,7947	84,55357	157,9623	141,5991	119,6377	132,5929	148,4295
Wool 3	160,3528	121,5107	155,1935	141,5991	103,8678	122,6569	146,3849
Ctr 1		139,9892	189,9569	177,4793		167,7512	191,3656
Ctr 2	191,5544	150,3155	188,4187	171,851	135,4077	154,7579	175,009
Ctr 3	195,3528	128,8477	190,5722	205,6206	132,375	149,4078	173,9867
Blank	0,356533	-0,25753	-5,08735	19,53603	15,73786	14,23947	7,547767

Tables D 11-D 12 show the free concentration of 1-methylphenanthrene and fluoranthene for determination of fibre concentration.

Table D 11 free concentration of 1-methylphenanthrene for determination of sufficient fibre concentrations. Concentrations are given in µg/L

	1d	2d	3d
PES-W 4 mg	47,24021	41,59134	
PES-W 16 mg	35,19698	27,9663	25,34244
PES-W 32 mg	28,17177	21,25859	
PA-W 4 mg	26,16456	20,42013	17,51528
PA-W 16 mg	18,33647	14,23646	
PA-W 32 mg	17,13214	14,02684	
PAC-B 4 mg	56,27263	51,02406	
PAC-B 16 mg	56,27263	47,87982	
PAC-B 32 mg	49,24741	45,78366	
Wool 4 mg	37,20419	39,49518	
Wool 16 mg	31,18257	29,01438	27,78843
Wool 32 mg	23,95664	21,57302	
Ctrl 1	56,27263	49,97598	55,91729
Ctrl 2	58,27983	51,02406	58,36327
Ctrl 3	53,26182	53,12022	55,91729

Table D 12 free concentration of fluoranthene for determination of sufficient fibre concentrations. Concentrations are given in µg/L

	1d	2d	3d
PES-W 4 mg	46,03703	41,22745	
PES-W 16 mg	30,9382	26,4097	10,36292
PES-W 32 mg	23,99274	19,70272	
PA-W 4 mg	19,4631	16,73917	5,669257
PA-W 16 mg	15,08444	12,46542	
PA-W 32 mg	13,98222	13,15171	
PAC-B 4 mg	53,58645	53,70556	
PAC-B 16 mg	47,54692	47,4665	
PAC-B 32 mg	43,01727	36,54816	26,28056
Wool 4 mg	38,48762	38,10792	
Wool 16 mg	24,5967	24,53798	14,24029
Wool 32 mg	20,06705	18,45491	
Ctrl 1	55,09633	55,26532	46,68779
Ctrl 2	55,09633	55,26532	50,76924
Ctrl 3	53,58645	55,26532	50,76924

Appendix E: Concentrations determined from samples from sorption kinetics experiments

Tables E 1 to E 6 shows the calculated free concentrations of PAHs from the sorption kinetics study.

Table E 1 Calculated free concentration of 1-methylphenanthrene in seawater at 20 °C. Concentrations are given in µg/L

	2t	4t	6t	1d	2d	3d	4d	7d	10d
PES-W	265,8395	277,4709	287,0497	235,6925	243,6941	211,5673	191,6537	191,591	181,5123
PES-W	256,2607	284,3129	276,1025	249,078	249,2764	219,9403	196,8193	212,4524	190,9528
PES-W	264,4711	281,5761	265,8395	266,9253	253,4631	235,3983	211,6706	222,5466	210,5081
PES-B	252,8397	276,7867	254,2081	257,258	236,0184	228,9575	208,4421	203,0311	184,2096
PES-B	269,9447	274,7341	256,2607	240,898	226,2493	203,1942	189,7166	186,2075	173,4205
PES-B	248,7345	269,2605	258,3133	234,2052	218,5736	199,9738	185,1966	175,4403	161,957
PA-W	241,2084	239,84	217,9456	171,7396	164,8438	149,7353	137,4143	151,8872	153,8651
PA-W	226,8402	222,0508	196,0512	150,9177	141,8167	135,5655		143,8118	135,6585
PA-W	222,0508	219,314	194,6828	150,1741	146,7012	131,701	116,7517	130,3529	134,9841
Wool	191,9461	193,3144	196,7354	185,1251	194,8488	182,5835	161,9512	180,1509	188,9298
Wool	183,0515	196,7354	191,9461	183,6378	188,5686	172,9223	159,3683	173,4215	190,2785
Wool	189,2093	185,1041	193,3144	180,6633	192,7554	178,075	158,7226	190,2451	186,9069
Ctrl 1	280,8919	292,5233	292,5233	304,8509	284,8637	271,4669	254,2872	266,961	248,2701
Ctrl 2	259,6817	282,9445	284,9971	292,209	300,2151	286,9249	252,9958	285,8035	288,7294
Ctrl 3	252,8397	285,6813	293,2075	266,9253	281,3747	261,8057	235,5617	252,1562	257,7106
Blank	14,88912	14,97807	14,91649	12,31101	12,30688	17,32488	15,6663	16,86046	17,97588

Table E 2 Calculated free concentration of 1-methylphenanthrene in seawater at 10 °C. Concentrations are given in µg/L

	2t	4t	6t	1d	2d	3d	4d	7d
PES-W	149,9286	157,9106	148,5983	123,5823	135,0113	119,0252	113,9223	116,3887
PES-W	151,2589	150,5938	149,9286	115,6814	122,2957	114,7747	102,4323	107,586
PES-W	149,9286	149,2634	147,2679	122,8641	124,9727	118,3167	108,1773	111,6488
PES-B	144,6073	143,2769	140,6163	106,3439	114,934	105,5655		96,0749
PES-B	149,9286	141,9466	141,9466	104,1891	114,934	98,48142	90,94227	96,75203
PES-B	152,5893	147,9331	142,6118	109,9353	124,3034	106,9823	104,5867	96,75203
PA-W	152,5893	150,5938	147,9331	100,5978	98,20302	74,39566	64,37158	62,21859
PA-W	152,5893	149,2634	148,5983	95,56992	96,86453	77,22928	66,52596	60,18721
PA-W	147,9331	137,2904	131,3039	84,07765	82,81047	63,76959	60,06281	52,73882
Wool	117,3354	108,0231	100,7062	74,74018	85,48744	69,43683	68,68034	
Wool	117,3354	112,0141	106,6927	72,58538	85,48744	78,64609	69,39846	75,76112
Wool	117,3354	112,6792	103,3669	75,45845	88,1644	71,56204	67,96221	74,40686
Ctrl 1	152,5893	147,2679	147,2679	124,3006	139,696	128,9428	115,3586	105,5547
Ctrl 2	151,9241	149,2634	150,5938	125,0189	144,3807	126,1092	110,3317	127,8998
Ctrl 3	145,9376	151,2589	149,9286	119,2727	141,0344	132,4848	126,8486	135,3482
Blank	19,75537	19,6556	19,69551	14,79364	16,87684	5,09244	5,564166	5,68532

Table E 3 Calculated free concentration of 1-methylphenanthrene in seawater at 5 °C. Concentrations are given in µg/L

	2t	4t	6t	1d	2d	3d	4d	7d
PES-W	109,0224	97,69469	99,20506	102,4836	72,83882	75,75958	78,36274	53,17342
PES-W	111,288	106,7569	110,5328	118,6636	84,54348	91,00373	83,4833	62,42537
PES-W	108,2673	100,7154	102,2258	113,5154	85,23199	88,71711	89,45729	70,35561
PES-B	108,2673	96,93951	104,4913	114,9864	85,9205	88,71711	87,75044	71,67732
PES-B	109,7776	95,42914	103,7362	116,4573	87,98603	88,71711	92,871	56,47769
PES-B	113,5535	95,42914	109,7776	118,6636	85,9205	90,24152	90,31072	66,39049
PA-W	121,8606	103,7362	104,4913	116,4573	85,9205	89,47932	89,45729	56,47769
PA-W	121,8606	102,981	107,5121	111,3091	82,47795	83,38166		56,47769
PA-W	96,18433	97,69469	95,42914	103,9545	77,65838	76,52179	68,97504	51,85172
Wool	73,52883	84,1014	70,5081	84,83255	69,39627	74,23517	59,58735	57,7994
Wool	76,54957	77,30475	73,52883	84,83255	68,01925	71,18634	63,00106	61,10367
Wool	74,28402	75,0392	74,28402	81,89071	68,01925	76,52179	63,85448	55,15598
Ctrl 1	103,7362	108,2673	115,8191	129,6955	115,5264	134,4496	112,4998	92,82463
Ctrl 2	105,2465	116,5743	123,3709	129,6955	121,0345	131,4007	113,3532	91,50292
Ctrl 3	97,69469	112,7984	116,5743	129,6955	116,2149	135,2118	114,2067	93,48548
Blank	6,54409	6,430813	6,476124	30,80575	19,46556	18,7236	13,59617	19,14608

Table E 4 Calculated free concentration of 1-methylphenanthrene in freshwater at 20 °C. Concentrations are given in µg/L

	2t	4t	6t	1d	2d	3d	4d	7d
PES-W	404,6973	428,1431	414,644	375,6798	377,0169	342,2409	323,0506	285,6025
PES-W	423,8802	413,9335	455,8517	391,2168	384,5873	348,7298	352,4242	307,7867
PES-W	436,6688	389,7773	426,7221	389,8658	410,7398	349,4508	333,595	297,768
PES-B	426,7221	446,6155	430,985	399,3231	374,264	300,4233	326,8165	275,5838
PES-B	420,3278	456,5622	430,985	367,5735	354,3055	292,4924	325,3101	277,015
PES-B	422,4593	426,0117	437,3793	361,4938	365,3171	315,5642	332,0887	280,5931
PA-W	433,1164	427,4326	440,2212	309,4784	273,7833	242,744	261,2907	212,6093
PA-W	420,3278	427,4326	422,4593	308,8029	281,3538	246,349		253,3996
PA-W	415,3545	408,9602	418,1964	278,4043	252,4484	229,0452	256,7717	236,9404
Wool	354,9639	344,3067	347,1486	317,5847	315,765	306,9123	328,3228	329,2553
Wool	347,1486	342,1753	342,8857	331,0952	324,0237	311,2382	326,8165	312,0804
Wool	326,5448	340,0438	342,8857	308,8029	319,8943	311,2382	323,0506	303,493
Ctrl 1	443,0631	481,4289	472,9032	429,0462	479,5622	414,34	442,8046	453,0574
Ctrl 2	474,3241	474,3241	438,8003	454,0406	446,5274	430,9229	433,0134	430,1576
Ctrl 3	428,1431	494,2175	435,2479	420,2644	447,9039	429,4809	453,349	420,8545
Blank	11,39812	11,54732	11,53311	9,376969	14,05469	5,833301	15,44868	13,81025

Table E 5 Calculated free concentration of fluoranthene in seawater at 20 °C. Concentrations are given in μg/L

	2t	4t	6t	1d	2d	3d	4d	7d	10d	14d
PES-W	41,42277	40,36596	36,13871	32,97097	30,71833	24,5942	26,06135	22,13606	21,34368	18,9275
PES-W	43,5364	42,47959	37,19553	32,97097	31,69371	28,98824	29,14452	25,00911	25,19454	22,82126
PES-W	44,59321	42,47959	37,19553	33,97477	30,71833	25,69271	26,06135	22,35707	21,87852	19,72622
PA-W	46,70683	37,19553	30,85466	23,93676	22,42765	17,89329	19,79224	18,15799	18,13462	17,72942
PA-W	44,59321	36,13871	29,79784	23,03334	21,2572	16,46523	18,35342	16,83197	16,851	16,33166
PA-W	44,59321	35,0819	29,79784	23,93676	21,64735	17,12434	19,68946	17,49498	17,81372	17,72942
Wool	34,02509	29,79784	27,68422	26,94816	28,76758	24,5942	28,1168	25,00911	26,26422	25,81647
Wool	35,0819	30,85466	27,68422	28,95576	28,76758	25,69271	29,14452	27,21915	26,26422	25,81647
Wool	31,91147	28,74103	26,62741	26,94816	26,81683	24,5942	26,06135	23,90409	26,26422	25,81647
Ctrl 1	50,93408	54,10452	47,76365	49,03177	50,22583	48,76141	49,699	46,00449	44,44885	42,78929
Ctrl 2	55,16133	51,99089	49,87727	48,02797	50,22583	49,85992	50,72672	48,21453	48,72758	46,78289
Ctrl 3	55,16133	49,87727	45,65002	47,02417	46,32433	46,56439	47,64355	44,89947	44,44885	43,78769
Blank	13,02624	13,03681	12,88885	13,99512	14,32228	9,401815	12,73691	11,78424	11,63095	11,93869

Table E 6 Calculated free concentration of fluoranthene in seawater at 20 °C. Concentrations are given in µg/L

	2t	4t	6t	1d	2d	3d	4d	7d	10d	14d
PES-W	27,05417	25,00158	22,94898	18,47577	17,19141	21,43412	19,50825	19,98966	21,02382	22,48256
PES-W	27,73837	25,68578	23,63318	18,32704	17,26119	21,11208	18,92712	20,72991	21,02382	22,28301
PES-W	27,05417	14,7386	24,31738	20,03741	18,65677	22,59347	20,47681	20,93179	21,36098	23,48031
PA-W	27,05417	22,94898	21,51216	14,9063	14,60959	18,66457	17,24828	18,03812	19,20315	20,75312
PA-W	27,73837	23,63318	21,3069	14,83194	14,40025	18,72898	16,79629	18,03812	18,93342	20,75312
PA-W	27,05417	23,63318	21,58058	15,35249	14,74915	19,05102	17,11914	18,3073	19,20315	21,01919
PAC-B	30,47517	29,79097	29,10677	26,73015	26,68136	29,29193	26,99845	29,41092	29,11567	31,52883
PAC-B	31,15937	29,79097	30,47517	26,73015	26,68136	30,5801		29,41092	29,11567	31,52883
PAC-B	29,79097	29,79097	29,79097	26,73015	28,07694	29,93601	28,28987	30,75681	30,46432	32,194
Wool	22,94898	21,3069	20,41745	17,5834	17,67987	21,88498	19,76654	21,47015	22,37246	24,34503
Wool	22,94898	21,37532	21,03322	11,85739	18,02876	21,88498	20,2831	22,27768	22,57476	25,07671
Wool	22,94898	21,37532	20,96481	17,95522	17,95898	22,33584	20,15396	22,14309	22,77705	24,74413
Ctrl 1	35,94876	33,89616	33,89616	31,19198	31,56589	35,08867	31,5184	34,12154	33,1616	36,185
Ctrl 2	33,89616	33,89616	33,89616	26,73015	32,26368	35,08867	32,16411	36,14038	35,18457	36,85017
Ctrl 3	33,89616	33,21196	33,89616	29,70471	28,77473	34,44459	31,5184	36,14038	35,18457	37,51534
Blank	14,88912	14,86175	15,01228	11,85739	12,34177	17,27979	15,42093	16,76625	18,06355	19,63564

Appendix F: Concentrations of samples from adsorption isotherm experiments

Tables F 1 to F 6 shows the calculated free concentrations of PAHs from the adsorption isotherm studies

Table F 1 Free concentrations of phenanthrene for PES-W, PES-B, PA-W, wool and control sample in seawater at 20 °C for adsorption isotherm studies.

	Replicate				Replicate		
PES-W	1	2	3	PES-B	1	2	3
10 %	26,9363552	24,6618422	22,3873292	10 %	23,1455002	23,9036712	23,1455002
25 %	81,524667	83,79918	79,250154	25 %	64,844905	72,426615	68,63576
40 %	140,662005	133,080295	152,792741	40 %	133,838466	133,838466	132,322124
55 %	226,335327	243,015089	265,760219	55 %	172,505187	195,250316	208,139223
70 %	297,603401	261,211193	348,400858	70 %	309,734137	275,616442	295,328888
85 %	371,145988	384,034895	394,649289	85 %	320,348531	299,877914	323,381215
100 %	523,538358	518,231161	475,015414	100 %	352,191713	351,433542	359,015252

	Replicate				Replicate		
PA-W	1	2	3	Wool	1	2	3
10 %	20,1128162	20,1128162	21,6291582	10 %	33,7598942	39,0670912	40,5834332
25 %	61,8122211	61,8122211	58,7795371	25 %	96,6880869	103,511626	96,6880869
40 %	113,367849	114,884191	102,753455	40 %	167,19799	171,747016	162,648964
55 %	155,067254	171,747016	154,309083	55 %	245,289602	237,707892	258,178509
70 %	231,642524	232,400695	228,60984	70 %	297,603401	326,413899	285,472665
85 %	272,583758	250,596799	262,727535	85 %	376,453185	377,969527	356,740739
100 %	283,956323	261,211193	286,230836	100 %	459,851994	481,080782	428,008812

	Replicate		
Control	1	2	3
10 %	53,4723401	54,2305111	52,7141691
25 %	148,243715	149,001886	137,629321
40 %	246,047773	260,453022	244,531431
55 %	334,75378	335,511951	318,832189
70 %	467,433704	462,884678	447,721258
85 %	564,479592	574,335815	568,270447

	Replicate				Replicate		
100 %	660,767308	639,53852	653,943769				

Table F 2 Free concentrations of phenanthrene for PES-W, PES-B, PA-W, wool and control sample in seawater at 10 °C for adsorption isotherm studies.

	Replicate				Replicate		
PES-W	1	2	3	PES-B	1	2	3
10 %	21,4911371	19,983791	21,4911371	10 %	22,9984833	22,2448102	22,2448102
25 %	47,1160222	45,608676	42,5939837	25 %	51,6380608	59,1747917	53,1454069
40 %	75,7555997	74,2482535	81,7849844	40 %	84,0460037	87,060696	84,7996768
55 %	126,251697	126,251697	120,975985	55 %	135,295774	137,556793	129,266389
70 %	172,225755	159,413313	154,137601	70 %	175,994121	177,501467	169,211063
85 %	243,824699	222,721852	195,589621	85 %	215,938795	200,11166	203,126352
100 %	231,012256	217,446141	224,229199	100 %	252,868776	239,30266	243,824699

	Replicate				Replicate		
PA-W	1	2	3	Wool	1	2	3
10 %	18,4764448	16,9690986	17,7227717	10 %	27,5205219	28,274195	28,274195
25 %	37,318272	33,5499066	35,8109259	25 %	59,1747917	60,6821379	62,189484
40 %	59,1747917	56,9137724	59,1747917	40 %	97,6121193	97,6121193	99,8731386
55 %	91,5827346	76,5092728	84,7996768	55 %	121,729658	129,266389	128,512716
70 %	100,626812	120,222312	109,670889	70 %	169,211063	164,689024	163,935351
85 %	129,266389	135,295774	148,861889	85 %	179,762486	180,516159	165,442697
100 %	183,530852	174,486775	197,85064	100 %	459,851994	481,080782	428,008812

	Replicate		
Control	1	2	3
10 %	43,3476568	43,3476568	40,3329644
25 %	96,1047731	100,626812	102,134158
40 %	160,166986	151,876582	166,950044
55 %	215,185121	202,372679	225,736545
70 %	277,739988	288,291411	282,262027
85 %	305,625892	304,118546	304,872219
100 %	287,537738	326,728739	290,552431

Table F 3 Free concentrations of phenanthrene for PES-W, PES-B, PA-W, wool and control sample in seawater at 4 °C for adsorption isotherm studies.

	Replicate				Replicate		
PES-W	1	2	3	PES-B	1	2	3
10 %	5,1	5,34	4,82	10 %	5,87	5,13	5,22
25 %	34,7054572	29,4326886	27,9261832	25 %	30,1859412	27,9261832	33,1989519
40 %	50,5237633	48,2640053	43,7444892	40 %	53,5367739	55,7965319	53,5367739
55 %	78,394112	82,913628	70,1083326	55 %	80,65387	72,3680906	78,394112
70 %	83,6668806	95,7189233	110,783977	70 %	95,7189233	93,4591653	101,744945
85 %	146,940105	146,940105	115,303493	85 %	125,84903	125,84903	114,55024
100 %	128,108788	127,355535	123,589272	100 %	130,368546	146,186852	140,914083

	Replicate				Replicate		
PA-W	1	2	3	Wool	1	2	3
10 %	5,87	5,1	3,84	10 %	8,3	2,99	3,89
25 %	26,4196779	27,1729306	25,6664252	25 %	33,1989519	33,9522046	32,4456992
40 %	37,7184679	42,2379839	45,2509946	40 %	53,5367739	52,7835213	55,7965319
55 %	56,5497846	52,7835213	53,5367739	55 %	70,1083326	72,3680906	73,874596
70 %	76,8876066	87,433144	73,874596	70 %	83,6668806	87,433144	85,9266386
85 %	95,7189233	85,173386	89,692902	85 %	102,498197	101,744945	105,511208
100 %	113,043735	116,056745	118,316503	100 %	139,407578	130,368546	142,420589

	Replicate		
Control	1	2	3
10 %	10,07	18,8	13,53
25 %	57,3030373	55,7965319	55,7965319
40 %	94,212418	92,7059126	95,7189233
55 %	130,368546	128,862041	130,368546
70 %	157,485642	169,537685	169,537685
85 %	192,135265	194,395023	198,914539
100 %	231,304404	211,719834	220,005613

Table F 4 Free concentrations of phenanthrene for PES-W, PES-B, PA-W, wool and control sample in freshwater at 20 °C for adsorption isotherm studies. Experiment for PA-W was done separately.

	Replicate				Replicate		
PES-W	1	2	3	PES-B	1	2	3
10 %	40,8358147	40,8358147	40,8358147	10 %	35,8272203	35,8272203	37,2582473
25 %	103,801002	109,52511	102,369975	25 %	110,240623	102,369975	101,654461
40 %	198,964296	202,541863	196,817756	40 %	181,076459	188,231594	191,809161
55 %	265,507051	289,834509	289,118996	55 %	283,394888	277,67078	211,843539
70 %	393,583965	9,42477251	355,66175	70 %	370,687534	380,704722	379,273695
85 %	466,566341	460,12672	453,687098	85 %	465,135314	451,540558	446,531964
100 %	570,315797	11,0704535	569,600284	100 %	533,824609	589,634662	551,712447

	Replicate				Replicate		
PA-W	1	2	3	Wool	1	2	3
10 %	45,8699992	54,4574311	44,4387606	10 %	52,2840306	52,2840306	52,9995441
25 %	103,835164	117,431931	113,138216	25 %	135,283595	8,56615633	132,421541
40 %	181,122051	183,268909	189,709483	40 %	222,576241	249,05024	232,59343
55 %	282,739995	278,446279	277,73066	55 %	306,291319	335,627373	344,213534
70 %	352,870689	324,961535	354,301927	70 %	416,480397	422,204505	422,920018
85 %	427,295098	451,626155	511,022559	85 %	483,738665	484,454178	493,04034
100 %	507,444462	503,150746	503,866366	100 %	599,65185	590,350175	353,51521

	Replicate						
Control	1	2	3	Control (PA-W)	1	2	3
10 %	74,4649487	75,8959757	72,3184083	10 %	88,8071586	95,9633518	95,2477325
25 %	198,964296	197,533269	197,533269	25 %	214,04054	228,352927	233,362262
40 %	322,74813	305,575806	318,455049	40 %	344,998876	319,9522	260,555796
55 %	451,540558	417,911424	452,256071	55 %	469,516638	434,451291	463,076064
70 %	597,50531	629,703417	596,789796	70 %	611,209264	609,778026	603,337452
85 %	715,565036	719,142603	709,125414	85 %	772,223612	805,142101	791,545334
100 %	664,048064	778,530223	806,435249	100 %	770,792373	831,620016	772,223612

Table F 5 Free concentrations of 1-methylphenanthrene for PES-W, PA-W, wool and control sample in seawater at 4 °C for adsorption isotherm studies.

	Replicate				Replicate		
PES-W	1	2	3	PA-W	1	2	3
40 %	27,2640243	27,2640243	27,2640243	40 %	19,8101675	22,5298179	20,2130787
50 %	26,2567463	27,2640243	28,2713022	50 %	20,8174454	19,8101675	21,2203566
60 %	30,2858581	30,2858581	35,3222478	60 %	22,6305457	22,4290901	22,5298179
70 %	37,3368037	37,3368037	39,3513596	70 %	24,2421904	24,2421904	23,2349125
80 %	44,3877493	48,4168611	36,3295258	80 %	26,2567463	26,2567463	25,2494684
90 %	45,3950273	46,4023052	49,4241391	90 %	29,2785802	27,2640243	29,2785802
100 %	50,431417	50,431417	52,4459729	100 %	30,2858581	30,2858581	29,2785802

	Replicate				Replicate		
Wool	1	2	3	Control	1	2	3
40 %	27,2640243	27,2640243	26,2567463	40 %	42,3731935	45,3950273	45,3950273
50 %	29,2785802	29,2785802	28,2713022	50 %	50,431417	52,4459729	52,4459729
60 %	33,3076919	32,300414	32,300414	60 %	59,4969185	61,5114744	60,5041965
70 %	35,3222478	36,3295258	36,3295258	70 %	68,56242	69,569698	71,5842539
80 %	37,3368037	40,3586376	38,3440817	80 %	72,5915318	76,6206436	74,6060877
90 %	41,3659155	42,3731935	43,3804714	90 %	85,6861451	84,6788671	83,6715892
100 %	46,4023052	48,4168611	48,4168611	100 %	90,7225348	91,7298128	91,7298128

Table F 6 Free concentrations of fluoranthene for PES-W, PA-W, wool and control sample in seawater at 4 °C for adsorption isotherm studies.

	Replicate				Replicate		
PES-W	1	2	3	PA-W	1	2	3
40 %	22,0184587	20,8518138	19,9768301	40 %	13,268622	13,1227914	12,6852995
50 %	26,5392076	25,0809015	23,6225954	50 %	14,8727587	13,8519444	14,7269281
60 %	25,0809015	26,5392076	25,0809015	60 %	16,1852342	14,5810975	15,893573
70 %	33,8307382	35,2890443	35,2890443	70 %	16,7685567	17,7893709	16,6227261
80 %	46,9554932	41,1222688	38,2056565	80 %	19,5393383	18,0810322	17,6435403
90 %	48,4137993	41,1222688	49,8721055	90 %	19,1018464	18,518524	20,2684913
100 %	55,7053299	55,7053299	55,7053299	100 %	22,4559505	20,2684913	22,6017811
	Replicate				Replicate		
Wool	1	2	3	Control	1	2	3
40 %	18,9560158	19,5393383	19,8309995	40 %	39,6639627	39,6639627	41,1222688
50 %	21,2893056	20,9976444	22,4559505	50 %	48,4137993	48,4137993	49,8721055
60 %	25,0809015	25,0809015	25,0809015	60 %	58,6219421	57,163636	57,163636
70 %	26,5392076	26,5392076	26,5392076	70 %	64,4551666	71,7466972	70,2883911
80 %	29,4558199	29,4558199	29,4558199	80 %	77,5799216	77,5799216	74,6633094
90 %	32,3724321	32,3724321	33,8307382	90 %	76,1216155	84,8714522	79,0382277
100 %	35,2890443	35,2890443	35,2890443	100 %	84,8714522	89,2463705	76,1216155

Appendix G: Calculated isotherm parameters

Tables G 1 – G 4 shows the calculated parameters for each fibre type in different conditions that was fitted with SSE, MWSE and EABS.

Table G 1 Calculated isotherm parameters for all PES-W

	PHE SW 20 °C			PHE SW 5 °C			PHE SW 10 °C		
LM	SSE	MWSE	EABS	SSE	MWSE	EABS	SSE	MWSE	EABS
Q	0,546535	0,418617	0,611689	0,465437	0,276051	0,464131	0,289517	0,299892	0,326916
K_L	0,005973	0,007955	0,004555	0,005402	0,012601	0,005284	0,02202	0,013116	0,017362
R^2	0,762185	0,71384	0,758843	0,941067	0,905076	0,93984	0,725041	0,683287	0,713159
Error	0,123763	0,077055	1,237504	0,005017	0,048457	0,267932	0,044068	0,067205	0,757302
FM	SSE	MWSE	EABS	SSE	MWSE	EABS	SSE	MWSE	EABS
K_F	0,023197	0,014083	0,016212	0,00651	0,008118	0,006544	0,036948	0,013934	0,031835
1/n	0,469184	0,531028	0,51929	0,696324	0,638622	0,693323	0,35072	0,516279	0,398666
R^2	0,744102	0,712067	0,733563	0,941425	0,930865	0,941121	0,663256	0,616807	0,643653
Error	0,136438	0,076925	1,333969	0,004981	0,021296	0,253582	0,058967	0,100435	0,914107
RP	SSE	MWSE	EABS	SSE	MWSE	EABS	SSE	MWSE	EABS
K_r	0,002038	0,004907	0,003674	0,147323	8,404816	0,020405	0,00342	0,003156	0,086001
a_r	2,38E-05	0,064045	0,017593	21,97789	1034,689	2,534652	5,39E-05	2,56E-05	2,377297
g	1,791033	0,725613	0,86323	0,30763	0,361475	0,333739	1,983219	2,105447	0,623538
R^2	0,768294	0,717257	0,74882	0,897717	0,930863	0,941052	0,837137	0,840597	0,648567
Error	0,119689	0,078533	1,266086	0,011034	0,022483	0,255603	0,022607	0,031036	0,906163
Sips	SSE	MWSE	EABS	SSE	MWSE	EABS	SSE	MWSE	EABS
Q_S	0,490107	0,661518	0,804813	0,936119	0,891008	0,356493	0,235201	0,215746	0,239517
B_S	1,183229	0,745475	0,852165	0,813731	0,696069	1,115069	2,579774	2,423588	1,947906
K_S	0,00305	0,011453	0,006081	0,00493	0,008243	0,004825	9,11E-05	0,0002	0,000865
R^2	0,763198	0,718729	0,751583	0,897171	0,9163	0,937596	0,783724	0,762974	0,774861
Error	0,123078	0,078955	1,238437	0,011101	0,026158	0,274434	0,032047	0,034466	0,595804
DA	SSE	MWSE	EABS	SSE	MWSE	EABS	SSE	MWSE	EABS
Q^0	0,414962	0,387885	0,532679	0,321978	0,621728	1,332496	0,233248	0,213785	0,225754
b	1,837174	1,315973	0,739198	1,11278	0,652074	0,413036	3,956298	3,999132	4,119366
E	8,964517	10,47401	13,36158	7,705199	5,633549	3,005144	7,272893	7,508814	7,352938
R^2	0,765024	0,719923	0,713016	0,941736	0,93236	0,925141	0,786588	0,766474	0,7836
Error	0,121835	0,079098	1,438207	0,004954	0,018065	0,281953	0,031506	0,033904	0,565187
DR	SSE	MWSE	EABS	SSE	MWSE	EABS	SSE	MWSE	EABS
q_s	0,390563	0,246653	0,372268	0,197595	0,171745	0,222017	0,235172	0,21186	0,229041
k_ad	1128,448	139,0523	951,3375	289,1098	198,8409	292,8237	148,8839	118,0317	129,3783
r^2	0,736738	0,600791	0,734166	0,883402	0,855248	0,83631	0,77469	0,749215	0,77196
Error	0,142632	0,129483	1,393954	0,010635	0,187898	0,391054	0,033777	0,035885	0,607945
	PHE FW 20 °C			1-MP SW 20 °C			FLA SW 20 °C		
LM	SSE	MWSE	EABS	SSE	MWSE	EABS	SSE	MWSE	EABS
Q	0,982551	0,932389	1,468687	0,001544	0,018784	0,006826	0,103065	0,110469	0,093196
K_L	0,002664	0,002562	0,00147	0,972942	0,002153	0,007917	0,075514	0,050107	0,084879
R^2	0,852963	0,838895	0,826863	0,510783	0,706884	0,717803	0,578435	0,565553	0,567552
Error	0,114761	**0,030095**	1,070198	2,89E-06	0,034934	0,003929	0,003395	0,033714	0,241695

FM	SSE	MWSE	EABS	SSE	MWSE	EABS	SSE	MWSE	EABS
K_F	0,013267	0,006837	0,004099	8,31E-05	4,63E-05	8,23E-05	0,029561	0,019192	0,028424
1/n	0,604738	0,706339	0,81686	0,797088	0,940582	0,813544	0,257609	0,360278	0,249042
R^2	0,833165	0,816295	0,775404	0,723426	0,70532	0,709384	0,558544	0,54648	0,551298
Error	0,133332	0,040813	1,084592	1,15E-06	0,035087	0,003934	0,003682	0,036854	0,250714
RP	SSE	MWSE	EABS	SSE	MWSE	EABS	SSE	MWSE	EABS
K_r	0,002155	0,002128	0,002129	0,001935	0,000884	0,001245	0,003229	0,002807	0,061409
a_r	0,000121	0,000175	0,00092	10,3161	18,09786	14,29154	5,9E-05	2,45E-05	1,956087
g	1,440224	1,403746	1,074355	0,418192	0,062084	0,192732	2,495008	2,654603	0,770011
R^2	**0,86296**	0,846821	0,833404	0,701711	0,705323	0,709412	0,684208	0,658457	0,552715
Error	**0,10571**	0,030649	1,071887	1,28E-06	0,037036	0,003934	0,002151	0,023989	0,249724
Sips	SSE	MWSE	EABS	SSE	MWSE	EABS	SSE	MWSE	EABS
Q_S	0,755513	0,764011	1,571472	0,004308	0,001902	0,004967	0,081784	0,081784	0,081784
B_S	1,318968	1,118242	0,985402	1,257159	4,042679	1,19603	5,936402	5,936402	5,936402
K_S	0,000782	0,00198	0,001452	0,00566	1,75E-06	0,006188	2,4E-08	2,4E-08	2,4E-08
R^2	0,857152	0,839776	0,822833	0,728483	0,731315	0,710672	0,68475	0,68475	0,68475
Error	0,110943	0,031116	**1,067801**	**1,12E-06**	0,032249	0,003888	0,002147	**0,023623**	0,189971
DA	SSE	MWSE	EABS	SSE	MWSE	EABS	SSE	MWSE	EABS
Q^0	0,626614	0,589993	1,485362	0,003119	0,00175	0,067152	0,081464	0,066379	0,080164
b	1,890982	1,702257	0,811561	1,03268	7,096087	0,250096	10,23174	94,18918	9,352277
E	7,966617	8,585318	6,09945	8,212635	4,163579	0,370662	4,513673	299,5324	4,565149
R^2	0,858845	0,841246	0,740985	0,709815	0,731317	0,706772	0,691439	0,5	0,686987
Error	0,10941	0,030607	1,121138	1,23E-06	0,031668	0,004012	**0,002079**	0,061072	**0,185648**
DR	SSE	MWSE	EABS	SSE	MWSE	EABS	SSE	MWSE	EABS
q_s	0,555162	0,369236	0,459975	0,001505	0,002305	0,002516	0,089083	0,087824	0,086902
k_ad	2362,651	442,2929	1237,886	1,004155	122,4376	124,9879	36,62545	43,95018	37,5744
r^2	0,79936	0,66071	0,758472	0,503095	0,726812	0,729669	0,616073	0,605255	0,612978
Error	0,168375	0,081521	1,562387	2,98E-06	**0,031505**	**0,003776**	0,002903	0,027699	0,222062

Table G 2 Calculated isotherm parameters for all PES-B

	PHE SW 20 °C			PHE SW 5 °C		
LM	SSE	MWSE	EABS	SSE	MWSE	EABS
Q	10,09666	0,99013	2,610264	0,465437	0,276051	0,464131
K_L	0,000199	0,003303	0,000986	0,005402	0,012601	0,005284
R^2	0,8894	0,825936	0,876541	0,941067	0,905076	0,93984
Error	0,125998	0,035776	1,158972	0,005017	0,048457	0,267932
FM	SSE	MWSE	EABS	SSE	MWSE	EABS
K_F	0,003561	0,007643	0,005146	0,00651	0,008118	0,006544
1/n	0,888471	0,736045	0,832275	0,696324	0,638622	0,693323
R^2	0,892626	0,862882	0,883541	0,941425	0,930865	0,941121
Error	0,121688	**0,03143**	1,066057	0,004981	0,021296	**0,253582**
RP	SSE	MWSE	EABS	SSE	MWSE	EABS
K_r	0,018227	0,023503	0,026321	0,147323	8,404816	0,020405
a_r	4,306968	2,411657	4,380048	21,97789	1034,689	2,534652
g	0,122712	0,293694	0,181221	0,30763	0,361475	0,333739
R^2	0,768294	0,861598	0,883509	0,897717	0,930863	0,941052
Error	**0,119689**	0,033144	1,068159	0,011034	0,022483	0,255603
Sips	SSE	MWSE	EABS	SSE	MWSE	EABS
Q_S	580,3927	1,691529	2,590056	0,936119	0,891008	0,356493
B_S	0,888963	0,850316	0,945437	0,813731	0,696069	1,115069
K_S	6,12E-06	0,003255	0,00132	0,00493	0,008243	0,004825
R^2	0,763198	0,840047	0,879865	0,897171	0,9163	0,937596
Error	0,123078	0,034606	1,155194	0,011101	0,026158	0,274434
DA	SSE	MWSE	EABS	SSE	MWSE	EABS
Q^0	78,25252	1,025911	4,402821	0,321978	0,621728	1,332496
b	0,212015	0,937417	0,477606	1,11278	0,652074	0,413036
E	0,055492	7,38206	2,796423	7,705199	5,633549	3,005144
R^2	**0,913107**	0,868046	0,890587	0,941736	0,93236	0,925141
Error	**0,096239**	0,033109	**0,987378**	**0,004954**	**0,018065**	0,281953
DR	SSE	MWSE	EABS	SSE	MWSE	EABS
q_s	0,077124	0,8	0,372268	0,197595	0,171745	0,222017
k_ad	5000	5000	951,3375	289,1098	198,8409	292,8237
r^2	0,661635	0,554261	0,734166	0,883402	0,855248	0,83631
Error	0,698796	0,237828	2,77736	0,010635	0,187898	0,391054
	PHE SW 10 °C			PHE FW 20 °C		
LM	SSE	MWSE	EABS	SSE	MWSE	EABS
Q	0,982551	0,932389	1,468687	0,001544	0,018784	0,006826
K_L	0,002664	0,002562	0,00147	0,972942	0,002153	0,007917
R^2	0,852963	0,838895	0,826863	0,510783	0,706884	0,717803
Error	0,114761	**0,030095**	1,070198	2,89E-06	0,034934	0,003929
FM	SSE	MWSE	EABS	SSE	MWSE	EABS
K_F	0,013267	0,006837	0,004099	8,31E-05	4,63E-05	8,23E-05
1/n	0,604738	0,706339	0,81686	0,797088	0,940582	0,813544
R^2	0,833165	0,816295	0,775404	0,723426	0,70532	0,709384
Error	0,133332	0,040813	1,084592	1,15E-06	0,035087	0,003934
RP	SSE	MWSE	EABS	SSE	MWSE	EABS

K_r	0,002155	0,002128	0,002129	0,001935	0,000884	0,001245
a_r	0,000121	0,000175	0,00092	10,3161	18,09786	14,29154
g	1,440224	1,403746	1,074355	0,418192	0,062084	0,192732
R^2	**0,86296**	0,846821	0,833404	0,701711	0,705323	0,709412
Error	**0,10571**	0,030649	1,071887	1,28E-06	0,037036	0,003934
Sips	SSE	MWSE	EABS	SSE	MWSE	EABS
Q_S	0,755513	0,764011	1,571472	0,004308	0,001902	0,004967
B_S	1,318968	1,118242	0,985402	1,257159	4,042679	1,19603
K_S	0,000782	0,00198	0,001452	0,00566	1,75E-06	0,006188
R^2	0,857152	0,839776	0,822833	0,728483	0,731315	0,710672
Error	0,110943	0,031116	**1,067801**	**1,12E-06**	0,032249	0,003888
DA	SSE	MWSE	EABS	SSE	MWSE	EABS
Q^0	0,626614	0,589993	1,485362	0,003119	0,00175	0,067152
b	1,890982	1,702257	0,811561	1,03268	7,096087	0,250096
E	7,966617	8,585318	6,09945	8,212635	4,163579	0,370662
R^2	0,858845	0,841246	0,740985	0,709815	0,731317	0,706772
Error	0,10941	0,030607	1,121138	1,23E-06	0,031668	0,004012
DR	SSE	MWSE	EABS	SSE	MWSE	EABS
q_s	0,555162	0,369236	0,459975	0,001505	0,002305	0,002516
k_ad	2362,651	442,2929	1237,886	1,004155	122,4376	124,9879
r^2	0,79936	0,66071	0,758472	0,503095	0,726812	0,729669
Error	0,168375	0,081521	1,562387	2,98E-06	**0,031505**	**0,003776**

Table G 3 Calculated isotherm parameters for all PA-W

	PHE SW 20 °C			PHE SW 5 °C			PHE SW 10 °C		
LM	SSE	MWSE	EABS	SSE	MWSE	EABS	SSE	MWSE	EABS
Q	294,7366	10,29806	15,95347	0,59802	0,71493	0,53857	2,146745	2,72096	2,802622
K_L	4,02E-05	0,001428	0,000811	0,00734	0,005384	0,009023	0,015499	0,007222	0,009507
R^2	0,93445	0,904183	0,907962	0,949456	0,944695	0,946183	0,798563	0,739162	0,770381
Error	1,842303	0,019592	4,918805	0,008326	0,028287	0,341125	1,279326	0,066279	3,814459
FM	SSE	MWSE	EABS	SSE	MWSE	EABS	SSE	MWSE	EABS
K_F	0,009979	0,02397	0,017628	0,009367	0,005747	0,008989	0,147319	0,040403	0,074592
1/n	1,030206	0,857503	0,920306	0,717844	0,8237	0,728329	0,462748	0,709778	0,629217
R^2	0,93507	0,915622	0,929199	0,938044	0,928326	0,937873	0,736759	0,672109	0,678152
Error	1,82406	0,015384	4,613808	0,010332	0,024694	0,406298	1,810808	0,096535	4,637412
RP	SSE	MWSE	EABS	SSE	MWSE	EABS	SSE	MWSE	EABS
K_r	0,066504	2,704174	0,090248	0,003552	0,953406	0,033036	0,019229	0,01636	0,233776
a_r	4,654956	111,952	3,627857	3,8E-05	165,0106	2,810073	3,52E-07	2,33E-10	2,634951
g	0	0,143161	0,126446	2,003956	0,176893	0,312509	2,942744	4,312419	0,39554
R^2	0,934807	0,915612	0,916474	0,958863	0,928341	0,938538	**0,944293**	0,96197	0,680836
Error	1,831522	0,016241	4,614713	0,00671	0,026068	0,403829	**0,299619**	**0,013634**	4,599003
Sips	SSE	MWSE	EABS	SSE	MWSE	EABS	SSE	MWSE	EABS
Q_S	13,02992	37,04014	4,020222	0,311673	3,792676	0,310459	1,538748	1,483029	1,940035
B_S	1,249516	0,887031	1,998415	1,955425	0,846817	1,954095	2,576846	2,108944	1,727002
K_S	0,000296	0,000586	3,66E-05	0,000548	0,001452	0,000548	7,36E-05	0,000444	0,000975
R^2	0,927948	0,909353	0,888165	0,960498	0,932005	0,960402	0,867895	0,850201	0,818471
Error	2,041502	0,017059	6,959002	**0,006437**	0,026064	**0,282482**	0,7711	0,025388	2,959168
DA	SSE	MWSE	EABS	SSE	MWSE	EABS	SSE	MWSE	EABS
Q^0	172,5232	13,60792	28,77144	0,290061	0,665834	0,358362	1,518697	1,445981	1,799331
b	0,329211	0,689943	0,540004	3,005265	0,98399	1,700902	3,834039	3,29151	2,516853
E	0,441934	4,338032	2,586681	6,776541	6,361658	8,092689	7,094462	7,570144	7,312661
R^2	**0,947106**	0,935127	0,943106	0,958279	0,927195	0,948258	0,868023	0,850192	0,818806
Error	**1,466581**	**0,014323**	**3,726188**	0,006818	**0,026055**	0,332748	0,770163	0,025595	**2,955763**
DR	SSE	MWSE	EABS	SSE	MWSE	EABS	SSE	MWSE	EABS
q_s	3,616088	1,540471	3,347947	0,278611	0,257311	0,277311	1,546044	1,290365	1,522019
k_ad	2227,314	124,6345	2065,789	212,1289	179,2126	195,1123	191,5401	106,9762	218,0602
r^2	0,83866	0,585033	0,834284	0,948255	0,936884	0,94596	0,850109	0,788693	0,845492
Error	5,128032	0,168051	9,026997	0,008554	0,173903	0,326179	0,894442	0,043599	3,737012
	PHE FW 20 °C			1-MP SW 20 °C			FLA SW 20 °C		
LM	SSE	MWSE	EABS	SSE	MWSE	EABS	SSE	MWSE	EABS
Q	9,778431	7,997247	6,23796	52,75523	167,3832	0,115417	1056,872	2868,016	5,050862
K_L	0,000944	0,001175	0,001663	6,77E-06	1,87E-06	0,003494	2,72E-05	9,32E-06	0,00639
R^2	0,91037	0,902428	0,88898	0,759498	0,692901	0,736015	0,82225	0,78295	0,799072
Error	2,006862	0,026832	5,415904	4,36E-05	0,054425	0,024873	0,074503	0,025249	1,133198
FM	SSE	MWSE	EABS	SSE	MWSE	EABS	SSE	MWSE	EABS
K_F	0,023818	0,01946	0,025039	1,65E-05	6,64E-06	2,53E-05	0,009335	0,004857	0,005108
1/n	0,786593	0,814425	0,760627	1,948894	2,21898	1,827196	1,38981	1,610464	1,601293
R^2	0,910396	0,905396	0,8772	0,902185	0,88519	0,89151	0,869024	0,853148	0,85357
Error	2,006089	**0,02555**	**5,262523**	1,49E-05	0,022663	0,012097	0,051826	**0,011241**	0,834962
RP	SSE	MWSE	EABS	SSE	MWSE	EABS	SSE	MWSE	EABS

K_r	0,0132	0,018674	0,052426	0,001304	0,001183	0,005517	0,032983	0,040676	0,029711
a_r	0,055071	0,290783	1,620103	2,650482	2,771727	13,88902	0,14781	0,521799	0,000843
g	0,48119	0,315184	0,26023	0	0	0	0	0	0,006896
R^2	0,910562	0,905194	0,882113	0,75956	0,692921	0,75615	0,822349	0,783077	0,815568
Error	2,002005	0,026912	5,284933	4,36E-05	0,057446	0,023199	0,074452	0,026644	1,084638
Sips	SSE	MWSE	EABS	SSE	MWSE	EABS	SSE	MWSE	EABS
Q_S	17,51932	47,03771	18,00981	0,016705	0,022869	0,035064	0,707296	0,742764	0,707296
B_S	0,888592	0,838991	0,854741	4,391232	3,550652	2,430164	5,432833	4,779071	5,432833
K_S	0,000875	0,000377	0,000919	8,74E-07	6,66E-06	0,00014	5,42E-07	2,76E-06	5,42E-07
R^2	0,910799	0,905361	0,879023	**0,913947**	0,900895	0,898344	**0,945311**	0,942007	0,945311
Error	1,996184	0,026938	5,319316	**1,291E-05**	0,02322	0,011634	**0,019893**	0,005316	**0,535476**
DA	SSE	MWSE	EABS	SSE	MWSE	EABS	SSE	MWSE	EABS
Q^0	4,849839	5,034157	4,273983	0,017742	0,028637	0,031843	0,717207	0,767302	0,726004
b	1,123065	1,043612	1,112482	4,676485	2,897227	2,367598	8,19486	6,746212	8,200401
E	7,242724	7,05112	7,672121	4,720619	4,539204	4,694786	5,509147	5,593464	5,496643
R^2	0,910813	0,905347	0,882657	0,91387	0,900062	0,89976	0,94278	0,938821	0,941945
Error	**1,995834**	0,026927	5,294444	1,292E-05	0,023309	0,011421	0,020869	0,005547	0,542702
DR	SSE	MWSE	EABS	SSE	MWSE	EABS	SSE	MWSE	EABS
q_s	3,122118	1,856147	2,943955	0,024561	0,025837	0,022306	1,061002	1,102597	1,112836
k_ad	3800,801	635,1461	2238,845	124,8326	134,8942	110,6601	44,82385	47,80299	47,44266
r^2	0,813887	0,639935	0,788823	0,913569	0,904509	0,904071	0,924048	0,920554	0,921149
Error	4,713711	0,113556	8,312288	1,3E-05	**0,022376**	**0,010833**	0,028262	0,006018	0,629269

Table G 4 Calculated isotherm parameters for all wool

	PHE SW 20 °C			PHE SW 5 °C			PHE SW 10 °C		
LM	SSE	MWSE	EABS	SSE	MWSE	EABS	SSE	MWSE	EABS
Q	3,992706	197,9699	3,416907	0,640456	1,236154	0,572183	0,364009	0,325704	1,012099
K_L	0,000323	5,28E-06	0,000384	0,00426	0,001722	0,004516	0,009318	0,005823	0,002074
R^2	0,885242	0,860813	0,885053	0,898796	0,881599	0,88379	0,665574	0,604394	0,584254
Error	0,079582	0,053793	1,006491	0,01314	0,080692	0,470074	0,098002	0,147947	1,064978
FM	SSE	MWSE	EABS	SSE	MWSE	EABS	SSE	MWSE	EABS
K_F	0,001501	0,000866	0,001056	0,005391	0,003019	0,005122	0,017035	0,004818	0,001464
1/n	0,955262	1,035939	1,030208	0,772502	0,885352	0,77004	0,495796	0,675202	1,025203
R^2	0,883831	0,868403	0,862172	0,886813	0,870114	0,875815	0,631094	0,581036	0,473625
Error	0,080676	**0,052808**	0,990274	0,014895	**0,077603**	0,485446	0,11392	0,180972	1,068321
RP	SSE	MWSE	EABS	SSE	MWSE	EABS	SSE	MWSE	EABS
K_r	0,001245	0,003756	0,006579	0,002292	0,981459	0,012612	0,002255	0,001617	0,008426
a_r	9,81E-08	2,600046	4,338286	4,7E-08	324,1946	3,716176	7,05E-07	2,43E-10	4,09022
g	2,284049	0	0	3,233433	0,114845	0,096234	2,631309	4,090231	1,4E-06
R^2	0,888121	0,861036	0,872401	0,930815	0,87012	0,875151	0,7637	0,758283	0,483275
Error	0,07735	0,056742	0,994856	0,008683	0,081917	0,452761	**0,061754**	**0,058449**	1,070123
Sips	SSE	MWSE	EABS	SSE	MWSE	EABS	SSE	MWSE	EABS
Q_S	0,974691	4,337366	1,296049	0,247931	1,112514	0,259086	0,247672	0,188718	0,379414
B_S	1,456486	1,07777	1,343593	2,761929	0,964678	2,718619	3,528007	2,382357	1,676842
K_S	0,000146	0,000171	0,000203	1,36E-05	0,002201	1,38E-05	2,96E-07	7,91E-05	0,000376
R^2	0,8898	0,868942	0,869965	**0,936126**	0,872524	0,934124	0,723731	0,65191	0,657051
Error	0,07602	0,055557	0,968241	**0,007984**	0,084868	**0,359632**	0,074457	0,098121	0,900917
DA	SSE	MWSE	EABS	SSE	MWSE	EABS	SSE	MWSE	EABS
Q^0	0,621542	0,700612	0,719357	0,24081	0,832834	0,265861	0,244604	0,184282	0,308103
b	1,428111	1,069869	1,329879	3,319675	0,741097	2,529274	3,964596	3,231263	2,017716
E	5,691037	5,652971	5,53448	5,669381	4,46535	5,919735	5,169247	6,572148	5,919627
R^2	**0,89003**	0,868902	0,871083	0,933366	0,847745	0,927032	**0,724976**	0,655021	0,669928
Error	**0,075841**	0,055491	**0,967551**	0,008352	0,078649	0,364385	**0,074012**	0,096504	**0,89813**
DR	SSE	MWSE	EABS	SSE	MWSE	EABS	SSE	MWSE	EABS
q_s	0,545381	0,232428	0,555465	0,250316	0,215433	0,268902	0,261325	0,176491	0,268058
k_ad	5123,348	534,3849	4662,774	415,7932	309,4929	510,449	596,5499	244,6091	679,0133
r^2	0,842624	0,597487	0,835381	0,922193	0,895401	0,915421	0,708777	0,629342	0,707935
Error	0,115631	0,188129	1,266458	0,009883	0,183903	0,414034	0,080133	0,102727	1,000245
	PHE FW 20 °C			1-MP SW 20 °C			FLA SW 20 °C		
LM	SSE	MWSE	EABS	SSE	MWSE	EABS	SSE	MWSE	EABS
Q	1,646576	1,666118	3,086467	0,007559	37,1776	0,019686	121,1396	609,928	0,259337
K_L	0,000769	0,000647	0,000398	0,007644	1,12E-06	0,002556	2,91E-05	5,43E-06	0,024129
R^2	0,824844	0,797578	0,798342	0,794914	0,817814	0,835316	0,848348	0,81793	0,7301
Error	0,120211	**0,05198**	1,144017	1,12E-06	0,024416	0,00343	0,002451	0,020854	0,26148
FM	SSE	MWSE	EABS	SSE	MWSE	EABS	SSE	MWSE	EABS
K_F	0,002661	0,001693	0,000967	1,17E-05	5,67E-06	1,32E-05	0,001694	0,000808	0,002069
1/n	0,828695	0,884865	1,019901	1,369611	1,564331	1,339699	1,217681	1,433558	1,146141
R^2	0,818267	0,7948	0,754542	0,908948	0,894938	0,906076	0,866839	0,849222	0,849333
Error	0,125717	0,053049	1,099173	4,34E-07	0,009704	0,002428	0,002104	0,011765	0,178792
RP	SSE	MWSE	EABS	SSE	MWSE	EABS	SSE	MWSE	EABS

	SSE	MWSE	EABS	SSE	MWSE	EABS	SSE	MWSE	EABS
K_r	0,007557	0,005811	0,004616	0,000638	0,000573	0,000982	0,013222	0,003317	0,003655
a_r	2,090889	2,565561	3,232351	13,20361	12,7543	20,88239	2,753591	0,000922	0,080196
g	0,199787	0,137315	0	0	0	0	0	0,001	2,79E-08
R^2	0,818481	0,79489	0,757804	0,859865	0,81783	0,859833	0,848472	0,818146	0,834035
Error	0,125537	0,056315	1,105025	7,08E-07	0,02577	0,003174	0,002449	0,022006	0,191639
Sips	SSE	MWSE	EABS	SSE	MWSE	EABS	SSE	MWSE	EABS
Q_S	0,696153	1,691322	1,051464	0,008595	0,002731	0,004469	0,132805	0,132805	0,132805
B_S	1,712509	0,997817	1,596834	1,720849	3,829912	2,227138	5,064045	5,064045	5,064045
K_S	4,73E-05	0,000643	5E-05	0,000477	1,66E-06	0,000199	1,84E-07	1,84E-07	1,84E-07
R^2	**0,83338**	0,797527	0,790337	0,919333	0,956431	0,929008	**0,94323**	0,94323	0,94323
Error	**0,113212**	0,055228	1,148009	3,8E-07	0,004444	0,002027	**0,000824**	0,006219	0,116611
DA	SSE	MWSE	EABS	SSE	MWSE	EABS	SSE	MWSE	EABS
Q^0	0,574034	0,62195	0,985502	0,005224	0,002476	0,00247	0,132326	0,140402	0,123424
b	1,782733	1,183386	1,071127	1,456507	4,503216	4,624406	6,288358	5,090056	8,708725
E	6,137942	6,824752	5,761571	4,392325	4,137671	4,105984	4,654498	4,77629	4,517781
R^2	0,833234	0,797547	0,765307	0,920776	**0,960442**	0,960289	0,94091	0,93584	0,920758
Error	0,113311	0,055112	**1,093993**	3,73E-07	**0,004192**	**0,001477**	0,00086	**0,005947**	**0,107178**
DR	SSE	MWSE	EABS	SSE	MWSE	EABS	SSE	MWSE	EABS
q_s	0,552229	0,276095	0,42372	0,003403	0,00349	0,003467	0,18333	0,187833	0,185057
k_ad	7805,698	795,1735	3664,715	185,1825	193,6844	189,6169	91,19268	96,46609	92,44006
r^2	0,803174	0,616823	0,764708	0,954246	0,952546	0,953727	0,923545	0,920741	0,9234
Error	0,139929	0,127922	1,527698	**2,08E-07**	0,004475	0,001589	0,001134	0,006231	0,137804

Appendix H: Salt concentrations for TG 201

Table H 1 shows the salt content and concentrations for TG 201 freshwater media.

Table H 1 Salt content and concentrations for TG 201 freshwater media

Component	AAP mg/L	mM	OECD mg/L	mM
$NaHCO_3$	15.0	0.179	50.0	0.595
$NaNO_3$	25.5	0.300		
NH_4Cl			15.0	0.280
$MgCl_2 \cdot 6(H_2O)$	12.16	0.0598	12.0	0.0590
$CaCl_2 \cdot 2(H_2O)$	4.41	0.0300	18.0	0.122
$MgSO_4 \cdot 7(H_2O)$	14.6	0.0592	15.0	0.0609
K_2HPO_4	1.044	0.00599		
KH_2PO_4			1.60	0.00919
$FeCl_3 \cdot 6(H_2O)$	0.160	0.000591	0.0640	0.000237
$Na_2EDTA \cdot 2(H_2O)$	0.300	0.000806	0.100	0.000269*
H_3BO_3	0.186	0.00300	0.185	0.00299
$MnCl_2 \cdot 4(H_2O)$	0.415	0.00201	0.415	0.00210
$ZnCl_2$	0.00327	0.000024	0.00300	0.0000220
$CoCl_2 \cdot 6(H_2O)$	0.00143	0.000006	0.00150	0.00000630
$Na_2MoO_4 \cdot 2(H_2O)$	0.00726	0.000030	0.00700	0.0000289
$CuCl_2.2(H_2O)$	0.000012	0.00000007	0.00001	0.00000006
pH	7.5		8.1	